

Argonne National Laboratory, with facilities in the states of Illinois and Idaho, is owned by the United States government, and operated by The University of Chicago under the provisions of a contract with the Department of Energy.

NOTICE

This report was prepared as an account of work sponsored by an agency of the United States Government. Neither the United States Government nor any agency thereof, or any of their employees, makes any warranty, express or implied, or assumes any legal liability or responsibility for any third party's use, or the results of such use, of any information, apparatus, product or process disclosed in this report, or represents that its use by such third party would not infringe privately owned rights.

Available from

Superintendent of Documents
U. S. Government Printing Office
Post Office Box 37082
Washington, D.C. 20013-7982

and

National Technical Information Service
Springfield, VA 22161

ARGONNE NATIONAL LABORATORY
9700 South Cass Avenue
Argonne, Illinois 60439

REVIEW OF FROSION-CORROSION
IN SINGLE-PHASE FLOWS

by

G. Cragolino*

Materials Science Division
Department of Applied Science

and

C. Czajkowski

Nuclear Waste Management and Materials
Science Division
Department of Nuclear Energy

Brookhaven National Laboratory
Upton, New York 11973

and

W. J. Shack

Materials and Components Technology Division

Argonne National Laboratory
Argonne, Illinois 60439

Report completed
April 1988

Prepared for the Division of Engineering Technology
Office of Nuclear Regulatory Research
U.S. Nuclear Regulatory Commission
Washington, D. C. 20555
Under Interagency Agreement DOE 40-550-75
NRC FIN No. A2212

*Now at Comision Nacional de Energia Atomica
Buenos Aires, Argentina

REVIEW OF EROSION-CORROSION
IN SINGLE-PHASE FLOWS

by

G. Cragolino, C. Czajkowski, and W. J. Shack

ABSTRACT

This report contains two literature reviews (prepared by Brookhaven National Laboratory and Argonne National Laboratory, respectively) on the available data and current mechanistic understanding of erosion-corrosion, and a failure analysis (prepared by Brookhaven National Laboratory) of a tee-elbow joint from the Surry Unit 2 reactor that failed by erosion-corrosion in December 1986. It also includes suggestions for additional research that should be performed by the USNRC to increase the capability to rank plants and/or locations within plants in terms of susceptibility to erosion-corrosion and to ensure that proposed inspection and mitigation programs are soundly based.

NRC
FIN No.

FIN Title

A2212

Environmentally Assisted Cracking in Light-Water Reactors

TABLE OF CONTENTS

	<u>Page</u>
EXECUTIVE SUMMARY	v
I. Erosion-Corrosion in Nuclear Power Plants	1
1. Introduction	1
2. Erosion-Corrosion of Carbon and Low-Alloy Steels in Power Plants	4
3. Phenomenological Aspects of Erosion-Corrosion	5
4. Models of Erosion-Corrosion	32
5. Surry Unit 2	40
6. Trojan Power Station	42
7. Haddam Neck Feedwater Line Rupture and Toledo Edison Seminar	46
8. Ultrasonic Measurements of Two Surry Unit 2 Specimens	48
9. Conclusions	53
10. References	54
II. Erosion-Corrosion in Single-Phase Flows	58
1. Introduction	58
2. Phenomenology of the Erosion-Corrosion Process	58
3. Effect of the Flow Velocity on Erosion-Corrosion Rates	61
4. Effect of Temperature on Erosion-Corrosion Rates	65
5. Effect of pH on Erosion-Corrosion	72
7. Effect of Alloy Addition on Erosion-Corrosion	77
8. Empirical Estimates of Erosion-Corrosion Rates	83
9. Application of the Empirical Models to the Surry 2 Feedwater Line References	87 89

EXECUTIVE SUMMARY

Introduction

This report contains literature reviews prepared by Brookhaven National Laboratory and Argonne National Laboratory on the available data and mechanistic understanding of erosion-corrosion and also a failure analysis prepared by Brookhaven National Laboratory of a tee-elbow joint from the Surry Unit 2 reactor that failed by erosion-corrosion in December 1986. A companion report (NUREG/CR-5149, ANL-88-23) prepared by Jonas, Inc. reviews the actual range of water chemistry conditions and design characteristics of current feedwater piping systems including flow conditions, geometry, and materials. Another companion report (NUREG/CR-5131, ANL-88-20) prepared by Argonne National Laboratory reviews the data and techniques available to determine mass transfer rates in piping geometries of interest. This executive summary includes suggestions, based on the information presented in these reports, for additional research that should be performed by the U.S. Nuclear Regulatory Commission to increase our capability to rank plants and/or locations within plants in terms of susceptibility to erosion-corrosion and to ensure that proposed inspection and mitigation programs are soundly based.

The inspections triggered by the failure that occurred at the Surry Unit 2 in December 1986 have revealed numerous instances of significant erosion-corrosion at other U.S. reactors, primarily in wet-steam lines, but also in some single-phase lines. Although erosion-corrosion does occur most frequently in wet-steam systems, German data files for the period 1961 to 1976 show that one-third of the 96 cases reported were for single-phase conditions.

Accelerated wastage of piping systems can be produced by both mechanical and corrosion processes. Mechanical damage can be produced by the forces generated by the impact of liquid droplets in a two-phase flow on the metal surface or by the fluid dynamic forces arising from the collapse of gas bubbles in a fast-flowing liquid (cavitation). Wear of last-stage turbine blades by water droplets and also cavitation damage of pumps by steam bubbles are typical examples of these phenomena. Even without mechanical damage, accelerated wastage can be produced by more rapid dissolution of the corrosion film caused by the enhanced mass transfer associated with turbulent flows.

Susceptibility to damage by cavitation is generally assessed in terms of the cavitation number

$$K = \frac{P - P_v}{\frac{1}{2} \rho V^2}$$

where p is the pressure, p_v is the vapor pressure, ρ is the density, and V is the fluid velocity. For small K (< 0.5) cavitation becomes a concern. For feedwater piping, K is generally greater than 50, and cavitation seems unlikely. In a few plants, however, the feedwater pressure can approach the saturation pressure, and cavitation may become of more concern, especially in regions of high local flow velocity.

Mechanical damage by droplet impingement in two-phase flows is more likely. However, it is difficult to assess the relative contributions of accelerated dissolution and droplet impingement at the flow velocities in the two-phase regions of piping systems ($< 250 \text{ ft}\cdot\text{s}^{-1}$). Even in laboratory tests at room temperature and at relatively high velocities, there is evidence of significant contribution from dissolution. The strong dependences on pH and dissolved oxygen content observed in the field are also consistent with a dominant contribution from dissolution processes. Most investigators attribute the accelerated wear experienced in the single-phase regions of secondary-system piping in nuclear power plants to accelerated dissolution. Many also consider dissolution the dominant process in the two-phase regime. Most of the work reviewed in this report focuses on this process.

A substantial body of data and experience is available on erosion-corrosion in environments characteristic of secondary water systems in nuclear reactors. The primary factors influencing erosion-corrosion are

- (1) Fluid flow velocity and geometry;
- (2) Fluid temperature and chemistry (pH, dissolved oxygen level, and impurities); and
- (3) Chemical composition of the piping material.

Susceptibility to erosion-corrosion depends strongly on the interaction of these variables. Thus, one cannot usefully identify a "critical" velocity or geometry or pH for erosion-corrosion; only an integrated model that considers all these factors can predict whether erosion-corrosion will occur in a particular situation. Although the qualitative changes in the erosion-corrosion rates expected with changes in these variables are reasonably well understood and materials that are highly resistant to erosion-corrosion are available for replacement or new construction, quantitative predictions of erosion-corrosion rates in existing carbon steel piping systems are subject to large uncertainties.

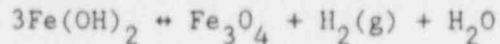
For currently operating plants, the most promising approach to mitigating erosion-corrosion in the short term would appear to be modification of the environmental factors, primarily pH and dissolved oxygen levels, and scrupulous attention to water purity. However, even in this case, important trade-offs must be considered. Raising the pH is generally beneficial for erosion-corrosion of carbon steel, but it may lead to unacceptably rapid wastage of copper alloy components in the system. Similarly, increasing the dissolved oxygen level could significantly reduce erosion-corrosion in the secondary-system feedwater train, but it could have substantial negative impact on steam generator materials.

Basic Processes of Erosion-Corrosion

In the deoxygenated solutions characteristic of typical secondary systems, iron dissolves to form ferrous hydroxide $[\text{Fe}(\text{OH})_2]$ according to the net corrosion reaction



At temperatures above 100°C, the ferrous hydroxide decomposes to form magnetite [Fe_3O_4] according to the Schikorr reaction



At even higher temperatures (> 200°C), Fe_3O_4 may be formed directly at the metal-oxide interface by transport processes involving the inward diffusion of H_2O through micropores in the oxide and a simultaneous outward diffusion of metal ions (Fe^{2+}) to the liquid. The net result is a double oxide layer with the inner layer growing into the metal as it oxidizes.

The stability of these films controls the erosion-corrosion process. The dissolution rate of the oxide films is a strong function of temperature, pH, and partial pressure of H_2 . Turbulent flow of the bulk fluid accelerates the corrosion process by removing the soluble corrosion products. The enhanced dissolution of the magnetite leads to accelerated metal loss as iron is oxidized to replace the dissolved film.

Effect of Flow Velocity and Geometry

Since the enhanced mass transfer associated with turbulent flows is the fundamental process in the accelerated dissolution of the magnetite corrosion film, the effect of the flow is best described in terms of the mass transfer coefficient k , which is a function of the flow velocity and geometry. For the nominal flow conditions generally found in PWR secondary-system feedwater piping, k is on the order of $1\text{-}3 \text{ mm}\cdot\text{s}^{-1}$.

Experimental data relating erosion-corrosion rates to k are frequently reported in terms of power law relationships of the form

$$\dot{m} \sim k^n$$

where \dot{m} is the mass loss per unit area and time. The exponent n describing the dependence of the erosion-corrosion rate on the mass transfer coefficient is a function of temperature, pH, and flow rate. Even for a restricted set of conditions characteristic of secondary-system feedwater piping in PWRs, a fairly wide range of values of n (1-3) has been reported. In piping systems k typically varies as $V^{0.9}$, where V is the flow velocity, so that the velocity dependence of the erosion-corrosion rate is $\sim V^{0.9-2.6}$.

The increased turbulence associated with changes in flow geometry increases the effective mass transfer coefficient over that for the straight pipe, and most instances of erosion-corrosion have occurred near flow discontinuities. Some data relating the mass transfer coefficient to flow velocity and geometry are available for a variety of configurations; these data suggest that for fittings such as elbows and tees, k can be 1-5 times the value for a straight pipe. However, it is difficult to obtain accurate values of k for many piping geometries. Mass transfer coefficients for two-phase flows are generally higher than those for single-phase flows with the same mass flow rate, because the reduction in the average density corresponds to higher velocities. Even fewer data on mass transfer coefficients for different flow geometries are available for two-phase flows.

In many cases the effects of flow geometry are estimated on the basis of a set of empirical factors developed by Keller from field observations in two-phase flows. However, the "Keller factors" are widely used for both single- and two-phase flows. The geometry factors are quite significant; the "Keller factor" for a 90° tee is 25 times larger than that for a straight pipe.

Effect of Temperature

Most reported cases of erosion-corrosion damage in single-phase flows have occurred within a temperature range of 80 to 230°C; for two-phase flow the range is somewhat higher, 140-260°C. Laboratory studies generally have found that erosion-corrosion rates drop off markedly at high and low temperatures with a strong peak at intermediate temperatures. However, considerable differences exist in the values reported for the temperature at which the maximum rate occurs and also in the temperature range for which erosion-corrosion rates are significant. Recently, an in-reactor instance of erosion-corrosion occurred at a reported temperature of 300°C in an evaporator unit of the Prototype Fast Reactor in the U.K. The reasons for this apparently anomalous behavior are unclear, although it might be attributed to exceptionally low trace levels of chromium in the material.

Several mechanistic explanations for the observed temperature dependence have been proposed. In one model, the decrease at high temperatures has been attributed to the decrease in the solubility of magnetite with increasing temperature, whereas at lower temperatures dissolution is kinetically limited in spite of the high equilibrium solubility. Another model also attributes the decrease at low temperatures to a decrease in the kinetics of the dissolution reaction, but the rapid decrease at higher temperatures is attributed to changes in the porosity of the oxide that inhibit access to the metal surface. With suitable choices of model parameters, both explanations give results fairly consistent with available data.

Effect of pH

Erosion-corrosion rates are strongly dependent on pH over the range of interest in reactor water systems. The data consistently show a decrease of more than an order of magnitude in erosion-corrosion rates over the pH range 8.5-9.5 typical of secondary-system feedwater. [Although the effect of pH is conventionally reported in terms of pH values at 25°C, the critical parameter is actually the corresponding high-temperature pH value. The relation of the high-temperature value to the reported value can be affected by the choice of control agents (e.g., morpholine or ammonia) and by impurities in the water.]

In two-phase flows the critical parameter is the pH of the liquid phase; this can be significantly affected by the partitioning of the control agent between the steam and liquid phases. Because morpholine has less tendency to enter the steam phase, PWRs in France use morpholine to control pH in the secondary system.

As was noted previously, raising the pH to the high end of the recommended ranges appears to be an attractive short-term mitigating action for erosion-corrosion of carbon steel, but may increase the corrosion rates of copper alloy components in the secondary system. Even for all-ferrous systems, operation above pH 9.3 may lead to unacceptably high resin exhaustion rates.

Effect of Impurities in the Water

Most studies of erosion-corrosion have been performed in relatively high-purity water. No studies are available on the effects of impurities like Cl^- or SO_4^{2-} , which can significantly affect magnetite solubility. Acidic impurities may be particularly deleterious. Organic acids, which can be generated by the thermal decomposition of organic impurities or ion exchange resin fines, are very stable in water, even at high temperatures. One disadvantage of the use of morpholine as a replacement for ammonia is the increase in cation conductivity of the water produced by the decomposition of the morpholine, which may mask small amounts of cooling water in-leakage.

Effect of Oxygen

In ammoniated water (pH ~ 9 at 25°C), very small amounts of dissolved oxygen (on the order of 2-10 ppb) appear to have dramatic effects on the erosion-corrosion rates. Relatively low levels of dissolved oxygen also have significant effects on the erosion-corrosion rates of carbon steel in neutral water, although the threshold levels needed to provide high erosion-corrosion resistance are not as well known as for more alkaline water.

The effect of oxygen can be explained in terms of its effects on the nature of the oxide film. In the presence of oxygen, the film probably contains hematite (Fe_2O_3) as well as magnetite (Fe_3O_4). Because the solubility of hematite is much less than that of magnetite, the oxide film is much more resistant to erosion-corrosion.

Although moderate levels of dissolved oxygen are very beneficial in terms of erosion-corrosion of the carbon steel feedwater, dissolved oxygen and oxide reaction products can have severely damaging effects on steam generator materials. Modern practice seeks to keep air ingress and dissolved oxygen levels as low as possible in PWR secondary systems. For BWRs, the EPRI/BWROG water chemistry guidelines suggest that dissolved oxygen levels in the feedwater be maintained at ≥ 20 ppb, even under hydrogen water chemistry conditions.

Effect of Material Composition

Alloying can greatly reduce susceptibility to erosion-corrosion. Austenitic stainless steels are considered virtually immune to erosion-corrosion, and even 2 1/4Cr-1 Mo steels give good performance in the field. Chromium is the most important alloying element for improving resistance, although other elements, such as molybdenum and copper, may also have a beneficial effect. The effect of chromium is readily understandable because of the high thermodynamic stability of chromium oxides. However, the degree of improvement associated with even low levels of chromium is somewhat surprising and may be due to progressive enrichment of the corrosion film by chromium as the less-stable oxides are dissolved. The basis for a beneficial effect of molybdenum and copper is less clear, and experimental data and plant experience are less consistent in demonstrating a beneficial effect of these elements.

Plant-to-plant variations in susceptibility (or even heat-to-heat variations within a plant) could be strongly influenced by variations in the levels of chromium present as a trace element in a nominally carbon steel. The specifications for the commonly used carbon steels (e.g., A106 Gr B, A234 Gr WPB) do not include chromium; however, experience suggests that chromium could be present as an "impurity" at levels ranging from 0.005-0.07 wt%. The available data on the effects of such levels of chromium are inconclusive. Some test data for high-pH, wet-steam conditions suggest that such low levels would have relatively little effect, but it is not clear that the test conditions were relevant to single-phase erosion-corrosion. Other test data for single-phase flows, which appear to better simulate the actual in-plant conditions, suggest a stronger role of low levels of chromium. However, in these tests most of the materials had relatively high levels of chromium, and the extrapolation of the data to the low levels of chromium that would be expected in nominally carbon steels is somewhat suspect.

Integrated Models for Erosion-Corrosion

As was noted previously, susceptibility to erosion-corrosion depends strongly on interaction of the flow, environmental, and material variables. Integrated models that consider all these factors have been developed by researchers at the Electricite de France (EDF), by Kastner in Germany, and by researchers at M.I.T. A modification of the model developed by EDF is being used by NUMARC (the CHEC code).

The EDF and Kastner models are based on dissolution models for erosion-corrosion and on experimental data for single-phase flows, although they are applied to both single-phase and two-phase flows. They have been calibrated and modified to improve agreement with in-plant data. The model developed at M.I.T. assumes that dissolution is the primary mechanism in single-phase flows, but it also includes a model for droplet impact damage for relatively high speed two-phase flows. The model of Kastner appears to be completely empirical; the EDF and M.I.T. models are semi-empirical, based on phenomenological models with empirical adjustments of the various constants to improve agreement with the available data.

All of the models are limited in their capabilities to consider the effects of complex piping geometries. Disturbances in turbulent flows can propagate through a distance of many diameters in piping systems. Thus the behavior at a particular location depends not only on the geometry at that location, but also on the upstream flow geometry. Even in the case of an isolated component, geometry effects in the EDF and Kastner models are taken into account through the "Keller factors," whose application to single-phase flows is somewhat suspect.

More mechanistically based models for certain aspects of erosion-corrosion have been proposed in the U.K. and France, but they cannot be used directly to predict erosion-corrosion in actual piping systems. An empirical modification of a mechanistically based model developed in the U.K. is outlined in this report.

No detailed comparisons of the models have been published, although some limited comparisons are given in this report. Significant differences exist between the models with respect to the predicted effects of variables like flow velocity and alloy content.

Recommended Research

The reviews of the literature and experience of utilities have revealed several areas where additional research is needed. These include

- (1) Parametric studies of available models. Three integrated models (CHEC, Kastner, and M.I.T.) are currently available for the analysis of erosion-corrosion. Comparisons of these models with each other and with the inspection results as they become available are needed to assess the usefulness of the models for developing inspection plans.
- (2) Effects of flow geometry on erosion-corrosion. Better techniques to account for the effects of flow geometry on erosion-corrosion are needed. Currently we rely primarily on the "Keller factors," even for single-phase flows and relatively complicated geometries instead of isolated simple geometries.
- (3) Studies on the effect of low chromium levels. It has been clearly established that chromium is an effective alloying element. However, lower levels of chromium, although not providing immunity, might significantly affect erosion-corrosion susceptibility. These studies may help to explain variations between plants with nominally similar conditions and also variations observed under well-controlled laboratory conditions.
- (4) Effects of water impurities on erosion-corrosion. Certain impurities can have significant effects on the solubility of magnetite. Erosion-corrosion is often thought to be primarily limited by mass transfer rates, but under certain circumstances it will be solubility-limited. Then impurities could have an important effect on erosion-corrosion rates. Most reactors are probably already committed to maintain water purity levels in the future as high as is reasonable to protect their steam generators; hence, no new guidelines are needed. However, data on these effects may help to rationalize results in existing plants. These data are clearly needed to develop an overall understanding of erosion-corrosion.
- (5) Field monitoring of erosion-corrosion. In situations where erosion-corrosion has occurred, further wear should be monitored by using ultrasonics, dc potential drop, or isotope-doping techniques. Such monitoring would provide realistic wear rates for comparison with models.
- (6) Evaluation of the effects of feedwater chemistry changes on other portions of the secondary system such as the steam generator, turbines, and condensers. Increasing the pH and dissolved oxygen levels has a generally favorable impact on erosion-corrosion. However, a more quantitative assessment of the positive and negative impacts of such changes is needed.

- (7) Rationalization of existing laboratory results. As has been noted, important quantitative differences exist between the results of different investigations of erosion-corrosion. For example, the power law exponent for the dependence of erosion-corrosion rate on the mass transfer coefficient for the same nominal environments and materials ranges from 1-3. These variations lead to considerable discrepancies in assessing the possible effects of flow velocity and geometry on erosion-corrosion. For example, doubling k might double the erosion-corrosion rate or increase it by a factor of eight. These differences in most cases are not due to uncertainties in the data, but appear to be due to some systematic effects that are not well understood. Similar systematic differences appear to occur in studies of temperature dependence. Insight into these differences can be obtained from the parametric model studies proposed above, but additional laboratory studies are also needed.

REVIEW OF EROSION-CORROSION IN SINGLE-PHASE FLOWS

by

G. Cragolino, C. Czajkowski, and W. J. Shack

I. EROSION-CORROSION IN NUCLEAR POWER PLANTS (C. Cragolino and C. Czajkowski)

1. INTRODUCTION

After the Surry Unit 2 (Virginia Electric Power Co.-VEPCO) catastrophic failure of a pipe in the "A" feedwater suction line, the U. S. Nuclear Regulatory Commission (USNRC) initiated a contract with Brookhaven National Laboratory (BNL). This program was to have as its objectives:

1. Evaluate Surry failure results and identify generic applicability;
2. Identify extent of erosion-corrosion problem in nuclear plants;
3. Evaluate data supplied by Office of Inspection and Enforcement and identify any trends or correlations; and
4. Identify problem areas that may need additional research to bound the problem.

An ultrasonic inspection of two pieces of the Surry Unit #2 piping was also made using both shear wave and longitudinal wave in order to evaluate the accuracy of the techniques. A review of the controlling variables in the erosion-corrosion phenomenon was prepared as a background information for further research.

1.1 Erosion-Corrosion

Erosion-corrosion is usually defined as the acceleration or increase in the rate of corrosion caused by the relative movement between a corrosive fluid and the metal surface. In principle, it should be distinguished from the effect of fluid flow that accelerates general corrosion by increasing the rate of mass transport of reactive species (i.e., a cathodic reactant, such as oxygen) to the metal surface, or the rate of removal of corrosion products from the metal surface. As illustrated schematically in Figure 1, at a given critical flow rate, a rather abrupt increase in the corrosion rate occurs within the turbulent flow regime. The critical fluid velocity, V_c , sometimes called erosional or breakaway velocity, depends on hydrodynamic parameters and the corrosion characteristics of the alloy/environment system. Below the critical fluid velocity the corrosion rate increases less abruptly due to an increase in the rate of mass transport of electroactive species. Within this regime the corrosion rate is governed by electrochemical and hydrodynamic phenomena under conditions varying from laminar to turbulent flow (Figures 2(a) and (b)). It should be noted, however, that for many alloy/environment systems the boundary between what is called flow-assisted corrosion and erosion-corrosion is not so well defined as suggested in Figure 1. This is precisely the case of carbon steel in high temperature deoxygenated water, as discussed in detail below.

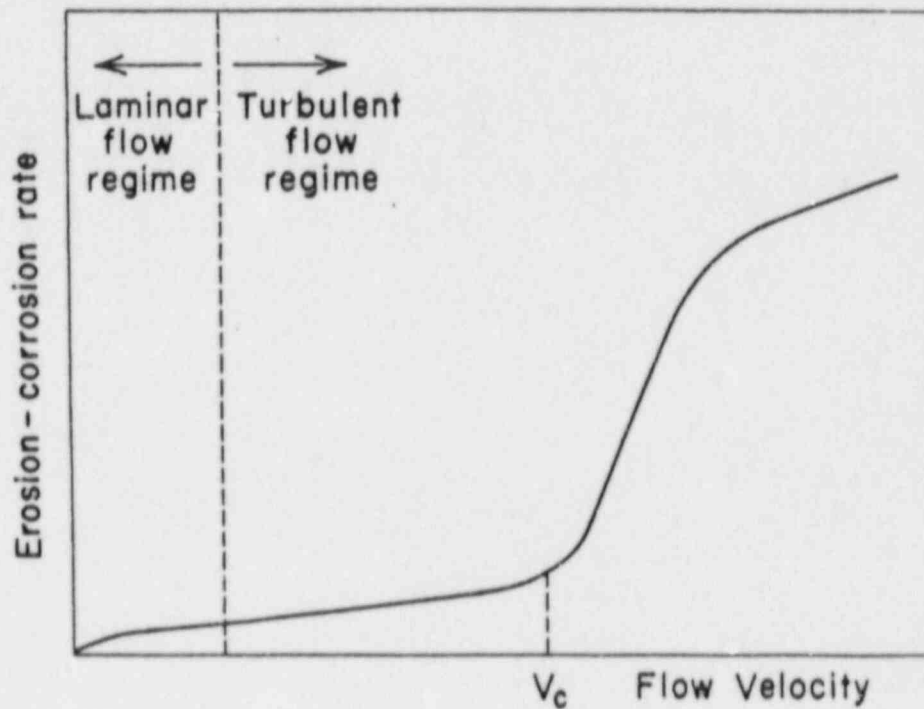


Figure 1. Schematic plot showing the effect of flow velocity on erosion-corrosion rate

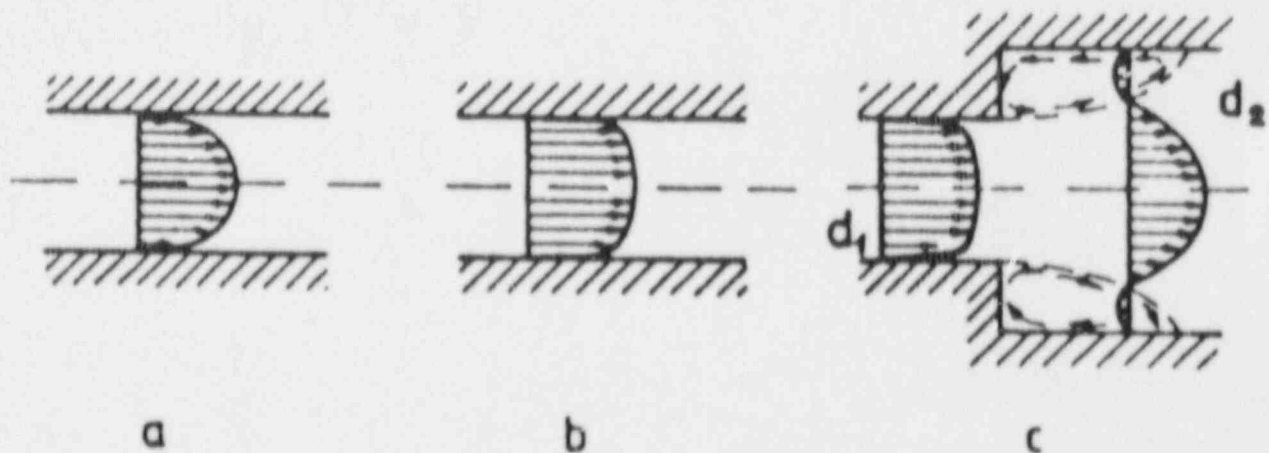


Figure 2. Velocity profile of fluid flow inside a pipe: a) established laminar flow, b) turbulent flow with logarithmic velocity profile, c) turbulent pipe with separation (complex velocity field with reverse flow).

Erosion-corrosion should also be distinguished from forms of erosion such as cavitation and impingement damage. Impingement damage involves the impact of liquid droplets present in a gaseous fluid through forces generally perpendicular to the metal surface, whereas cavitation arises from the collapse of gas bubbles contained in a fast flowing liquid phase, also through perpendicular pulsive forces. Wear of last-stage turbine blades by water droplets and cavitation damage of pumps by steam bubbles are typical examples of each phenomenon. Together with erosion by solid particles, they are essentially mechanical forms of metal deterioration, because the contribution of corrosion usually is thought to be almost negligible. In these three phenomena, direct damage of the metal occurs when the forces involved in the impact are higher than the material strength.

At lower energy transfer rates, erosion-corrosion predominates, characterized in appearance by grooves, ripples, gullies or smooth-bottomed shallow pits, usually exhibiting a directional pattern which makes evident the corrosive action of the environment. The flowing fluid can be a single-phase (liquid), a two-phase (liquid/gas or liquid/solid), or eventually a multiphase (gas/liquid/solid) system. Under certain conditions, the corrosive action of the flowing fluid is coupled to the mechanical effects noted above leading to enhanced rates of metal loss. This is particularly true when the liquid is water or an aqueous electrolyte and in this case is difficult to distinguish erosion-corrosion from pure erosion. Systems of interest in the steam-water cycle of nuclear power plants are obviously those in which a liquid (water, aqueous solution) and/or a gas (steam) phase are involved. It should be noted, however, that erosion-corrosion does not usually occur on surfaces exposed to dry steam, suggesting that the damage process is essentially an accelerated form of electrochemical aqueous corrosion.

Under erosion-corrosion conditions, the main effect of a fluid moving with a high flow rate is the localized removal of protective surface films, leading to accelerated corrosion, as depicted in Figure 1. However, the attack is less localized than in pitting or crevice corrosion, which are corrosion processes typical of stagnant fluids. In those locations where protective surface layers are removed, the electrochemical and hydrodynamic conditions determine the rate of corrosion in the presence of a physical separation between a small anodic area and a large cathodic surface. The rate of localized corrosion can be accelerated substantially in regions of high turbulence where reverse flow and eddying occur (Figure 1(c)).

As noted above, the boundary between flow-assisted corrosion and erosion-corrosion is not precisely defined for many alloy/environment systems under various hydrodynamic conditions. Different mechanistic interpretations of erosion-corrosion have been suggested, in which the emphasis for a particular system is displaced to the electrochemical or to the mechanical aspects of the phenomenon.

Erosion-corrosion in the steam-water cycle of power plants has been examined and discussed in recent conferences^(1,2) dealing mainly with problems encountered in feedwater heaters, moisture separators, boiler tubes, steam piping, pumps, etc. in both fossil-fueled and nuclear power plants. Several papers of particular interest have been presented in recent conferences on water chemistry of nuclear reactor systems organized by the British Nuclear Energy Society.^(3,4,5) The aim of this review is to update and complement with more recent information a previous overview on the subject.⁽⁶⁾

2. EROSION-CORROSION OF CARBON AND LOW-ALLOY STEELS IN POWER PLANTS

Carbon steels are extensively used in low pressure and high pressure turbine sections and feedwater heaters in both fossil-fueled and nuclear power plants. These materials are also used in many ancillary components of the steam-water circuit, such as moisture separators, reheaters, pipes, pumps, etc. In these components high flow velocities under single-phase (water) or two-phase (wet steam) conditions prevail.

Damage associated with erosion-corrosion under single-phase conditions has been observed at inlet ends in high pressure feedwater heater tubes,⁽⁷⁾ feedwater tube inlets in steam generators of gas-cooled reactor,^(8,9) feedwater pumps,⁽¹⁰⁾ and recently in the catastrophic failure of a suction line to the main feedwater pump at the Surry Unit 2 nuclear power plant.⁽¹¹⁾ Two-phase erosion-corrosion is a more widespread problem⁽¹²⁻¹⁶⁾ and it has been frequently observed in steam extraction piping, cross-over pipes from high pressure turbine to the moisture separator, and on the steam side of feedwater heat tubes,⁽⁷⁾ as well as in many other auxiliary components of the steam-water cycle. A complete compilation of the failure cases reported at the EdF meeting,⁽²⁾ including conditions for the occurrence of erosion-corrosion, components and materials affected, and estimated erosion-corrosion rates, was presented by Berge and Khan in the meeting's proceedings.

Damage of such power plant components generally occurs at locations where there is severe fluid turbulence adjacent to the metal surface, either as a result of inherently high fluid velocities (e.g., >2 m/s) or due to the presence of features (bend, tee, orifice, etc.) generating high local turbulence levels. In many cases the metal surface is characterized by the occurrence of overlapping "horseshoe" pits resulting in a scalloped appearance. Micro-pitting of the metal surfaces also occurs, being related to an accelerated attack on the pearlite grains of the carbon steel,^(9,14,17,18) which is probably the initial step in the damage process. A thin layer of oxide, 1 μm or less, is normally present on the corroding surface, but the rate of penetration in these localized areas deprived of the characteristic Potter-Mann double layer oxide film can reach values as high as 0.1 to 10 mm/year.^(9,15,17,18) Such rates of metal removal are indeed intolerable in power plants which have a design lifetime of 30 to 40 years, but even significantly lower rates of attack may generate undesirable high concentrations of corrosion products in the water circuits.

3. PHENOMENOLOGICAL ASPECTS OF EROSION-CORROSION

In recent years the fundamental aspects of erosion-corrosion of steels in high temperature flowing water have been studied by several authors^(9,17,18) particularly under single-phase conditions. For example, Bignold et al.⁽²¹⁾ have reported, as shown in Figure 3, that the total amount of metal loss increased linearly with time after a short non-linear initial period for carbon steel in deoxygenated water (pH 9.05) at 130°C. The slope of the line representing the steady state erosion-corrosion rate depends on the chemical composition of the steel (as illustrated in Figure 3), water chemistry, temperature and hydrodynamic conditions. However, under particular conditions, as indicated by Bignold et al.,⁽²¹⁾ there is a substantial initiation time before any erosion-corrosion loss is observed (Figure 4). Once initiated, the erosion-corrosion rate increases rapidly to a high value and remains constant for the duration of the test. These authors have pointed out that the initiation time can vary widely with the experimental conditions and may represent the time required to remove locally a protective magnetite film formed when specimens are initially exposed to a low flow environment. This conclusion is supported by results obtained by Berge et al.⁽¹⁸⁾ showing that preoxidation of carbon steel specimens (preoxidation conditions were not described) delays significantly (hundreds of hours) the initiation of erosion-corrosion in ammoniated water (pH₂₅ = 9.2) at 225°C. Delayed initiation times of the order of hundreds of hours are not expected to substantially affect evaluations of erosion-corrosion rates and metal losses in components exposed to a flowing fluid for many thousands of hours. However, these observations illustrate the potential risk of using data and kinetic expressions obtained in short term tests for predicting long term behavior without an adequate knowledge of the rate of metal loss as a function of time.

Prior to the discussion of the more important factors affecting erosion-corrosion of carbon steels in high temperature deoxygenated aqueous environments, a brief review of the general corrosion behavior of these steels is useful. According to the potential-pH diagram for iron in pure water, as shown in Figure 5,⁽²⁶⁾ a thermodynamically stable film of magnetite (Fe₃O₄) is formed in high temperature deoxygenated water. This film is stable at potentials close to that corresponding to the hydrogen evolution reaction (indicated as line a in Figure 5) over a wide range of pHs just above the pH of neutral water. The same general behavior is observed at temperatures ranging from 100 to 300°C.⁽⁶⁾ However, the solubility of magnetite in water containing H₂ changes with pH and also with temperature, as shown in Figures 6 and 7.⁽²⁷⁾ At neutral pHs (pH₂₅ = 7), the solubility reaches a maximum between 80 and 150°C and decreases again at higher temperatures.

The corrosion behavior in low flow rate (<2 m/s) circulating water can be directly related to the solubility of magnetite. As shown by Brush and Pearl,⁽²⁸⁾ iron release rates reached a maximum at about 100°C in water containing less than 3 ppb O₂. Only in the presence of >15 ppb O₂ a fully protective film of Fe₃O₄ is formed, which slows down significantly the iron release rate. At low temperatures (<100°C) iron dissolves slowly in deoxygenated water to form Fe(OH)₂ according to the overall equation,



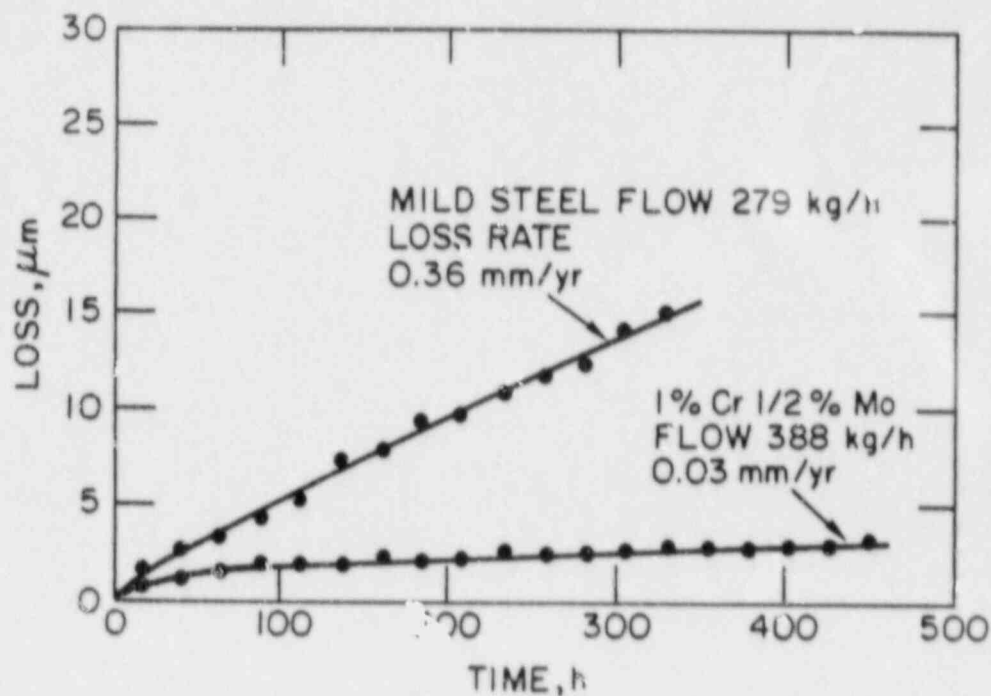


Figure 3. Erosion-corrosion loss versus time for mild and 1% Cr 1/2% Mo steel specimens in deoxygenated water flowing through an orifice at 130°C, pH 9.05. (Bignold et al., Ref. 21)

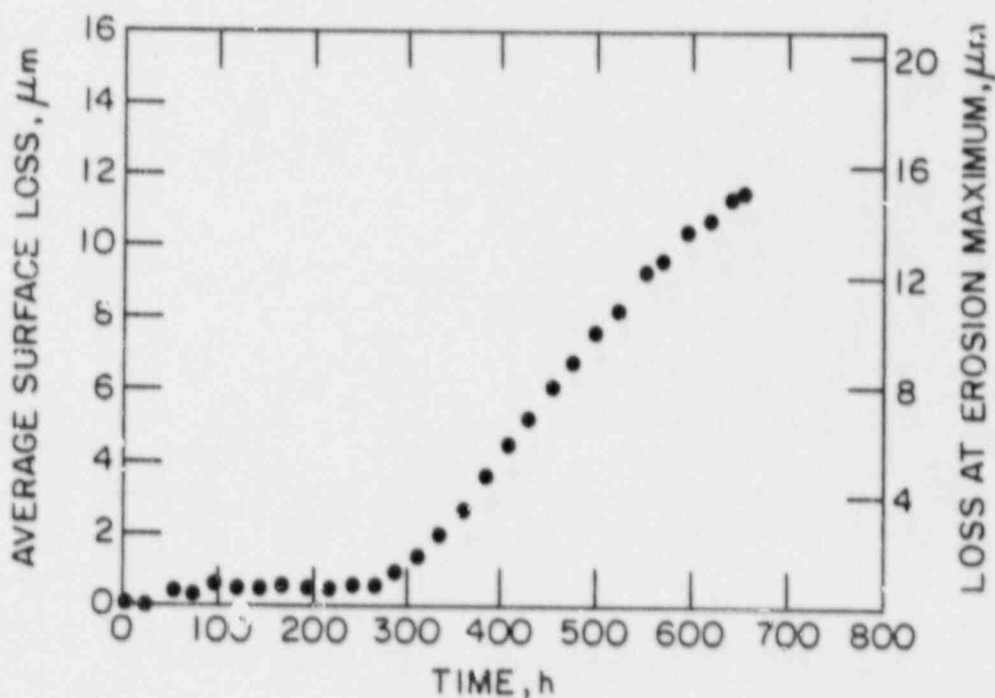
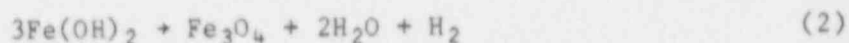


Figure 4. Average surface loss and loss at erosion maximum for mild steel in deoxygenated water flowing through an orifice at pH = 9.65; T = 148°C. (Bignold et al., Ref. 17)

whereas at temperatures above 100°C, Fe(OH)₂ is more rapidly formed and converted to magnetite according to the Schikorr reaction



At even higher temperatures (>200°C), it has been suggested, (29) as schematically shown in Figure 8, that Fe₃O₄ is formed directly at the metal/oxide interface by transport processes involving either the diffusion along grain boundaries of O²⁻ ions and the hopping of H⁺ ions between adjacent O²⁻ ions in the oxide lattice or the liquid diffusion of H₂O molecules through submicropores in the oxide towards that interface. These alternative processes are accompanied by the simultaneous outward movement of metal ions (Fe²⁺) via submicropores or grain boundaries (liquid or solid state diffusion) to the liquid phase. Under low flow rate conditions the liquid phase immediately adjacent to the oxide becomes saturated with soluble iron species and therefore an outer magnetite layer is nucleated and grows in the form of large crystals (0.5-5 μm) on top on the inner oxide. The net result is a double layer oxide (the so-called Potter-Mann oxide) with the inner layer occupying the volume of the metal oxidized.

The presence of H₂ dissolved in the environment or formed locally by the corrosion reaction, as well as the pH, determines the dissolution-deposition of magnetite at the oxide/solution interface according to the generalized equation proposed originally by Sweeton and Baes: (30)



where b = 0,1,2,3, depending upon the degree of hydrolysis of the ferrous ion.

In low flow rate or stagnant solutions, if atomic hydrogen is able to diffuse through the metal (as shown in Figure 8), a compact, non-porous oxide layer is formed representing a low general corrosion situation. On the other hand, in the presence of a high hydrogen concentration in the environment, a porous oxide layer is formed at a higher corrosion rate.

The previous discussion sets the basis for a physico-chemical understanding of the erosion-corrosion process. The most commonly accepted mechanism (17-24) for erosion-corrosion of carbon steels in high temperature deoxygenated water flowing at high flow rates is one of reductive dissolution of the magnetite (Fe₃O₄) film by enhanced mass transport of soluble Fe(II) species. If the rate of mass transfer of soluble Fe(II) species to the bulk of the solution is accelerated by the flow velocity, it is apparent from Eq. 3 that the enhanced dissolution of magnetite will lead to accelerated metal loss as iron oxidizes to replace the dissolved film. Under these conditions the outer oxide layer is not formed and erosion-corrosion occurs, under steady state conditions, through the simultaneous formation and dissolution of a film of

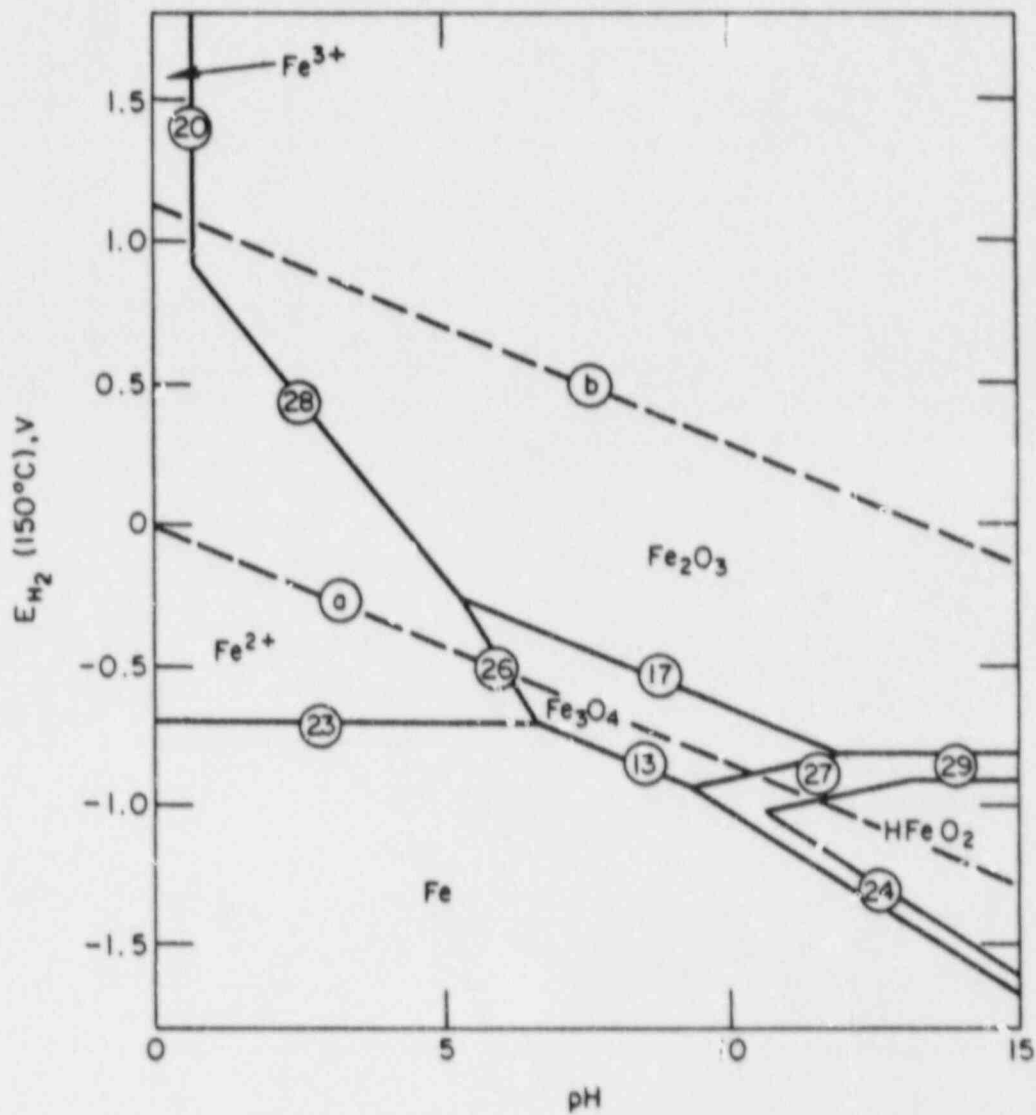


Figure 5. Potential -pH diagram for Fe-H₂O at 150°C. Activities of dissolved species taken as 10⁻⁶ mole/kg. Line a is drawn for $p_{H_2}=1$ at. (Townsend, Ref. 26). the pH of neutral water is 5.8 at 150°C.

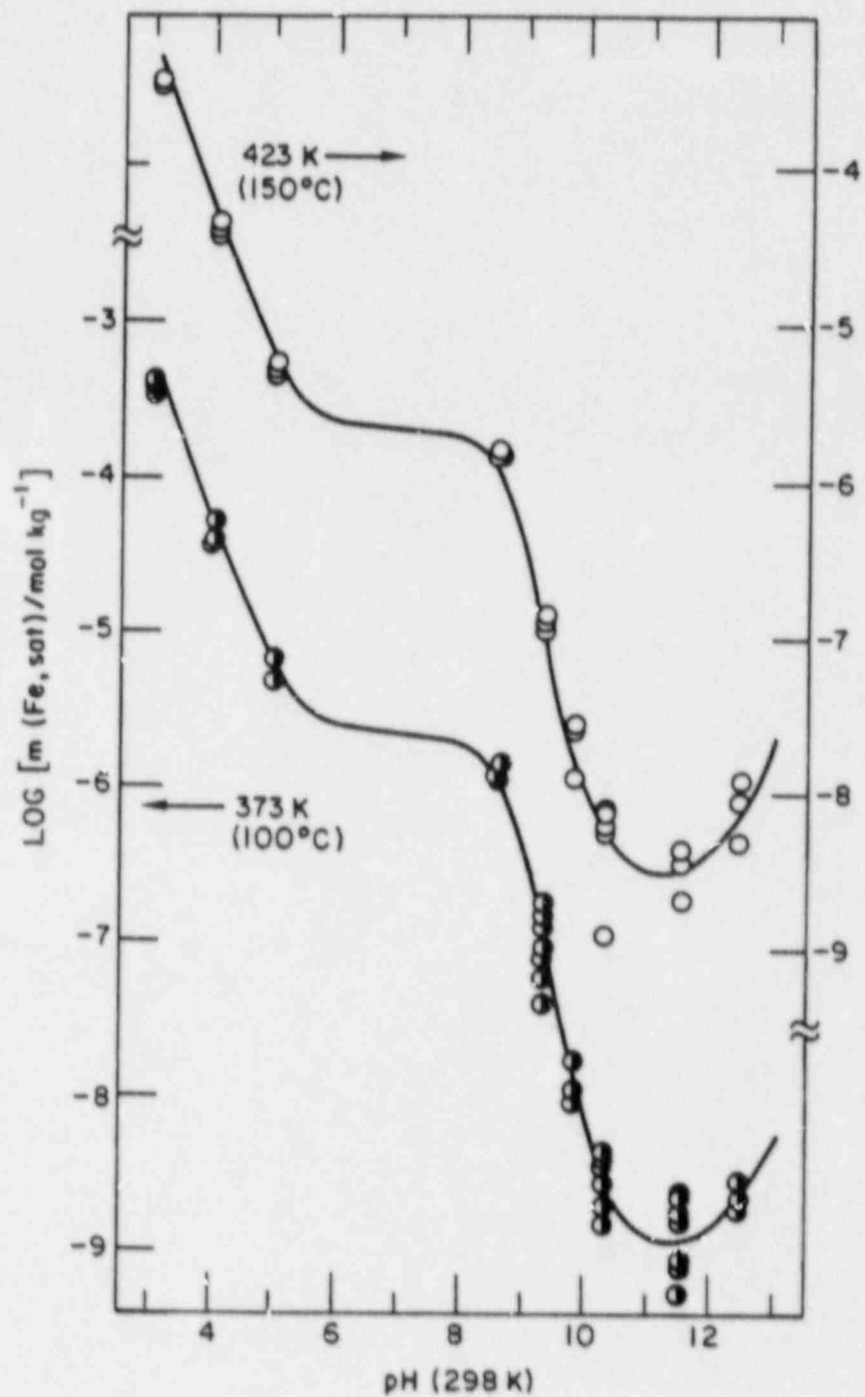


Figure 6 Experimental solubilities of magnetite at 423 and 373°K and 7790 mole-kg⁻¹ H₂. The solid line corresponds to the least-squares-fitted parameters listed in Table IV of the original publication. (Tremaine and LeBlanc, Ref. 27)

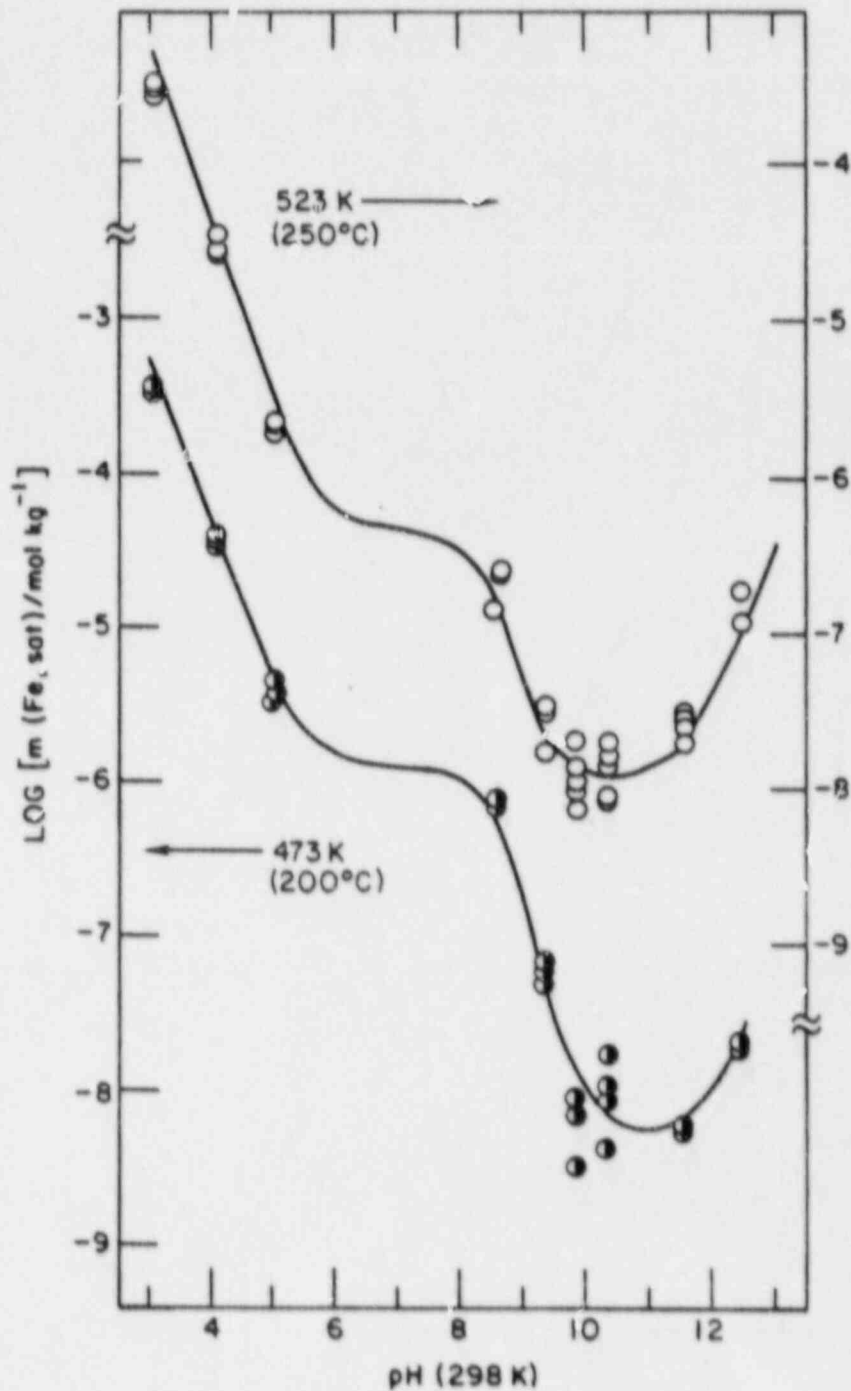


Figure 7 Experimental solubilities of magnetite at 523 and 473°K and 7790 mole·kg⁻¹ H₂. The solid line corresponds to the least-squares-fitted parameters listed in Table IV of the original publication. (Tremaine and LeBlanc, Ref. 27)

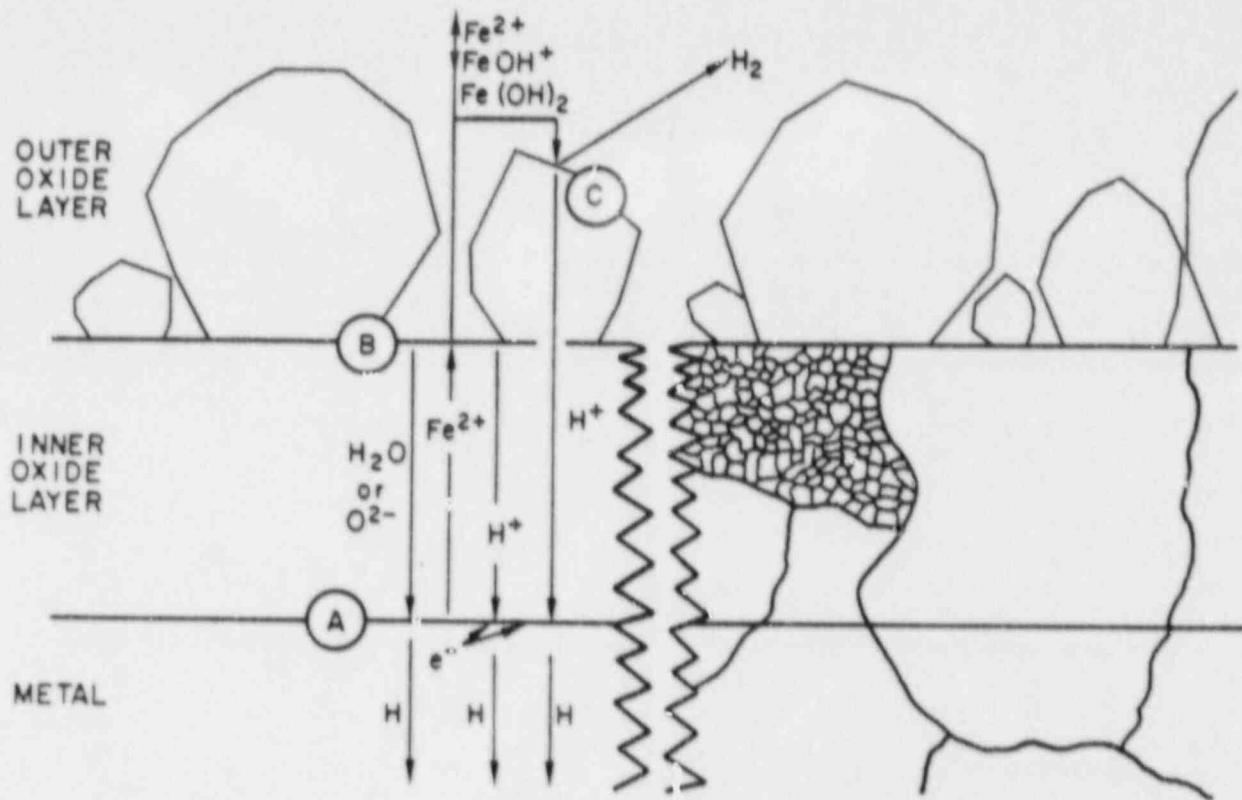


Figure 8. Model of steel corrosion by high temperature water ($\text{pH} < 11$). Diffusing species are shown on left-hand side. Grain structure is shown on right-hand side. The Fe/Cr spinel grain structure is shown within one ghost ferrite grain only. (Tonlinson, Ref. 29)

magnetite of constant thickness, and hence, at a constant rate of metal loss. If the overall process is controlled solely by mass transfer in solution, the rate of metal loss can be simply expressed as:

$$dm/dt = K(C - C_b) \quad (4)$$

where C is the concentration of Fe(II) species in solution at the oxide/solution interface, C_b is the concentration in the bulk, and K is the mass transfer coefficient, which varies with local hydrodynamic conditions.

With these basic concepts in mind, it is possible to discuss the role of the major influential factors in the occurrence of erosion-corrosion. They can be classified as follows:

- Hydrodynamic factors (flow rate, geometry of the flow path)
- Environmental factors (temperature, pH, oxygen concentration, water impurities content)
- Metallurgical factors (mainly the chemical composition of the steels)

The rate of metal loss depends in a complex manner on such factors. Therefore, it is not surprising that a satisfactory and comprehensive predicting model is not yet available. Nevertheless, several models have been developed which are capable of semi-quantitative predictions of metal loss. Following a review of the experimental data available, these models will be examined and the differences between them emphasized in the next section.

Hydrodynamic Factors

The strong dependence of erosion-corrosion rate on flow velocity for carbon steels in high temperature deoxygenated water is illustrated in Figure 9, as reported by Bignold et al.⁽¹⁷⁾ In this case the rate is proportional to the square of the fluid velocity, but it should be noted that these results were obtained for a particular geometry corresponding to the expansion of the flow from an axially located orifice (see Figure 2c). Although experimental results are many times reported in terms of fluid velocity, erosion-corrosion rate is not only determined by the flow rate, but also by the flow path geometry.

Following initial attempts by Gulich et al.,⁽³¹⁾ many other laboratory studies^(17,19,20,21,24) have confirmed that the local mass transfer coefficient (K), which can be defined as the ratio between the reaction rate and the concentration driving force for a process determined by mass transport, is the controlling parameter. This coefficient depends on a complex manner of fluid velocity, geometry of the flow and temperature, as related to dynamic and diffusional properties of the system, but it can be expressed in terms of nondimensional groups.^(32,33) In general, the Sherwood number, $Sh = K d/D$, where d is the characteristic length (for example, diameter of a pipe), and D is the diffusivity of the relevant species, is expressed as

$$Sh = Kd/D = \text{constant } Re^a Sc^b \quad (5)$$

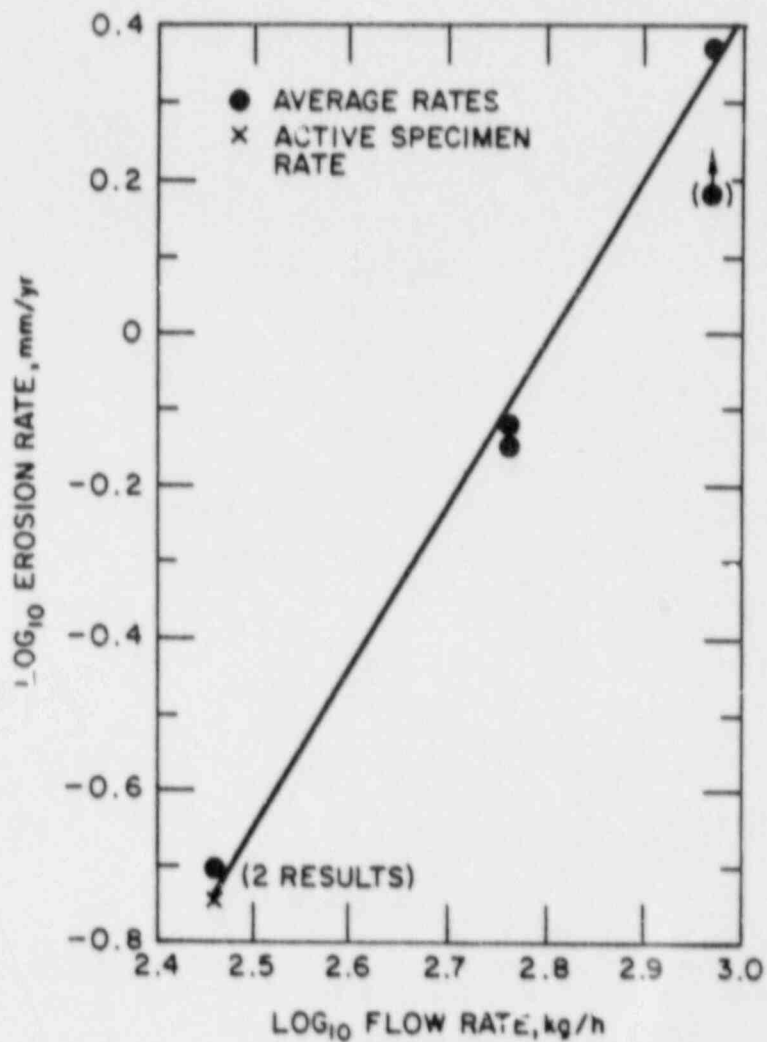


Figure 9. Variation of erosion-corrosion rate of mild steel with mass flow rate in deoxygenated water flowing through an orifice at pH 9.05, 149°C (slope of line = 2.1) (Bignold et al., Ref. 17).

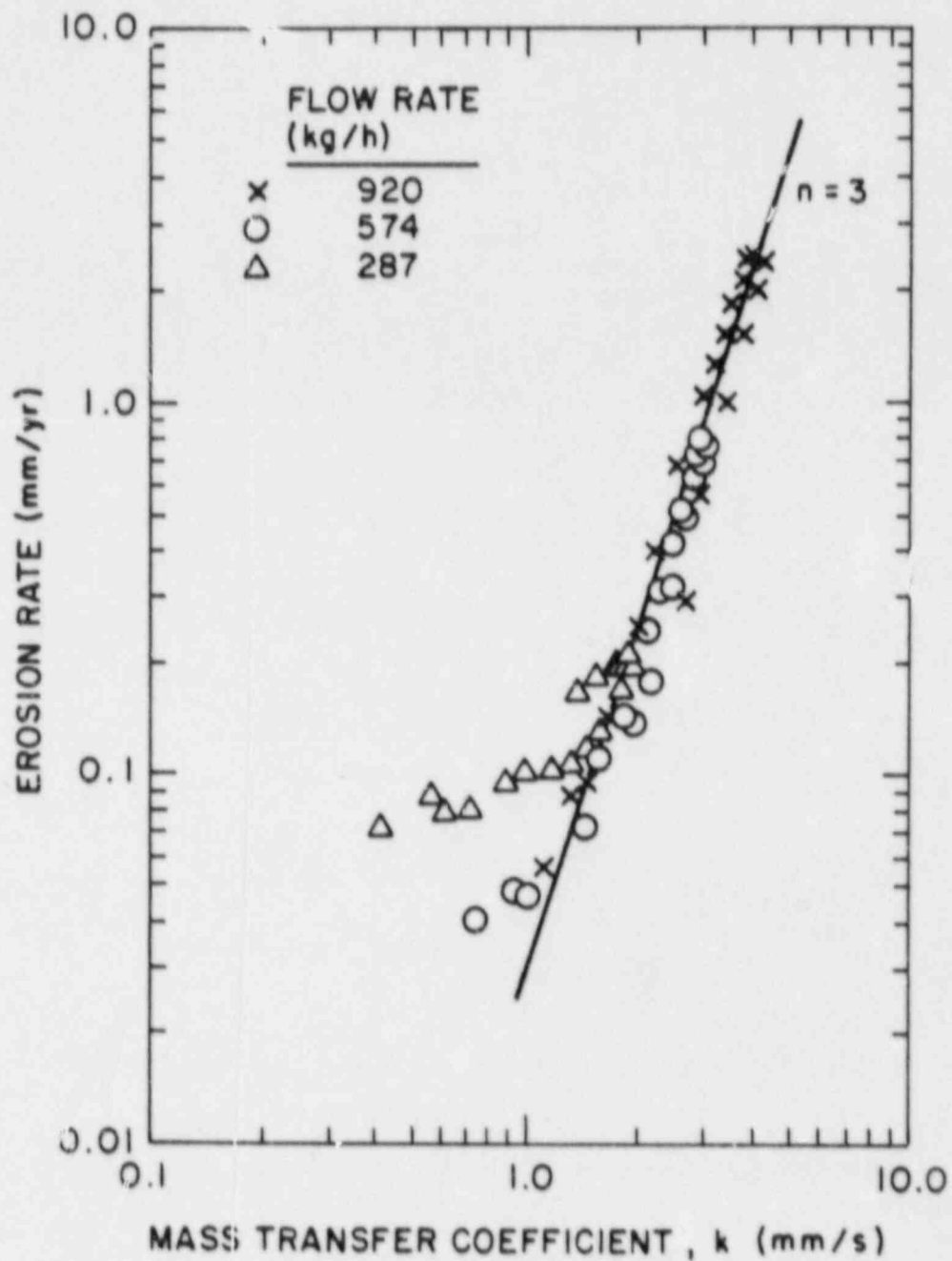


Figure 10. Correlation of erosion-corrosion rate downstream of orifice with corresponding mass transfer coefficient for mild steel in deoxygenated water at 148°C and pH=9.05 (Bignold et al., Ref. 17)

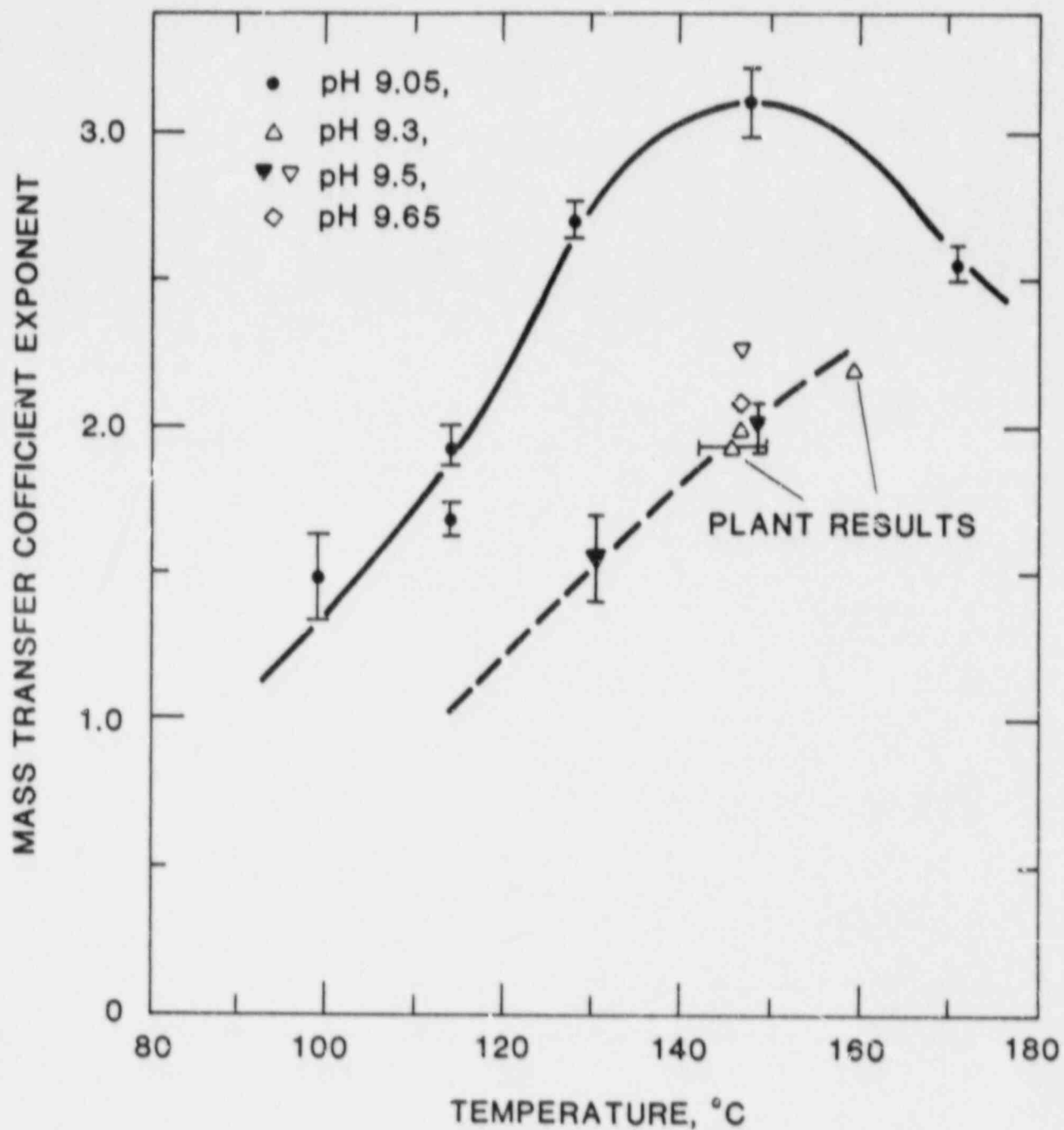


Figure 11. Temperature dependence of the exponent of the mass transfer coefficient on the erosion-corrosion rate of mild steel in flowing water at various pHs. (Bignold et al., Ref. 20)

where $Re = vd/\gamma$ is the Reynolds number, $Sc = \gamma/D$ is the Schmidt number, and v and γ are the velocity of the fluid and the kinematic viscosity, respectively. Usually $0.66 < \alpha < 0.875$ and $\beta = 0.33$. For example, Berger and Han⁽³⁴⁾ have shown that for fully developed turbulent flow in a smooth straight pipe

$$Sh = 0.0165 Re^{0.86} Sc^{0.33} \quad (6)$$

Since the mass transfer coefficients for simple flow geometries can be calculated by using expressions similar to Eq. (6), experimental correlations between erosion-corrosion rate and mass transfer coefficients under well defined environmental conditions can be used to predict that rate for other situations. For example, Figure 10⁽¹⁷⁾ shows that a cubic relationship exists between the erosion-corrosion rate for carbon steel in deoxygenated water at 150°C and the mass transfer coefficient over a wide range of flow rates. Since the mass transfer coefficient for flow downstream of an orifice is proportional to the flow velocity to the (2/3) power, the erosion-corrosion rate should be proportional to the square of velocity, as seen in Figure 9. However, as shown in Figure 11,⁽²⁰⁾ the exponent of the mass transfer coefficient is extremely dependent upon temperature and pH, indicating a more complex relation than that indicated in Figure 10 for a single temperature and pH.

Another author⁽²⁴⁾ have found a different relationship between erosion-corrosion rate and mass transfer coefficient, as shown in Figures 12 and 13. A linear relationship is observed for K values ranging from 3.5 to 16 mm/s in Figure 12, whereas Figure 13 indicates the existence of a threshold value of K , above which the rate increases linearly with the mass transfer coefficient. It should be noted that these results were obtained using flat specimens located perpendicularly to the water flow produced through a nozzle. Extremely high erosion rates were measured, although the water chemistry is similar to that employed by Bignold and consists of deoxygenated water (<5 ppb O_2) with $pH_{25} = 9.0$ by conditioning with ammonia and 20 ppb of hydrazine.

The comparison of these results indicates that despite the significance of the mass transfer coefficient as a controlling variable of the hydrodynamic conditions, it is difficult to establish the relevant value for a given geometry. Furthermore, as experimentally shown by Bignold,⁽¹⁷⁾ the mass transfer coefficient for water flowing through an orifice shows a well defined maximum at a distance beyond the orifice equivalent to 2 times its diameter, with a relatively abrupt decay to low values at about 7 times the tube diameter, in good agreement with calculations performed by Coney.⁽³³⁾ Thus, the local value of the mass transfer coefficient is the relevant variable, but in practical situations a distribution of values exists, giving rise to widely different erosion-corrosion rates. In addition, small alterations in the roughness of the surface or the presence of protrusions from welds and other irregularities may significantly alter those coefficient values calculated by taking into consideration a rather smooth surface. In particular, roughness due to the erosion-corrosion process itself may give rise to increasingly higher values of mass transfer, and hence an acceleration of erosion-corrosion

An empirical approach has been suggested by Keller⁽¹²⁾ to estimate erosion-corrosion rates for different flow path geometries under two-phase flow on the basis of observations of damage in wet steam-turbines. His approach will be presented in a later section.

Environmental Factors

Temperature. A very important variable affecting the erosion-corrosion resistance of carbon and low alloy steels is temperature. Most of the reported cases of erosion-corrosion damage under single-phase conditions have occurred within the temperature range of 80 to 230°C, whereas the range is displaced to higher temperatures (140 to 260°C) under two-phase flow. On the basis of laboratory work, several authors^(12,17,20,35,36) have reported a maximum in the erosion-corrosion rate at some intermediate temperature, as illustrated in Figure 14⁽²⁰⁾ for carbon steel in ammoniated, deoxygenated water (pH = 9.05). It is seen that the maximum becomes significantly more pronounced with increasing flow rate or mass transfer.

The precise location of the maximum seems to change with pH and other environmental variables, but under single-phase conditions is about 130 to 150°C.^(17,20,35) For two-phase conditions the location is displaced to approximately 180°C,⁽¹²⁾ but other authors⁽³⁶⁾ have reported a maximum at 150°C, also on the basis of plant experience. However, as reported recently by Tomlinson and Ashmore,^(37,38) severe erosion-corrosion (≈ 3 mm/year) was observed at 300°C in small ferrules used to control the flow of water (≈ 20 m/s) through individual tubes in evaporator units of the Prototype Fast Reactor in the U.K. Extrapolation of the data shown in Figure 14 would lead to very small erosion-corrosion rates at that temperature for an all-volatile treated (AVT) water with pH ranging from 8.6 to 9.2. On the contrary, the plant results indicate rates of erosion-corrosion which are similar in magnitude to those found between 100 and 160°C. The authors attribute these high erosion-corrosion rates to an exceptionally low level of chromium in the material, a factor to be discussed below. For this reason, among others, it seems very important to emphasize again the difficulties associated with the extrapolation of short term experiments to plant exposures (> 15,000 hours).

pH. It has been found (Figure 15) that an increase in the pH of the water above 9.2 (measured at room temperature) induces a decrease of more than one order of magnitude in the erosion-corrosion rate of carbon and low alloy steels.⁽³⁵⁾ This observation is in qualitative agreement with early studies of erosion-corrosion damage in feedwater heaters,⁽⁷⁾ indicating that attack occurred predominantly at pH values less than 9.0, but it was not normally observed at pH > 9.2.

According to the results of Bignold et al.,^(17,19) the erosion-corrosion of carbon steels in ammoniated, deoxygenated water at 148°C decreases with pH, as shown in Figure 16. For the upper solid line the rate is approximately proportional to $[H^+]^{1.5}$ over the pH range 9.05 to 9.65. However, the scatter in the data makes it difficult to define precisely the slope of the pH dependence. Some of the data points at pH = 9.5 seem to indicate an abrupt decrease of the erosion-corrosion rate above this pH, but it should be noted that this is a relatively high pH for plant operation. A less strong pH dependence has been observed by Apblett⁽³⁹⁾ over the pH range 8.0 to 9.5 at 99°C. In this case, the rate was found to be directly proportional to $[H^+]$.

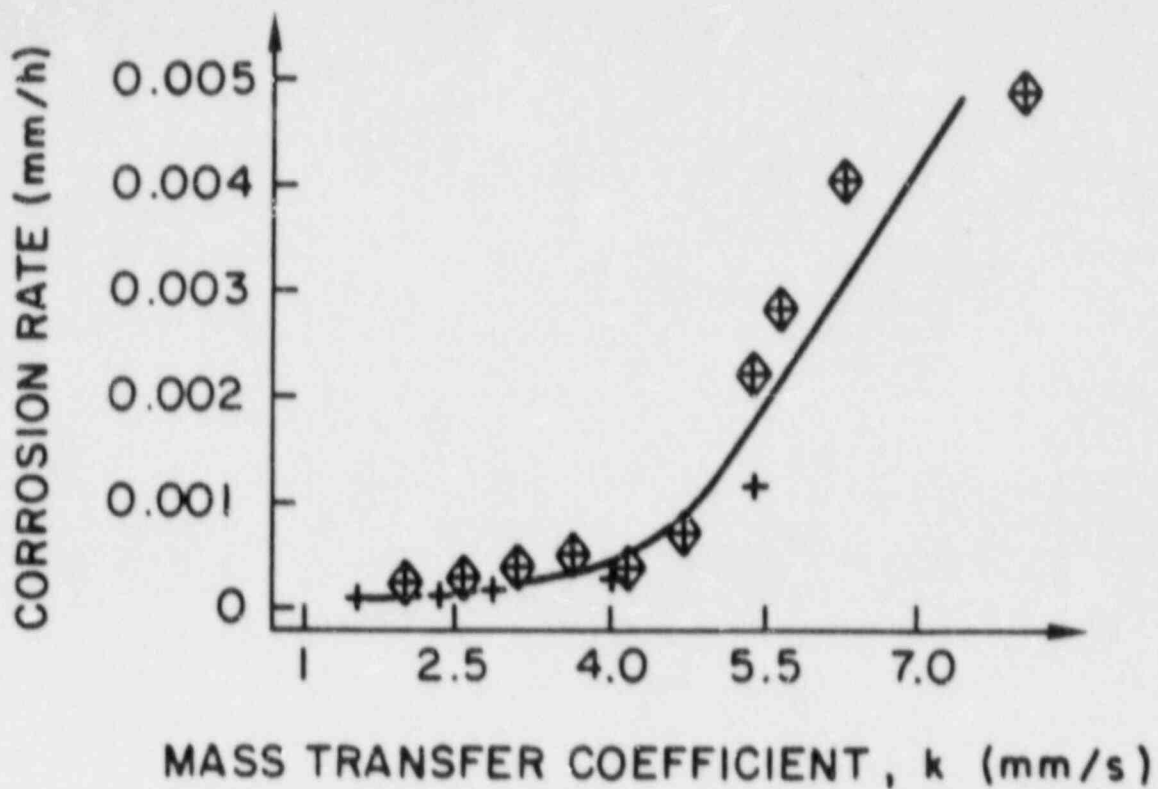


Figure 12. Correlation of erosion-corrosion rate with mass transfer coefficient for mild steel in deoxygenated water at 180°C. (Nozzle inner diameter ϕ 1.5 mm) (Ducreux, Ref. 24).

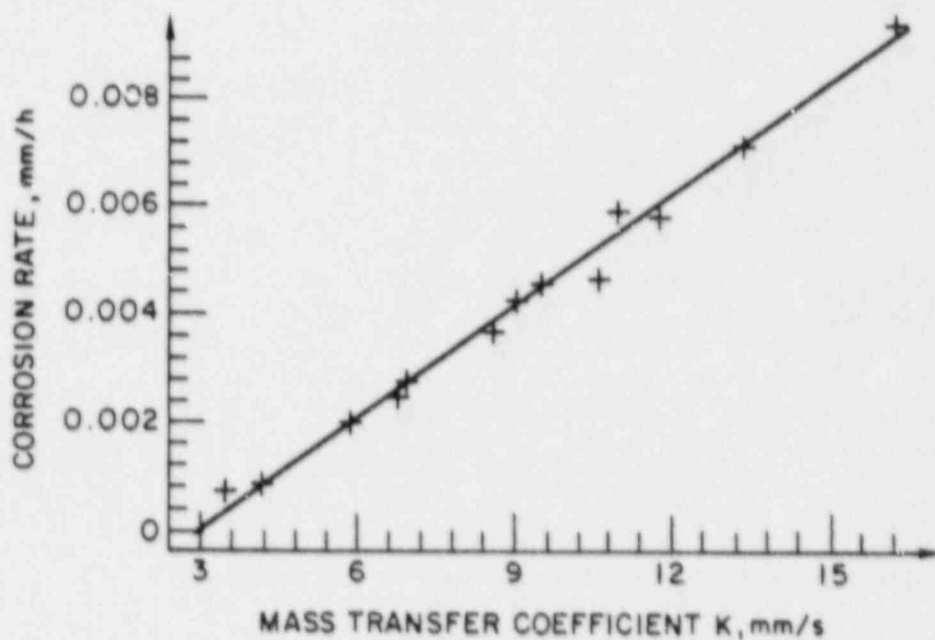


Figure 13. Correlation of erosion-corrosion rate with mass transfer coefficient for mild steel in deoxygenated water at 180°C. (Nozzle inner diameter ϕ 2.3 mm) (Ducreux, Ref. 24)

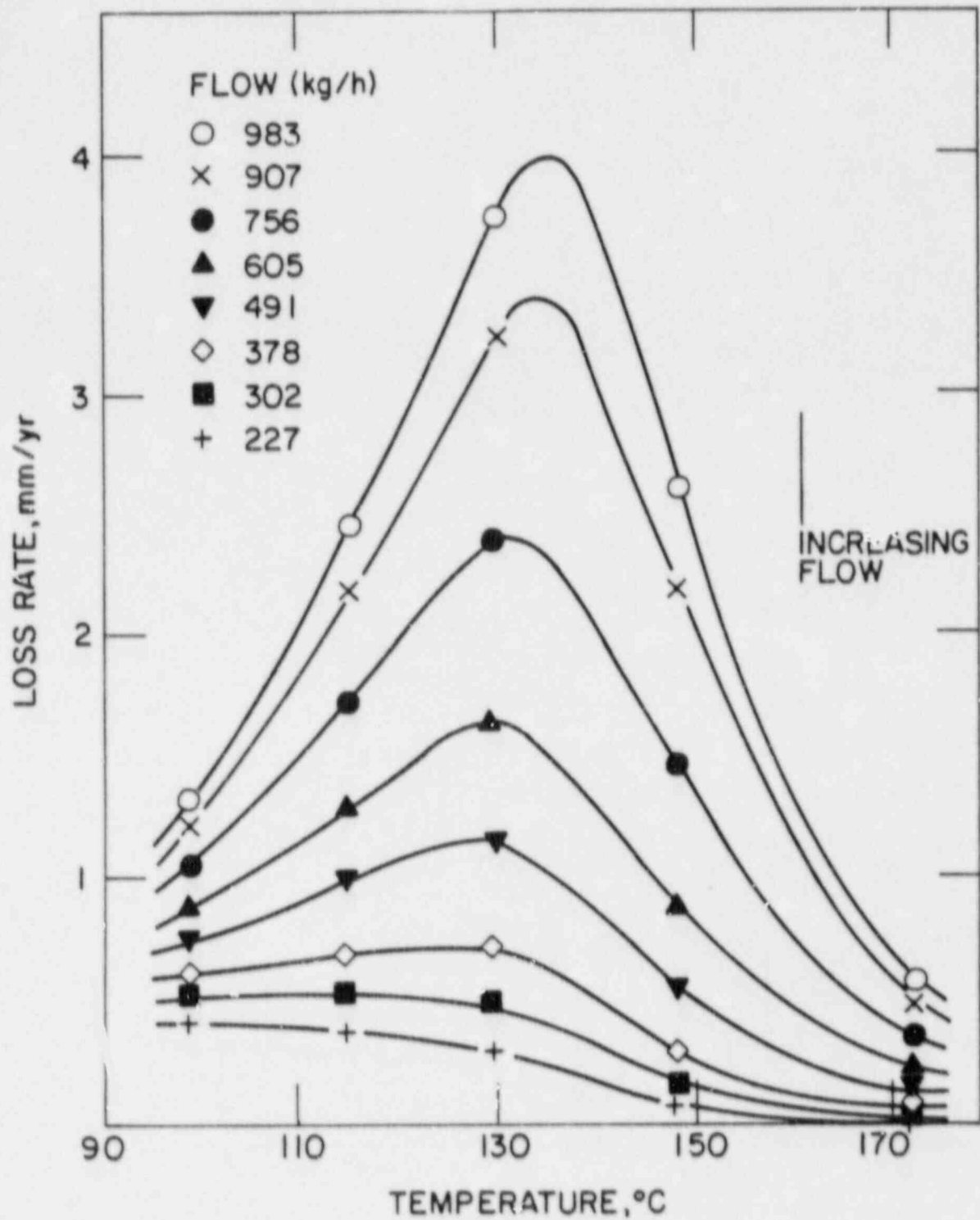


Figure 14. Temperature dependence of post-orifice erosion-corrosion rates for mild steel in deoxygenated water (pH = 9.05) (Bignold et al., Ref. 20)

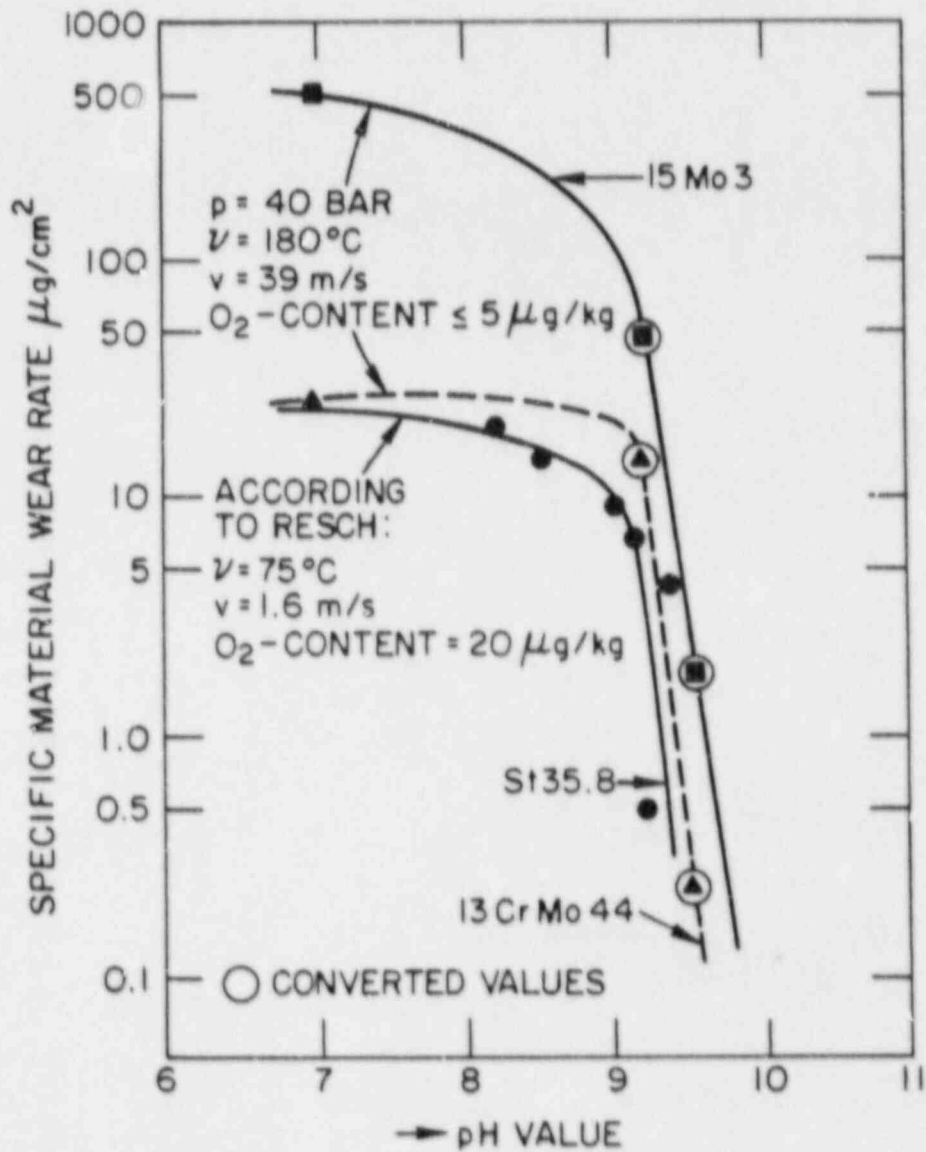


Figure 15. Effect of pH value on material wear rate due to erosion-corrosion for various steels in neutral water (Heitmann and Kastner, Ref. 35). Note that St 35.8 = A414 GrB (carbon steel); 15 Mo3 = A161 GrT1 (0.5 Mo) and 13 Cr Mo44 = A213 GrT12 (1Cr-0.5Mo).

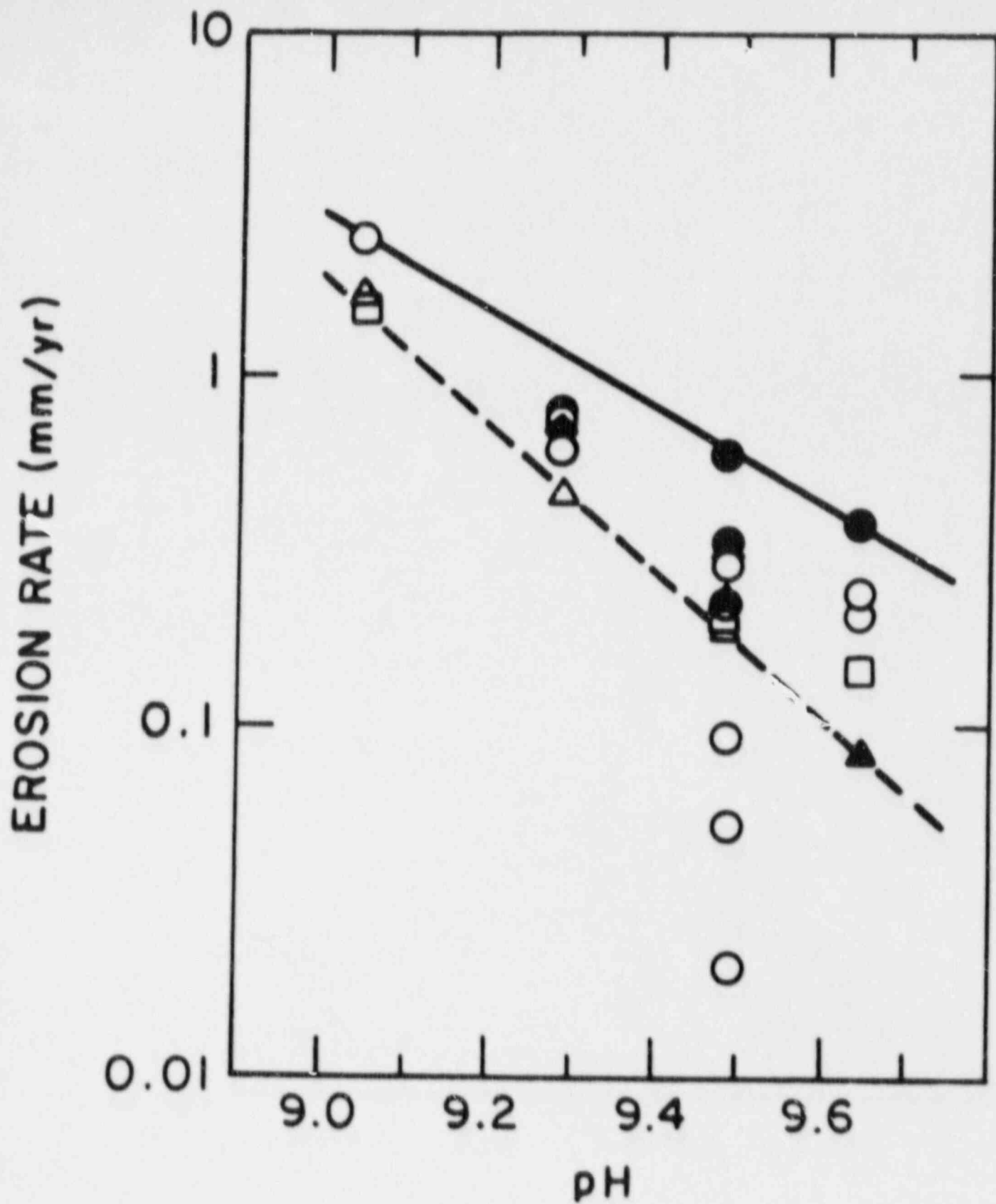


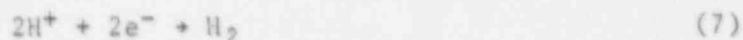
Figure 16. Erosion-corrosion rates in a restrictor tube downstream of the ferrule for mild steel in deoxygenated water as a function of pH ($T = 148^{\circ}\text{C}$) (Bignold et al., Ref. 17).

Regarding the effect of volatile bases added to the water to control the pH, Berge et al.⁽¹⁸⁾ have shown that the rate of metal loss for carbon steels in jet impingement tests with deoxygenated water at 225°C are significantly higher in the presence of ammonia (approximately 5 times) than in the presence of morpholine when the pH at 25°C is controlled at a value of 9.2. The lower rate of erosion-corrosion observed in the presence of morpholine should be attributed to the higher pH attainable at high temperatures with this additive. For two-phase application the beneficial effect of morpholine has been noted.⁽¹⁶⁾ Its more favorable partition coefficient between water and steam in comparison to ammonia leads to higher pH values in the liquid phase.

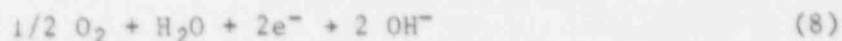
Oxygen Content. The beneficial effect on erosion-corrosion rate arising from the presence of dissolved oxygen in the water has been reported by various authors.^(35,36) It should be noted that iron release rates from carbon steel in pure water (neutral pH) decreased by up to two orders of magnitude over the temperature range of 38 to 204°C with increasing oxygen concentration from 1 to 200 ppb.⁽²⁸⁾ It can be expected that erosion-corrosion rates follow this type of behavior. As a matter of fact, additions of up to 300 ppb oxygen to the feedwater constitute the basis of the oxygen-dosed neutral water chemistry and the combined oxygen-ammonia water chemistry regimes used by German utilities for fossil-fueled power plants.^(40,41) No incidents of erosion-corrosion have been reported in these plants coupled with very low levels of iron detected in the feedwater. In both regimes the control of the water purity is critical, because small concentrations of aggressive anions such as Cl⁻ or SO₄²⁻ may lead to very high corrosion rates in the presence of relatively high oxygen contents.

In laboratory work the beneficial effect of oxygen on erosion-corrosion was reported initially by German researchers,^(35,42) as shown in Figure 17. However, in this figure it appears that relatively high levels of dissolved oxygen (>100 ppb) are required to reduce the erosion-corrosion to sufficiently low values. More recently, Bignold et al.⁽²¹⁾ have shown (Figure 18) that dissolved oxygen concentrations of about 8 ppb are sufficient to arrest erosion-corrosion of carbon steels (two different tests) in ammoniated water. When the dosing of oxygen was interrupted, there was a significant delay before erosion-corrosion restarted at the initial rate. The delay (from 50 to more than 200 hours in different experiments) is related to the duration and level of oxygen dosing, as well as to the severity of the hydrodynamic and environmental conditions in the reinitiation period.

In a more recent study,⁽²²⁾ similar data were obtained for oxygen inhibition of erosion-corrosion at 150°C and at a lower pH, around 7.8. In this case, the potential of the specimen was measured, as shown in Figure 19. It is seen that the addition of oxygen shifts the potential to more positive values. This effect has been interpreted as due to a change in the cathodic reaction from hydrogen evolution.



to oxygen reduction



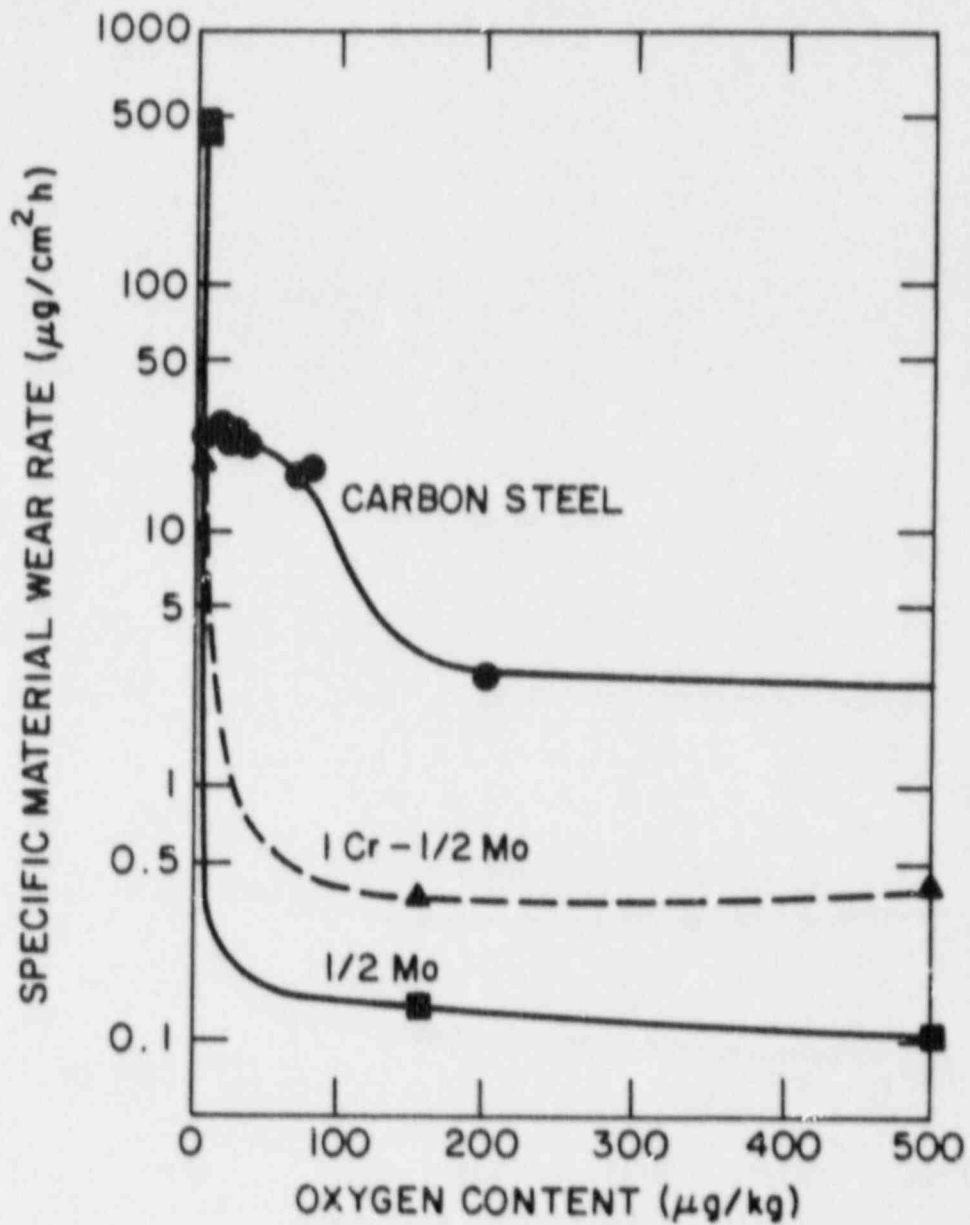


Figure 17. Effect of oxygen content on material wear rate due to erosion-corrosion for various steels in neutral water for steel denominations. (Heitmann and Schub, Ref. 49). See caption of Figure 15 for steel denomination.

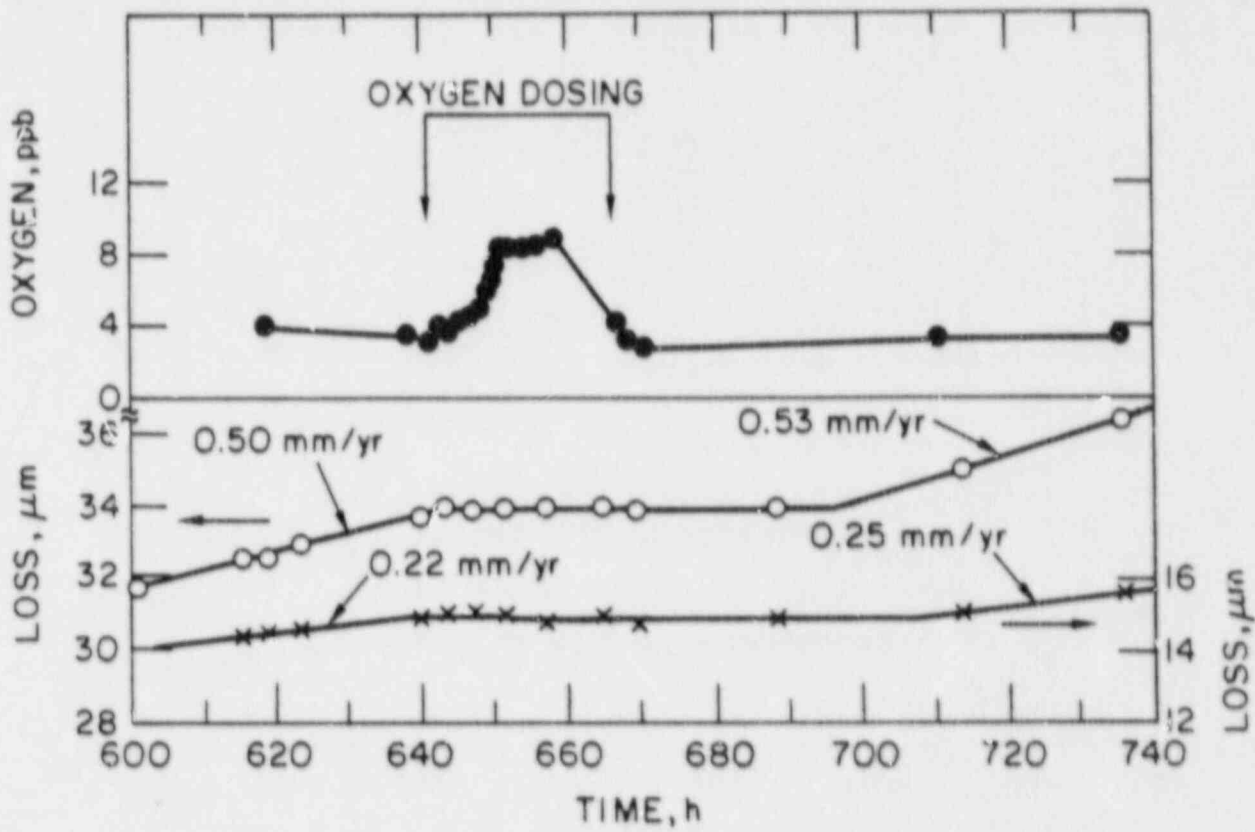


Figure 18. Effect of oxygen on erosion-corrosion of mild steel in deoxygenated water at 148°C, pH 9.4 (Bignold et al., Ref. 21).

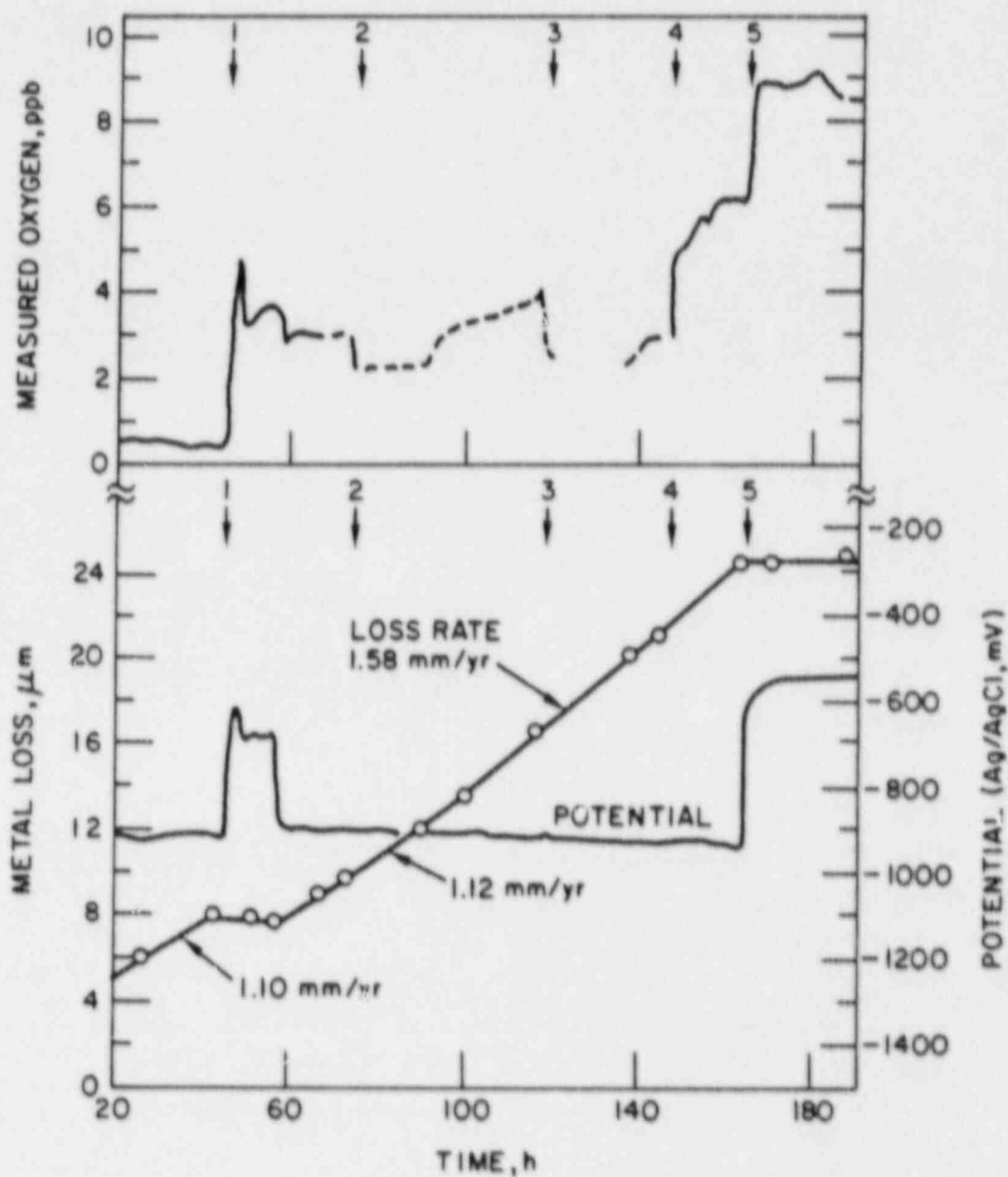


Figure 19. Influence of oxygen on erosion-corrosion of mild steel in deoxygenated water and specimen potential at 150°C 1) start O_2 dose; 2) O_2 dose switched to 2nd flow channel; 3) O_2 dose stopped; 4) start 2nd O_2 dose; 5) dose increased. (Woolsey, Bignold et al., Ref. 22)

The precise oxygen level required to inhibit erosion-corrosion depends on the local oxygen mass transfer coefficient to the eroding surface and the existing metal loss rate. An upper limit to the amount required for complete inhibition was estimated by calculating the mass transfer rate of oxygen required to balance the ongoing erosion-corrosion rate, according to the following expression:

$$K_{O_2} [O_2] \rho_w = \text{erosion-corrosion rate} \quad (9)$$

where K_{O_2} = local oxygen mass transfer coefficient

$[O_2]$ = concentration of oxygen in solution required to inhibit erosion-corrosion

ρ_w = density of water

Figure 20 shows a plot where the influence of dissolved oxygen on erosion-corrosion rate is indicated on the basis of experimental data obtained at 150°C.⁽²²⁾ Although the theoretical slope for the threshold oxygen concentration derived from Eq. (9) should be 0.285 and the experimental one differs by a factor of 4, the correlation seems to be satisfactory. This diagram is particularly useful to illustrate that substantial differences in erosion-corrosion resistance can be expected among different plants operating under rather similar conditions. Systems operating with nominally deoxygenated feedwater may suffer serious erosion-corrosion problems, while others which are apparently similar, but in reality have slightly higher oxygen content in the feedwater, may not be susceptible to damage.

An additional observation reported by Bignold et al.⁽²²⁾ deserves to be mentioned. They have found that dissolved oxygen inhibits erosion-corrosion and controls the potential of the steel even in the presence of relatively large concentrations of reducing agents, such as N_2H_4 and H_2 , at temperatures up to 250°C. Below this temperature the reduction or scavenging of oxygen by these species is sufficiently slow (particularly at about 150°C) that enough dissolved oxygen is available to inhibit erosion-corrosion. These experiments, as well as others conducted in a full-scale single-tube boiler rig⁽⁴³⁻⁴⁵⁾ have been used as a basis to qualify an oxygen-ammonia-hydrazine feedwater treatment as a remedy for erosion-corrosion problems in British AGR plants. The water chemistry consists of pH = 9.3 water controlled by ammonia, with the addition of 30 $\mu\text{g}/\text{kg}$ N_2H_2 and only 15 $\mu\text{g}/\text{kg}$ O_2 .

Water Impurities and Additives. Most of the reported laboratory work in single-phase erosion-corrosion, both in neutral or ammoniated water, has been conducted with feedwater of very low conductivity ($< 1 \mu\text{S}/\text{cm}$). No attempt has been made to study the effect of anionic impurities such as Cl^- or SO_4^{2-} , which are complexing agents for Fe^{2+} and may affect the magnetite solubility

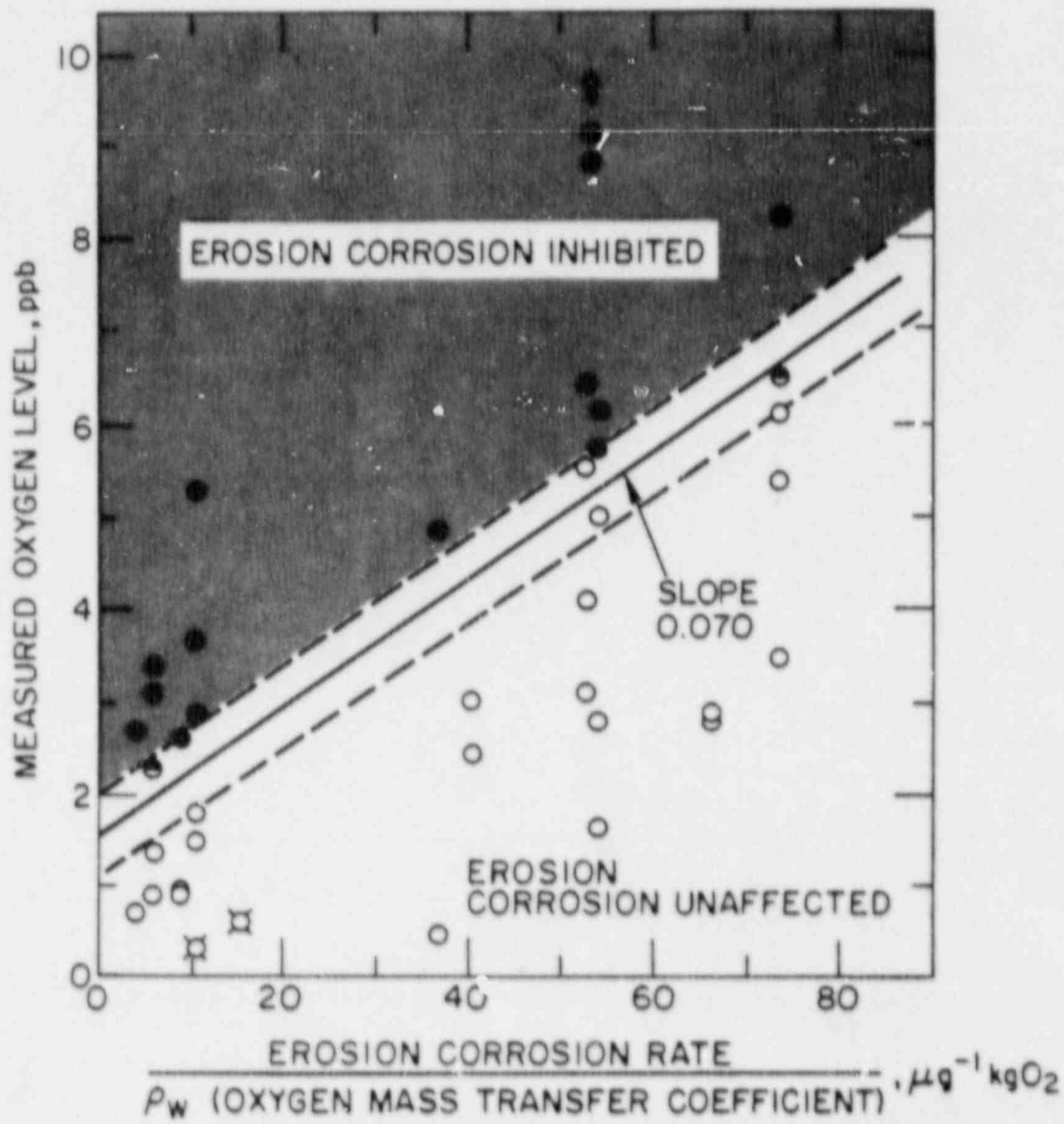


Figure 20. Oxygen concentration required to inhibit erosion-corrosion of mild steel in water at 150°C. Solid symbols, erosion-corrosion inhibited. Open symbols, erosion-corrosion unaffected. Half open symbols, erosion-corrosion slowed or inhibition anticipated in long term. (Woolsey et al., Ref. 22)

as expressed by Eq. (3). According to the accepted concepts for the erosion-corrosion process, any species that tends to displace Eq. (3) to the right may enhance erosion-corrosion rates. This is particularly true for acidic impurities, in particular with neutral feedwater. A particular risk in the case of air in-leakage through condensers arises from the presence of CO_2 . However, CO_2 can be formed also by decomposition of carbonates or other organic impurities. Organic acids, such as acetic acid, are very stable in aqueous solutions even at high temperature⁽⁴⁶⁾ and sufficiently acidic to enhance the dissolution of magnetite. They can be generated by decomposition of organic impurities (humic matter), ion exchange resins, etc. In particular, one of the main disadvantages in the use of morpholine or other amines to replace ammonia is the generation of CO_2 or carboxylic acids as products of their decomposition, with an associated increase in the cation conductivity which may mask small cooling water in-leakages.⁽⁴⁷⁾

Material Factors

Having discussed the role of hydrodynamic and environmental factors on the erosion-corrosion of steels, it is important to emphasize that the chemical composition of the steel has a predominant influence on the resistance to erosion-corrosion in high temperature water or wet steam. Whereas plain carbon steels are extremely susceptible to erosion-corrosion, austenitic stainless steels are essentially immune.⁽⁶⁾

Many authors have reported^(14,15,16,35,36) that the addition of chromium to steels has a profound beneficial effect on the resistance to erosion-corrosion under both single- and two-phase conditions. Even at chromium contents as low as 1 w/o, the erosion-corrosion rate can be reduced in more than one order of magnitude in comparison to plain carbon steel, as shown in Figure 3.⁽²¹⁾ However, in certain plant components these erosion-corrosion rates may still give rise to intolerable levels of soluble iron, and alloys with higher chromium contents (i.e., >2 w/o Cr) should be employed.^(14,15,48)

There are few systematic studies on the effect of alloying elements on erosion-corrosion of carbon and low alloy steels under conditions similar to those encountered in power plants. Although Heitmann et al.^(35,49) have reported data for a variety of commercial steels in high temperature flowing water, as shown in Figures 21 and 22 for the effect of flow velocity and temperature respectively, the separate effect of the main alloying elements cannot be assessed from their results. It is apparent from these figures, however, that low alloy steels with increasing chromium contents are more resistant to erosion-corrosion. At high flow velocities and at the peak temperature, erosion-corrosion rates can be reduced by almost two orders of magnitude by substituting 1 Cr-0.5 Mo steel for carbon steels.

Studies conducted by Huijbregts⁽⁵⁰⁾ using a large number of heats of carbon steels have shown that combinations of relatively small contents of chromium, molybdenum and copper (0.1 w/o) impart better resistance to erosion-corrosion in wet steam than steels deprived of these residual alloying elements. The relative resistance to erosion-corrosion (R) was represented by the following expression obtained by linear regression:

$$R = 0.61 + 2.43 \text{ Cr} + 1.64 \text{ Cu} + 0.3 \text{ Mo} \quad (10)$$

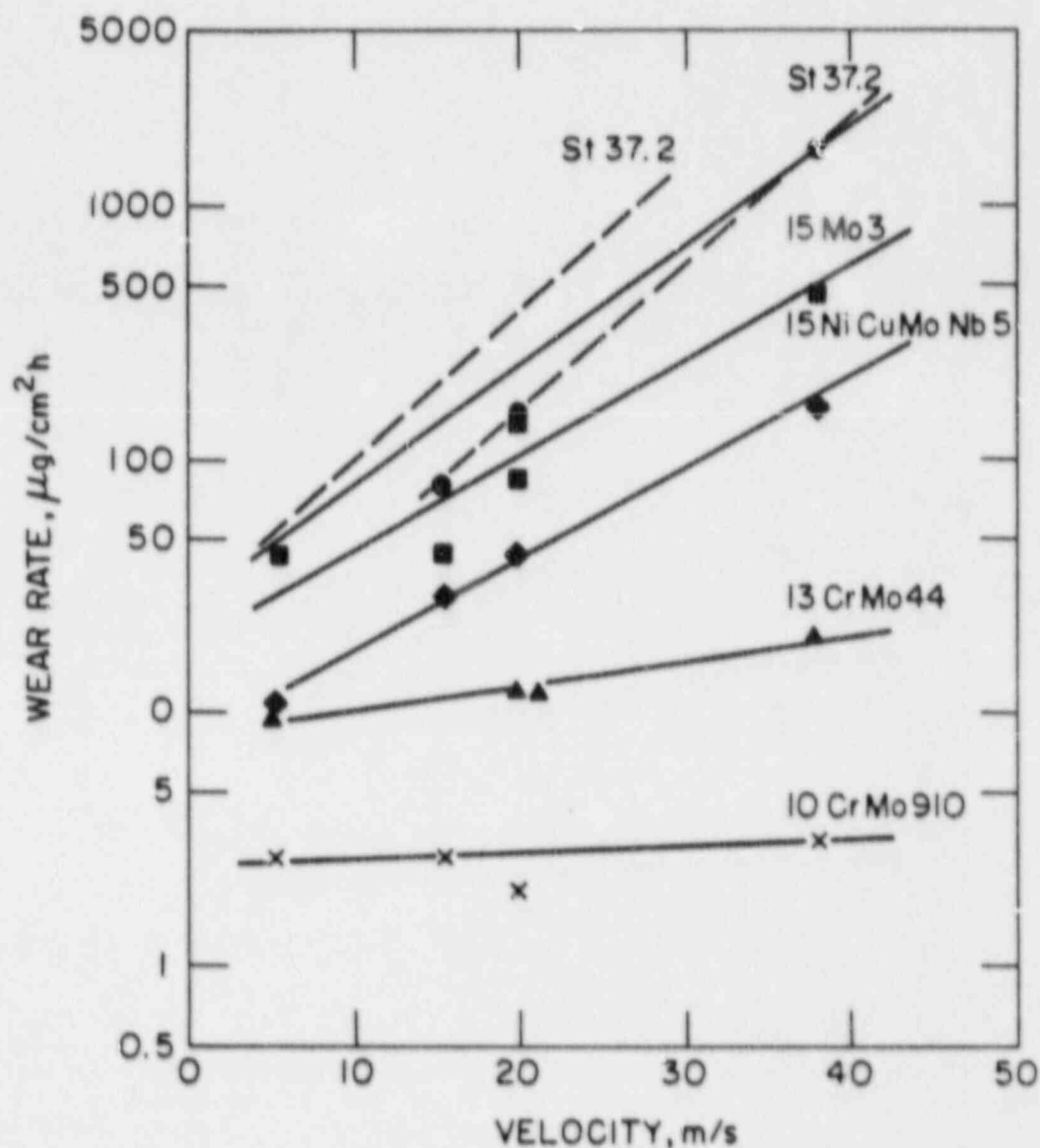


Figure 21. Effect of flow velocity on material wear due to erosion-corrosion in neutral water for various steels. (Heitman and Schub, Ref. 49) Note that St37.2 = A414 GrB (carbon steel); 15Mo3 = A161 GrTI (0.5Mo), 15NiCuMoNb5 = A714 GrVI (0.8Cr-1.1Ni-0.4Mo-0.8Cu), 13CrMo44 = A213 GrT12 (1Cr-0.5Mo) and 10 CrMo910 = A213 Gr T22 (2.2Cr-1Mo).

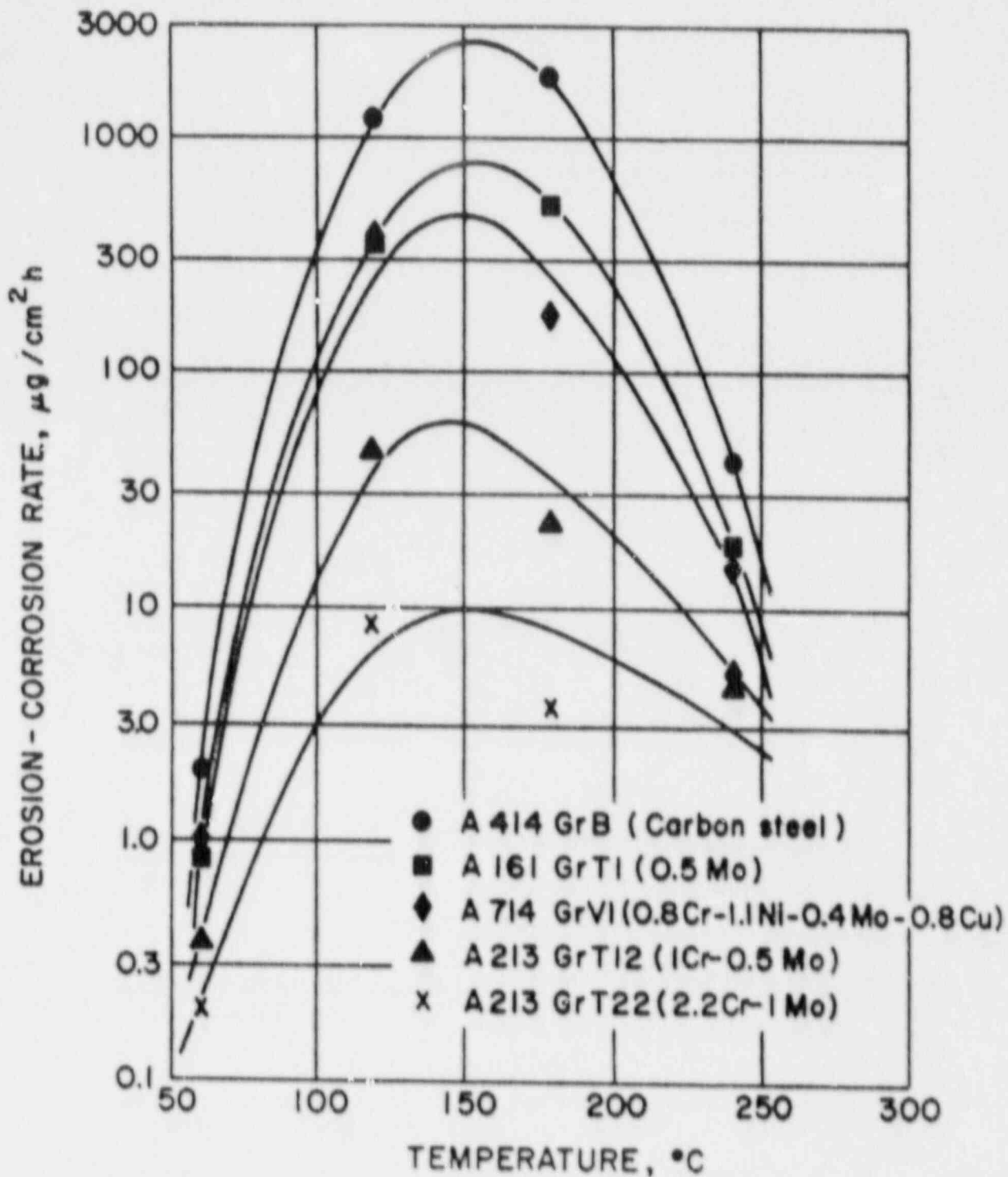


Figure 22. Erosion-corrosion rate vs. temperature for various steels in water. pH=7.0; p=40 bar; flow velocity=35 m/s; $\text{CO}_2 < 40$ ppb (Heitmann and Schub, Ref. 49)

where Cr, Cu and Mo are the weight percentages of these elements in the steel. A confidence level of $r^2 = 0.925$ was calculated for Equation 10 on the basis of tests conducted in high velocity (960 m/s) wet steam (10% water content) at 253°C. However, these results may not be applicable to single-phase flow, because an additional damage process associated with droplet impingement could render susceptible to erosion-corrosion those alloys which are not affected so much by high temperature flowing water.

The remaining systematic study on the effect of alloying elements was conducted by Ducreux.⁽⁵¹⁾ He studied low alloy steels (<2.3% Cr) in water (56 m/s) at 180°C, concluding that chromium is the more influential element. His results are summarized in the form of four equations:

- 1) Assuming that chromium alone confers resistance to erosion-corrosion,

$$R = 0.7 + 32.4 \text{ Cr} ; r^2 = 0.96 \quad (11)$$

$$R = 32 \text{ Cr}^{1.02} ; r^2 = 0.93 \quad (12)$$

- 2) Assuming that chromium, molybdenum and copper are responsible for the resistance to erosion-corrosion,

$$R = 5.2 + 28.9 \text{ Cr} + 51.9 \text{ Cu} + 11.5 \text{ Mo} ; r^2 = 0.98^a \quad (13)$$

$$R = 83.0 \text{ Cr}^{0.89} \text{ Mo}^{0.20} \text{ Cu}^{0.25} ; r^2 = 0.965$$

Although it is difficult to assess the relative value of these equations, there are experimental evidences confirming the dominant role of chromium in improving erosion-corrosion resistance. As shown by Bignold et al.⁽²¹⁾ using XPS to analyze the composition of the oxide film formed on 1 Cr-0.5 Mo steel in high temperature water, selective dissolution of iron promotes the formation of an oxide film highly enriched in chromium. The chromium enrichment was found to be 5 to 10 times that of the metal substrate and even several times higher near the oxide/solution interface. No molybdenum enrichment was observed. These results have been considered by Tomlinson and Ashmore^(37,38) to explain the abnormally high rate of erosion-corrosion observed in plant for carbon steel ferrules as noted before. They have pointed out that the chromium content of the steel ferrules was extremely low (0.006%) in comparison to that used by Bignold et al.⁽²¹⁾ in their studies. In the latter case the residual chromium content of the plain carbon steel was 0.07%. Although they also found a significant chromium enrichment in the oxide film, it was concluded that the chromium content of the steel was still extremely low to confer resistance to erosion-corrosion at 300°C. No similar enrichment was observed for Mo or Cu. From these results it seems that molybdenum contents up to 0.5 w/o without the simultaneous presence of chromium do not offer sufficient protection against erosion-corrosion, as illustrated in Figure 22. The beneficial effect of chromium is understandable in terms of the extremely low solubility of chromium oxide or chromium spinels, $(\text{Fe}_x\text{Cr}_y)\text{FeO}_4$ with $x+y=2$, in high temperature water. Only in those cases in which mechanical effects may affect the integrity of the chromium oxide film can high erosion-corrosion rates be expected for alloys with moderate chromium content (~2%).

4. MODELS OF EROSION-CORROSION

During the last decade several authors^(17,18,25) have developed analytical models based on the qualitative description of the relevant physicochemical processes presented before. In all these models the relevance of mass transport of Fe(II) species away from the oxide/solution interface, as described by Eq. (4), has been considered as one of the controlling factors in determining erosion-corrosion rates. However, there are differences between the various models arising from different assumptions that must be clarified.

1) Model of Berge et al.

According to this model, the erosion-corrosion rate is determined by two coupled processes. One is the dissolution of magnetite according to Eq. (3), assuming that the rate of reaction is given by:

$$dm/dt = 2k (C_{eq} - C) \quad (15)$$

where C_{eq} is the equilibrium concentration of Fe(II) species from Eq. (3) at a given pH and concentration of dissolved H_2 ; C is the true concentration at the interface oxide/solution; k is the rate constant for the chemical reaction, which is assumed to be of 1st order, and the coefficient 2 appears because it is assumed that the rate of corrosion is equal to two times the rate of dissolution of the magnetite.

The second process is the mass transport of soluble Fe(II) species to the bulk, as given by Eq. (4). Therefore,

$$dm/dt = [2kK/(2k+K)](C_{eq} - C_b) \quad (16)$$

This expression can be rearranged to give

$$dm/dt = [K/(1 + K/2k)](C_{eq} - C_b) \quad (17)$$

With the assumption that C_b is negligible, Berge et al.⁽¹⁸⁾ have shown that the rate of erosion-corrosion is proportional to C_{eq} , as calculated from the following equation.

$$C_{eq} = [K_1[H^+]^2 + K_2[H^+] + K_3 + K_4/[H^+]][H_2]_{1/3} \quad (18)$$

Using the Sweeton and Baes data⁽³⁰⁾ for different solution pHs as attained by the addition of NH_3 or morpholine. In addition, as shown in Figure 12, Ducreux⁽²⁴⁾ has found for a limited range of conditions a linear relationship between the erosion-corrosion rate and the mass transport coefficient. According to Eq. (17) this can be expected when $k \gg K$. The observation that $C_b > 0$ has an effect on erosion-corrosion rate and the possible existence of a threshold value for K_c above which erosion-corrosion takes place have been discussed in the context of this model.⁽²⁴⁾

One of the questionable assumptions in this model is the consideration of a first order kinetics for the dissolution of magnetite as a chemical reaction. The possibility of higher orders for this reaction was discussed,⁽¹⁸⁾ but it was concluded that the value adopted agrees reasonably well with the experimental data. Although valid to explain experimental results within a given range of conditions, this model cannot explain the temperature dependence shown, for example, in Figure 14. No quantitative correlations have been provided by the authors of this model.^(18,23,24)

2) Model of Bignold et al.

By considering initially that the erosion-corrosion rate is controlled solely by mass transport, Bignold et al.^(17,19-21) have derived an expression for C, the concentration of Fe(II) species at the oxide/solution interface. They have pointed out that in addition to pH and temperature, the value of C depends on the potential established at the metal oxide/solution interface because the dissolution of magnetite to release ferrous ions is a reductive process. By applying the Nernst equation for the electrode potential to Eq. (3), they have calculated the total ferrous ion concentration as given by

$$C = \sum [\text{Fe(II)}] = ([\text{H}^+]^{2/3} + [\text{H}^+]^{5/3}/K_1 + [\text{H}^+]^{8/3}/K_2) \exp(-2F(E-E_0)/3RT) \quad (19)$$

$$\text{where } K_1 = \frac{[\text{Fe(OH)}_2][\text{H}^+]}{[\text{Fe(OH)}^+]} \quad (20)$$

$$K_2 = \frac{[\text{Fe(OH)}_2][\text{H}^+]^2}{[\text{Fe}^{2+}]} \quad (21)$$

$$\text{or } C = \sum [\text{Fe(II)}] = C_{\text{eq}}^0 [\text{H}^+]^{2/3} \exp(-2FE/3RT) \quad (22)$$

where C_{eq}^0 is the standard solubility of magnetite at 1 bar partial pressure of hydrogen, and E is the electrode potential.

In addition, they have assumed that the hydrogen electrode reaction cannot be in equilibrium on the eroding surface, because typical H_2 concentrations in boiler feedwater will be too low to explain the erosion-corrosion rates. Sufficient hydrogen should evolve locally to depolarize the anodic reaction leading to an enhanced ferrous ion solubility, since the potential of the system could be depressed to a value considerably more negative than that corresponding to the hydrogen equilibrium value. The cathodic current for hydrogen discharge was assumed to vary with potential as follows:

$$i_c = i_0 \exp(-3FE/RT) \quad (23)$$

where B depends on pH according to the accepted hydrogen evolution mechanism. At the corrosion potential $i_a = i_c$, and with the assumption that i_a is entirely determined by mass transport, it follows from Eqs. (4) and (23) that

$$2FK(C-C_b) = FB \exp(-\beta FE/RT) \quad (24)$$

As a result, if C_b is assumed to be negligible and $\beta=1$, the following expression gives the concentration of ferrous ion:

$$C = 4K^2 C_{eq}^3 [H^+]^2 / B^2 \quad (25)$$

$$(dm/dt)_t = 4k^3 C_{eq}^3 [H^+]^2 / B^2 \quad (26)$$

This equation shows that the erosion-corrosion rate depends on the third power of the mass transfer coefficient. This was precisely the behavior observed in experiments carried out in ammoniated water of pH=9.05 at 149°C, as shown in Figure 10. However, as shown in Figure 11, the exponent of the mass transfer coefficient varies with temperature and pH. The decrease of the exponent at temperatures lower than 130°C has been explained by Bignold et al.⁽²⁰⁾ by assuming that activation-controlled film dissolution becomes important in determining the rate of the overall reaction because film dissolution is insufficient to maintain saturation of Fe(II) species at the oxide/solution interface. They suggested that the limiting rate would be expected to vary with temperature according to an Arrhenius relationship of the form.

$$(dm/dt)_k = A \exp(-\Delta G^*/RT) \quad (27)$$

By assuming $\Delta G^* = 67 \text{ kJ/mol}$ (16 kcal/mol) they were able to model the erosion-corrosion rate vs. temperature dependence observed in the rising part of the curves given in Figure 14. They have noted that the preexponential coefficient A in the equation should be pH dependent and also the limitations of Equation 27 because the rate of dissolution under activation control is potential dependent and a more complex expression must be required. Taking into consideration these limitations they indicated, however, that the introduction of the kinetic term $(dm/dt)_k$ will tend to reduce the mass transfer coefficient dependence compared with that predicted for a purely mass transfer limited rate $(dm/dt)_t$ when $(dm/dt)_k$ and $(dm/dt)_t$ are comparable. Other arguments were put forward to discuss the variation in mass transfer dependence and also the displacement of the maximum in the erosion-corrosion rate vs. temperature curves with pH.

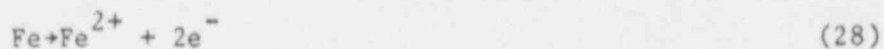
They have modeled the decay in the erosion-corrosion with increasing temperature in terms of mass transfer limitations, taking into consideration the variation in the solubility of magnetic with temperature. However, a

constant value of the exponent of the mass transfer coefficient equal to 3 was assumed, as well as an expression for B, as follows:

$$B = B_0 [H^+]^n \exp(-\Delta G^*/RT) \quad (27)$$

with $\Delta G^* = 20 \text{ kJ/mol}$.

The lack of agreement between the theoretical and experimental value for the exponent of the mass transfer coefficient cast doubts about the real physical validity of their interpretation. Leaving aside this problem, it seems that the qualitative description of some of the critical processes is a significant step forward in the consideration of erosion-corrosion. In particular the relevance of the cathodic reaction and its relation to the potential established at the eroding surface in controlling the erosion-corrosion rate should be emphasized. However, the assumption of a charge transfer coefficient for the hydrogen evolution reaction, $\beta=1$ is questionable. The model predicts that the potential of the surface should shift to more negative values with increasing erosion-corrosion rates. Conversely, by shifting the potential to more positive values, for example by the addition of oxidizing agents such as oxygen, the erosion-corrosion rate should be reduced. In this context, it should be noted that the anodic reaction that counterbalance the cathodic reaction at the corrosion potential is not the dissolution of magnetite according to Equation 3, (this is a reduction reaction) as inadvertently indicated by Ducreux,⁽²⁴⁾ but the overall anodic process



which takes place through the intermediate formation and dissolution of magnetite through oxidation and reduction reactions respectively. It is difficult, however, to envisage the charge transfer processes at both sides of the magnetite layer.

It can be concluded that despite the apparent general validity of this model, there are many uncertainties which precludes a precise prediction of erosion-corrosion rates. In particular, as noted by Bignold et al.⁽²⁰⁾ a full expression for erosion-corrosion rate in the mass transfer limited case is a polynomial of mass transfer and pH dependent terms, rather than the simplified expression given by Equation 26. This must be considered in combination with an expression for the dissolution kinetic limitation, which should be extremely complex because of its dependence on potential and pH.

Model of Sanchez Caldera

The main difference of this model with respect to those discussed above, is that Sanchez Caldera⁽²⁵⁾ considers the reaction producing $\text{Fe}(\text{OH})_2$, Equation 1, as the rate controlling process. By assuming this as a first order

reaction which occurs at the base of the pores in the magnetite film, it follows that:

$$(dm/dt)_1 = k\theta(C_{eq} - C_o) \quad (29)$$

where k is the rate constant, θ the porosity of the oxide, C_{eq} the equilibrium concentration of $Fe(OH)_2$ and C the actual concentration, both at the inner oxide surface.

The second step is the diffusion of ferrous ions through the pores of the oxide. These ions, accounting for one-half of the corroded iron diffuse through the thickness of the oxide,

$$(dm/dt)_2 = 0.5(dm/dt)_1 = (D\theta/L)(C_o - C_1) \quad (30)$$

where L is the oxide thickness, D the diffusion coefficient, and C_1 the concentration at the pore mouth (outer oxide surface). The final step is the removal of the ferrous ions by the connective action of the moving solution.

$$(dm/dt)_3 = (dm/dt)_2 = K\theta(C_1 - C_b) \quad (31)$$

By assuming that $C_b=0$, the set of equations can be solved to give

$$dm/dt = (dm/dt)_1 = C_{eq} \theta / \left[\frac{1}{k} + \frac{1}{2} \left(\frac{L}{D} + \frac{1}{K} \right) \right] \quad (32)$$

One of the important features in the Sanchez Caldera's model is the incorporation of the oxide porosity as a parameter. He assumed that the porosity decreases linearly with increasing temperature above $130^\circ C$. More recently Keck⁽⁵²⁾ has attempted to develop a physical model for the decrease in porosity. He emphasizes the existence of experimental data revealing magnetite porosity and the difficulties associated with the proper consideration of critical variables. Keck considers that porosity decrease is the result of the decrease in the number of pores available for the transport of the ferrous ions through the oxide as a consequence of the localized precipitation of magnetite in specific locations along the pore.

In the Sanchez Caljera's model, as suggested previously by Bignold et al, it was assumed a Arrhenius behavior to compute the effect of temperature on the reaction rate constant k .

This model is more simple than the Bignold's model and has similarities with Berge's model. However, its main difference is that the dissolution process is not associated with the dissolution of magnetite. The concept of reduced porosity with increasing temperature seems well justified and agrees

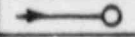
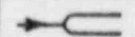

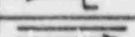
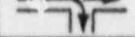
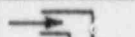
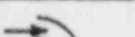

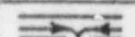
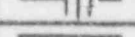

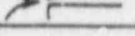


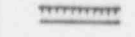
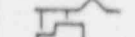
FLOW PATTERN		REFERENCE VELOCITY	K_d	
PRIMARY FLOW STAGNATION POINTS		AT PIPES	1	
		AT BLADES	1	
		AT PLATES	1	
		IN PIPE JUNCTIONS	1	
			0.8	
SECONDARY FLOW STAGNATION POINTS		R/D=0.5	IN ELBOW PIPES	0.7
		R/D=1.5		0.4
		R/D=2.5		0.3
		BEHIND PIPE JOINTS	0.2	
				
STAGNATION POINTS DUE TO VORTEX FORMATION		BEHIND SHARP EDGED ADMISSION PIPES	FLOW VELOCITY	0.2
		AT AND BEHIND BARRIERS		0.2
NO STAGNATION POINTS		IN STRAIGHT PIPES	FLOW VELOCITY	0.04
		IN UNTIGHT HORIZONTAL TURBINE JOINTS	VELOCITY CALCULATED FROM PRESSURE DROP	0.08
COMPLICATED FLOW THROUGH TURBINE PART		IN TURBINE GLAND SEAL	VELOCITY CALCULATED FROM PRESSURE DROP	0.08
		AT AND ABOVE TURBINE BLADES AND AT DRAINAGE COLLECTING WINGS	AVERAGE CIRCUMFERENTIAL BLADE VELOCITY	0.3

Figure 23. Influence of flow path configuration on erosion-corrosion damage under two-phase conditions derived from in-plant experience. (Keller, Ref. 12)

with observations about the protective properties of magnetite at temperatures above 250°C at low hydrogen partial pressures. The limitations again arise from the assumptions made to calculate relevant parameters, such as the reaction rate constant. Modelling is accomplished by fitting to a set of data, but is difficult to use for predictions of erosion-corrosion under different environmental conditions.

Other Models and Predictive Expressions

Whereas a relatively good understanding of erosion-corrosion under single-phase conditions has emerged in recent years as noted above, no theoretical work has been carried out for two-phase flowing conditions, with the exception of some modelling efforts by Sanchez Caldera.⁽²⁵⁾ Keller⁽¹²⁾ has proposed an empirical equation for predicting erosion-corrosion losses from carbon steels, based on observations in wet steam turbines. This has the form

$$S = [f(T) f(x) v K_c] - K_g \quad (33)$$

where S is the maximum local depth of material loss in $\text{mm}/10^4 \text{ h}$, $f(T)$ is a dimensionless coefficient denoting the influence of temperature on erosion-corrosion [a plot of $f(T)$ against temperature has a bell-shape form similar to that shown in Figure 14].

$f(x)$ is a dimensionless coefficient denoting the influence of steam wetness on erosion-corrosion loss. For subcooled water it has been suggested that $f(x) = 1$, but for two-phase mixtures $f(x) = (1-x)^{Kx}$, where x is the steam fraction and $0 < Kx < 1$, being $Kx = 0.5$ the more appropriate value,

v is the fluid velocity in m/s ,

K_c is a variable factor accounting for the effect of local geometry on the fluid flow. Values of K_c in $\text{mm s}/\text{ml}0^4 \text{ h}$ are summarized in Figure 23.

K_g is a constant which the first term in the equation must exceed before erosion-corrosion is observed. A value of $1.0 \text{ mm}/10^4 \text{ h}$ has been adopted by Keller.⁽²⁴⁾

Despite its practical significance Equation 33 does not contain any factor accounting for the influence of water chemistry which may have a dominant effect as discussed above. Nevertheless, the equation can be used as an appropriate guideline to evaluate the effect of various geometries and steam qualities in order to improve existing designs and operating practices.^(16,53)

The factor characterizing the geometry of the component considered has been incorporated to an empirical model, developed by Kastner⁽⁵⁴⁾ to predict metal loss due to erosion-corrosion in high temperature flowing water. This is a completely empirical model based on laboratory data^(35,42) in which the following parameters are considered: flow velocity, temperature, pH, oxygen

content, and chemical composition of the steel in terms only of the chromium and molybdenum contents. Comparison of values calculated from the model with measurements from laboratory experiments and power plants showed a considerable degree of scattering (up to 2 orders of magnitude), but a conservative low limit.

5. SURRY UNIT 2

In December 1986, an 18-inch suction line to the main feedwater pump A for the Surry Unit 2 power plant failed in a catastrophic manner. Four of the eight men working nearby on another pipe were killed during the event.

The condensate feedwater system flows from a 24-inch header to two 18-inch suction lines each of which supplies one of two feedwater pumps. The line temperature at this location is approximately 370°F (188°C), with a pressure of approximately 370 psig and a maximum flow rate of 5 million lb./hr. The fluid in the pipe at this point is considered to be liquid phase with no vapor present.

The following additional information was derived from the BNL failure investigation:

1. The pipe material is ASTM A-106 Grade B carbon steel. The pipe is 18-inch (46cm) diameter with a nominal wall thickness of 0.500 inches (1.27cm).
2. The elbow material is ASTM A-234 Grade WPB carbon steel, also with a nominal wall thickness of 0.500 inches (1.27cm).
3. Localized areas measured on the elbow were thinned to as low as .046 inch (1.17mm).
4. The flow velocity of the header was 12fps (3.05 m/s) while the pipe was 17fps (4.32 m/s).
5. The elbow developed two ruptures. Both ruptures in the elbow were separated by four inches and approximately two inches from the weld.

The BNL failure investigation revealed that the chemical and mechanical properties of the pipe, elbow and weld materials involved in the Surry failure were consistent with the expected properties of the specified materials. The report⁽¹¹⁾ concluded that the overall thinning of the elbow and pipe material at Surry 2 (Figure 24), in addition to the ductile tearing on all of the fracture examined, were a clear indication that the Surry Unit 2 feedwater pipe failed as a result of an erosion-corrosion mechanism under single phase conditions.

At the time of the failure investigation, it was believed that the Surry incident was the first case of single phase erosion-corrosion at a nuclear plant. The next section will reveal that this was not the case.



Figure 24. Photomicrograph of a cross section of the "worn" area near the weld on specimen 1A-4. The thinnest area measured approximately .015 inch (0.38 mm).

6. TROJAN POWER STATION

A review of the literature revealed⁽⁵⁶⁾ that, Surry Unit 2 was not unique in being the first nuclear unit to have a rupture caused by single phase erosion-corrosion. The first event took place at the Trojan Station and is described in part by NUREG/BR-0051 as follows:

"...On the evening of March 9, 1985, the plant was operating at 100% power. Average coolant temperature was 585 degrees F and reactor coolant system (RCS) pressure was 2235 psig. At about 9:50 p.m., a reactor trip occurred from automatic actuation of the reactor protection system, due to a main turbine trip. The turbine trip was caused by a spurious main turbine bearing high vibration signal. The reactor protection system and plant safety systems functioned as designed during the transient. Following the turbine trip, the resulting automatic main feedwater isolation produced a pressure pulse to approximately 875 psig in the heater drain and feedwater systems, as expected. However, the pressure surge caused an eroded section of the 14-inch diameter heater drain pump discharge piping to rupture, resulting in the release of a steam-water mixture of approximately 350 degrees F into the 45-foot (ground-level) elevation of the turbine building. In addition to the fire suppression (deluge) system actuation by heat sensors in the turbine building and damaged secondary plant equipment, one member of the plant operating staff received first and second degree burns on 50% of his body from the high temperature fluid. He was treated at a local hospital for three weeks before being released..."

Discussions with both USNRC Region V personnel and Portland General Electric⁽⁵⁷⁻⁵⁹⁾ (PGE-owner of Trojan) disclosed that a failure investigation was performed by the utility and that the cause of the failure was a single phase (water only) erosion-corrosion phenomenon.

Figure 25 is a photograph of the failed 14 inch diameter pipe from Trojan (Figures 25-28 are PGE supplied photographs of the Trojan failure). The failure occurred very close to a weld (Figure 26) on the pipe.

Figure 4 is a photograph of the eroded inside surface of the pipe on the wall opposite the failure. A "scalloped" surface typical of erosion-corrosion was seen on the inside surface of the pipe (Figure 28).

Table 1 is a listing of both, the chemical and mechanical property data from the failed piping at Trojan. It is evident from the table that the chemical and mechanical properties of SA 106 Gr.B material were satisfied. The table also shows that the alloying content of the failed pipe (Cr, Ni, C) were very low - .02%. These elements have been shown⁽⁶⁾ to reduce the propensity of erosion-corrosion attack if they are present in sufficient concentration.

The failure investigation also documented that the microstructure of the pipe material was normal for A 106 Gr.B material. This failure was considered by the utility to be caused by erosion-corrosion in a single phase system (450 psig and 350°F, with a bulk flow rate of 20-24 fps). This being the case, the Surry Unit was actually the second instance of this type of accelerated attack which appears to make the problem potentially generic.



Figure 25. Photograph of the failed 14 inch diameter pipe from the Trojan Station.

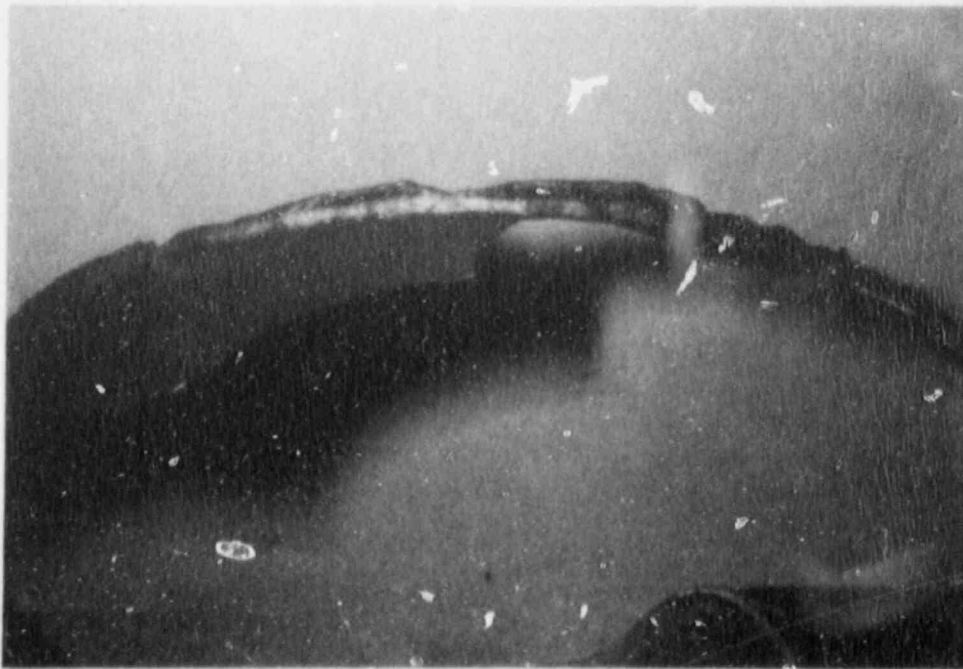


Figure 26. Close-up photograph of the weld area adjacent to the failure.

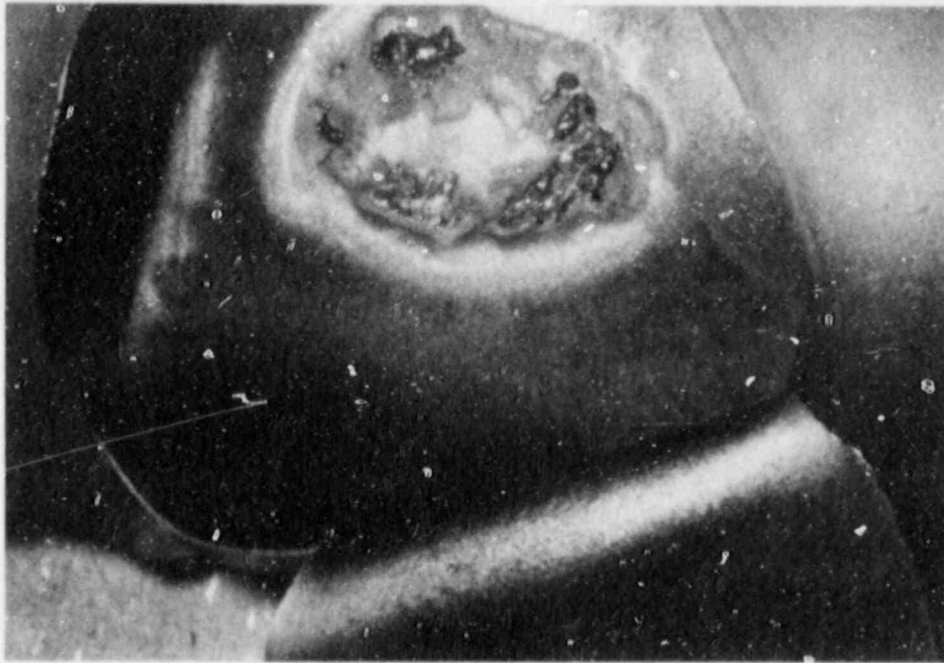


Figure 27. Photograph of eroded area on back side of pipe (opposite failed area).

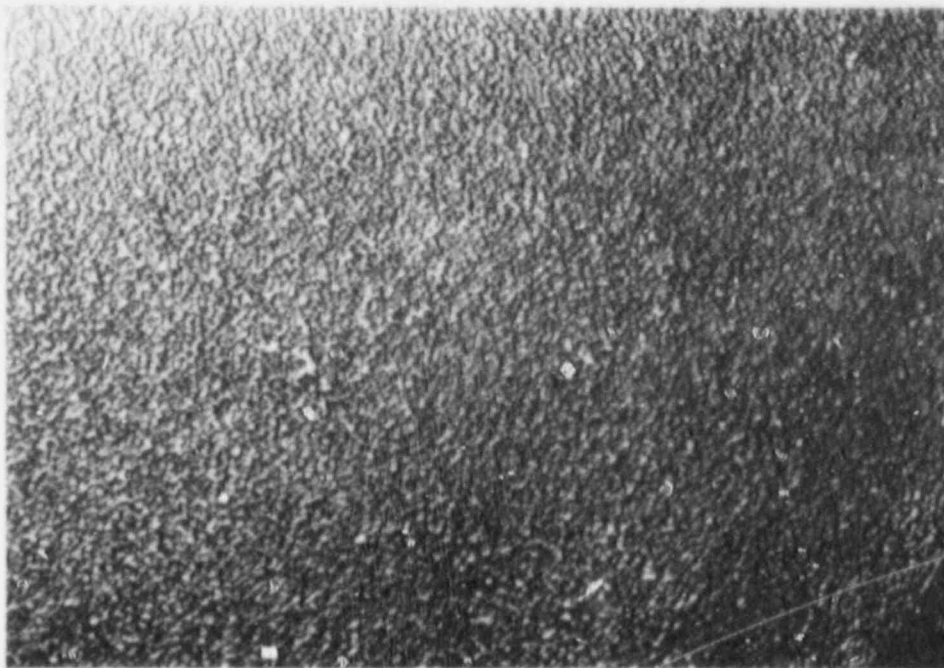


Figure 28. Photograph of inside surface of Trojan piping showing scalloping (typical of erosion-corrosion).

Table 1

Chemical and Mechanical Property
Data From Trojan Failure

Chemical Analysis		SA 106 Grade B Req.
C	0.24 w/o	0.30 max
Mn	0.80 w/o	0.29-1.06
Si	0.22 w/o	0.10 min
S	0.018 w/o	0.058 max
P	0.005 w/o	0.048 max
Cu	0.021 w/o	
Ni	0.02	
Cr	0.02	
Mo	0.003	
V	0.02	
Al	0.025	

<u>Mechanical Properties</u>	
Hardness:	Rb 75.2
UTS (estimated):	66 ksi
YS (estimated):	37 ksi

<u>ASTM Grain Size:</u>	7-8	Base Material
	10	WHAZ

7. HADDAM NECK FEEDWATER LINE RUPTURE AND TOLEDO EDISON SEMINAR

Seven days after the Trojan incident, a pipe failed at the Haddam Neck plant by an erosion-corrosion mechanism. The literature⁽⁵⁶⁾ reference describes the event in part:

"On March 16, 1985, a steam leak was discovered at Haddam Neck while the plant was operating at 100% power. The reactor and turbine were manually tripped due to the possibility of grounding the steam generator feed pump motor(s) and/or heater drain pump motor(s). After tripping the plant, one steam generator feed pump was shut down and the auxiliary steam generator feed pumps were started to ensure their availability. Condenser vacuum was lost due to air leaking through the turbine seals. The atmospheric steam dump valve was then used to control primary side pressure and temperature. Automatic initiation of auxiliary feedwater flow occurred due to low level in two steam generators. The cause of this event was a pipe rupture immediately downstream of the 1B feedwater heater normal level control valve. The eroded section of the pipe was replaced..."

Discussions with utility personnel⁽⁶⁰⁾ revealed that the failure occurred in 6 inch diameter 301 carbon steel piping and that the burst in the pipe measured approximately 1/2 inch by 2 1/4 inch in size. Although no formal failure analysis was performed by the utility, the following information was disclosed from the discussions:

1. The failure occurred near a camflex valve,
2. The operating conditions of the line were: pressure-220 psia, temperature-390°F, bulk velocity-7.34 fps.

These operating temperature and pressure conditions place this occurrence directly at the equilibrium point (water + steam 220.8 psi, 390.2°F) and although the incident was probably a two phase phenomenon (the utility suspected cavitation) it is reported here due to the conditions close proximity to equilibrium.

Table 2 is a partial listing of erosion-corrosion problems experienced by various utilities. This information was presented at an Erosion/Corrosion Seminar sponsored by Toledo Edison Co. on March 19-20, 1986. This list evidences the fact that virtually all (notable exceptions being Surry 2 and Trojan) of the erosion-corrosion problems experienced by nuclear utilities have occurred in two phase (water + steam) systems. This observation has been substantiated by an EPRI⁽⁶¹⁾ review of single phase erosion-corrosion. So, although the problem may be generic in nature it has not been widespread to date.

An observation made at this seminar as well as in reviewing the various I&E data is that of the overall utility response to the problem (after Surry). Virtually all the utilities listed have initiated or augmented inspection programs to diagnose potential problems before they become critical.

Table 2

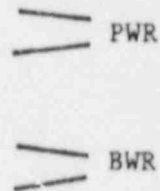
Erosion-Corrosion Problems Experience

Toledo Edison

MSR to Condenser (Drains, Large and Small)
Reheat Steam Line to Aux Boiler
Aux Boiler Sparger
O.T.S.G. Blow Down Line to Condenser
H.P. F.W. Heater to Deareator Heater

NYP&A

Cross Over/Cross Under Lines
Cold Reheat
Extraction Line to LP Heater (M.C. 10%)
Feedwater Discharge Line to LP Heaters



Baltimore Gas & Electric

Extraction Steam from Cold Reheat
Third Stage Extraction to the HP Feedwater Heater
MSR Drains
First Stage MSR Drain Tank to FW Heater
Steam Generator Blowdown (2, 4, 6, inch lines)
FW Recirc Lines
HP Feedwater Heater Drain to Fifth FWH

WPPSS

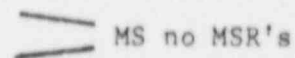
Aux Boiler Problems

Duquesne Power

No Piping Problems (Beaver Valley)
MSR
Cold Reheat

OPPD

Extraction HP Turbine Lines
Extraction Drain from LP Turbine (2")



8. ULTRASONIC MEASUREMENTS OF TWO SURRY UNIT 2 SPECIMENS

Two pieces from the Surry 2 failure investigation were subjected to examination ultrasonically ("D" meter-longitudinal wave and 45° shear wave). These specimens numbered 4A-1 and 4A-2⁽¹¹⁾ were cut from the weld joint between the fabricated tee joint and the header from Surry Unit 2 (Figure 29). Both of these specimens had significant erosion damage on the inside surface of the pipe adjacent to the weld (Figure 30).

Both of these specimens had a grid pattern stencilled on the outside surface of the pipe and were subjected to ultrasonic thickness measurements in addition to physical (caliper) measurements. A pictorial representation of the grid pattern and associated measurements are seen in Figures 31 and 32. The number on top of each "fraction" corresponds to the "D" meter measurement while the "denominator" is the actual caliper measurement. (Note--the angle beam technique elicited no decipherable response.) These figures do show that a difference is noted between even calibrated equipment and actual thickness measurements.

One point worthy of note is the importance of the grid spacing used when making field measurements as shown in areas 12, 15, and 16 in specimen 4A-2. The figure clearly shows that in a very small area (≈3 inches) the ultrasonic measurements can show a difference of .164 inch. This difference of thickness (approximately one third of the original .500 inch thickness) may not have been revealed if a larger (3, 4, 6 inch) grid pattern had been utilized.

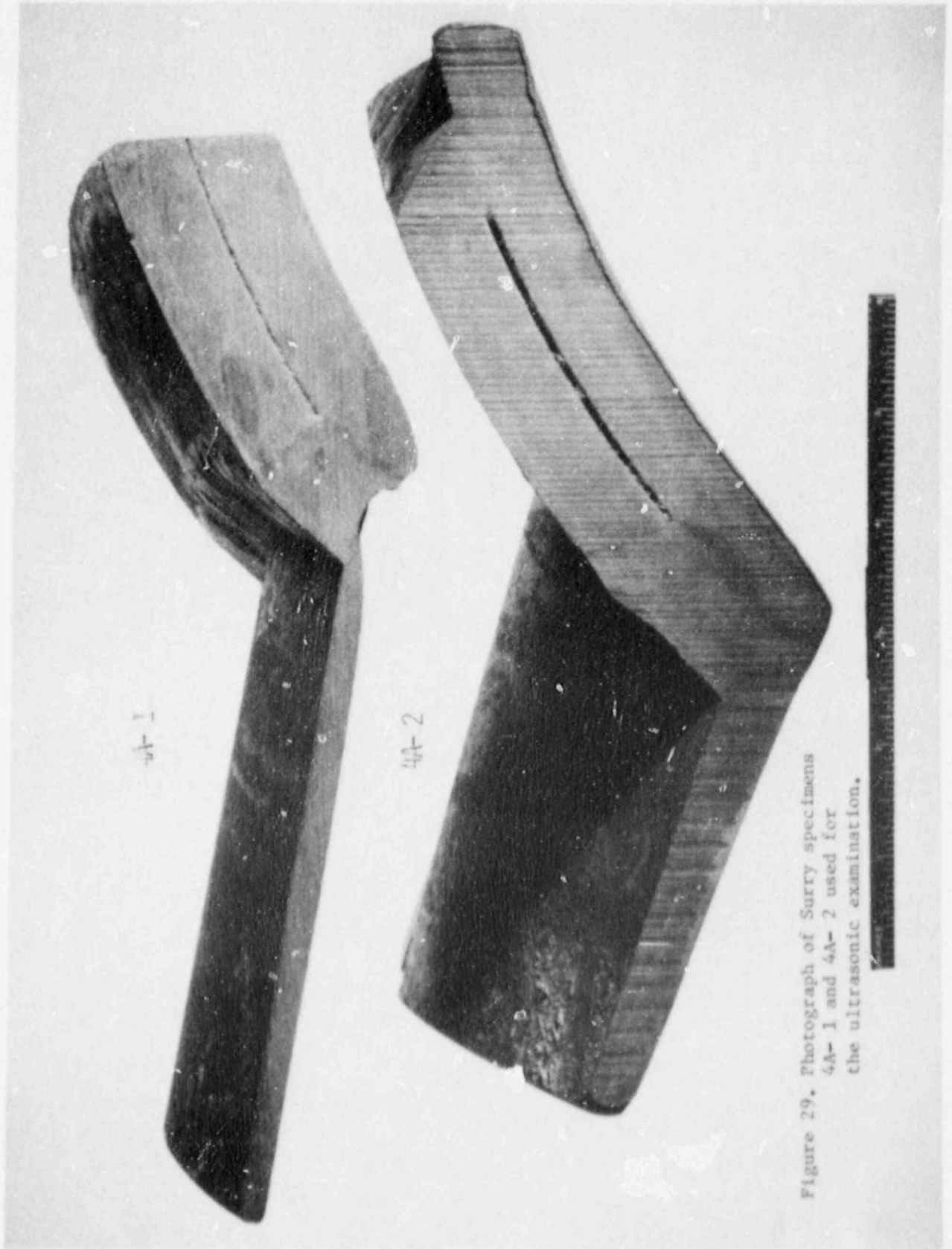


Figure 29. Photograph of Surry specimens 4A-1 and 4A-2 used for the ultrasonic examination.

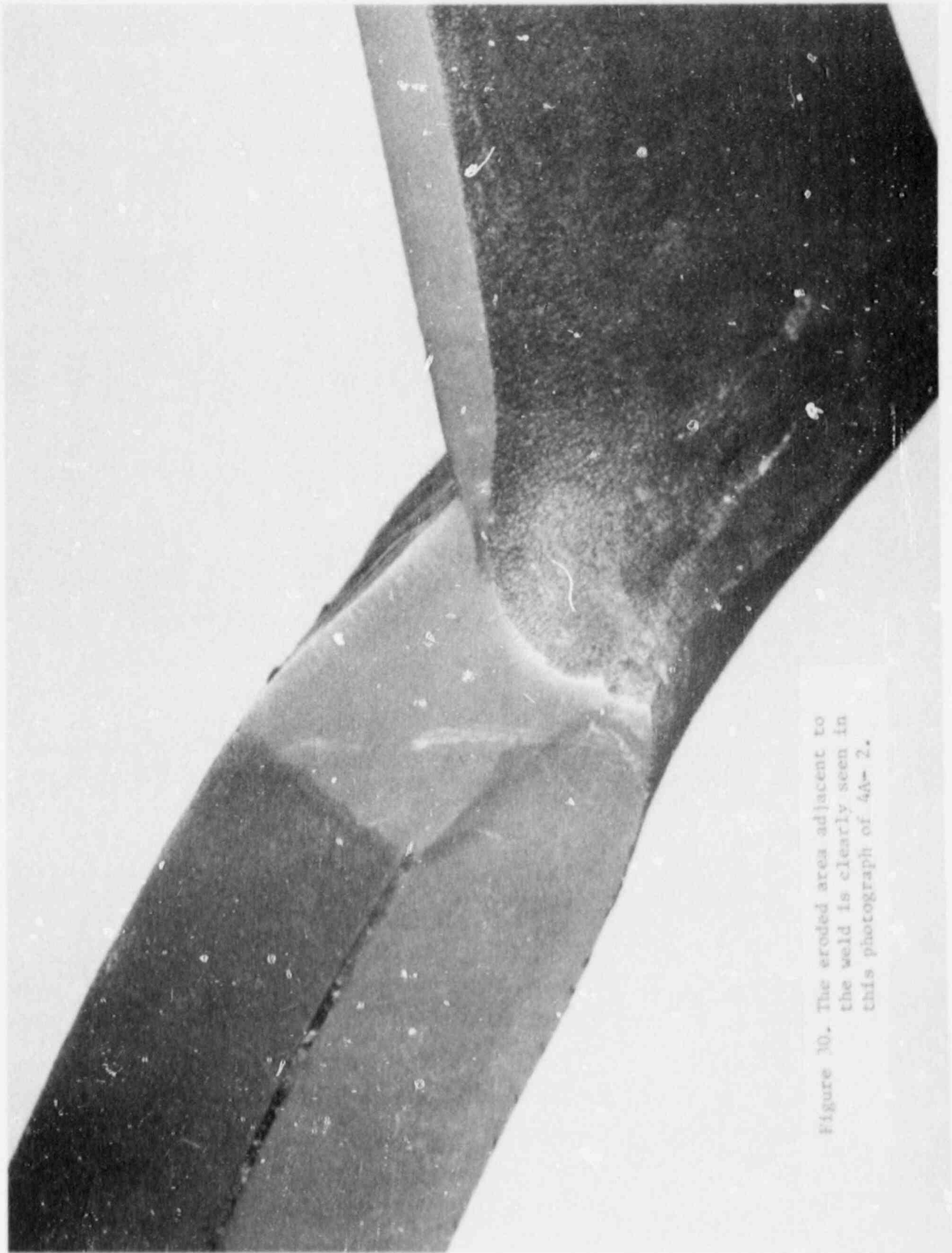


Figure 10. The eroded area adjacent to the weld is clearly seen in this photograph of 4A-2.

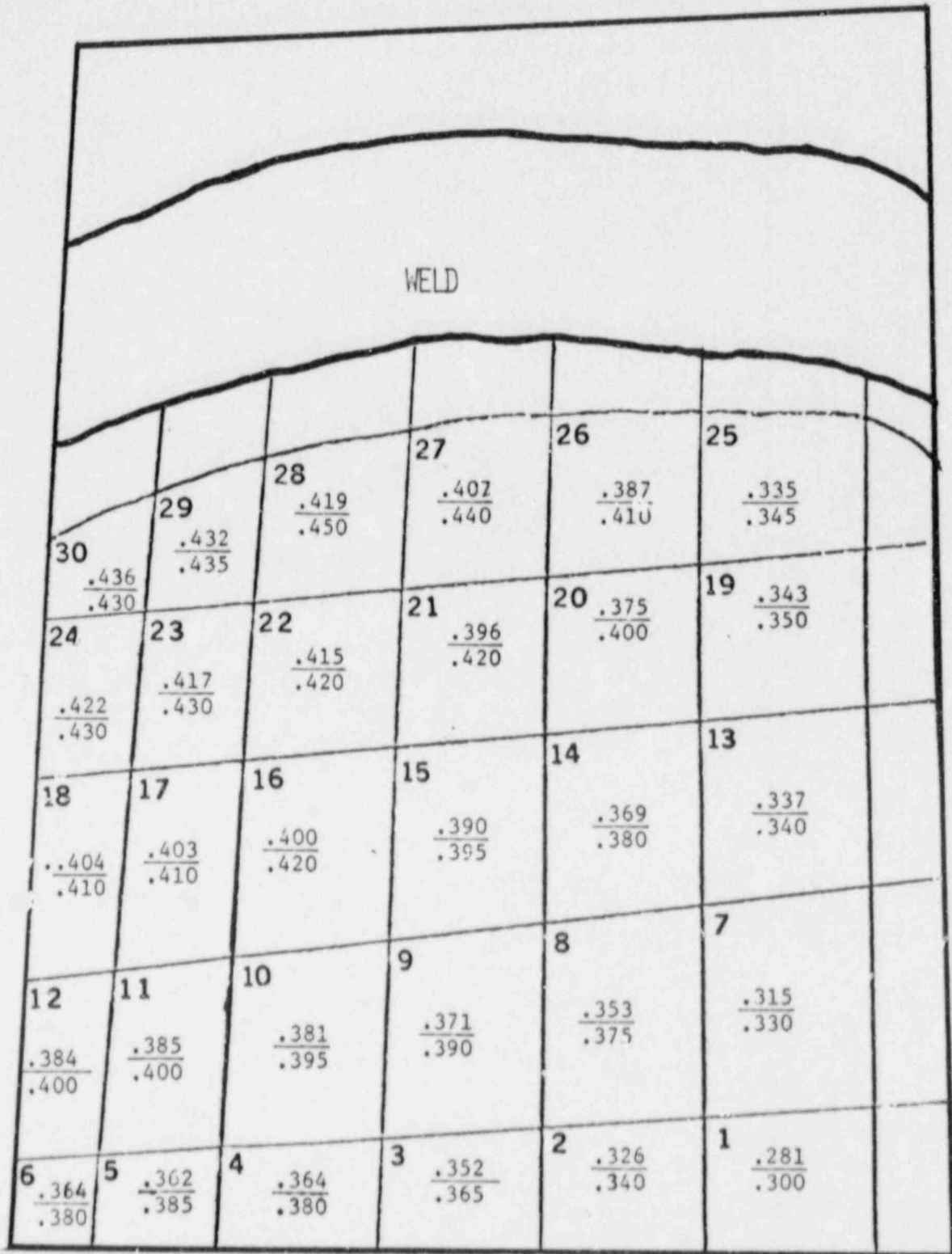


Figure 31. Sketch of the grid pattern used for the examination of specimen 4A- 1.

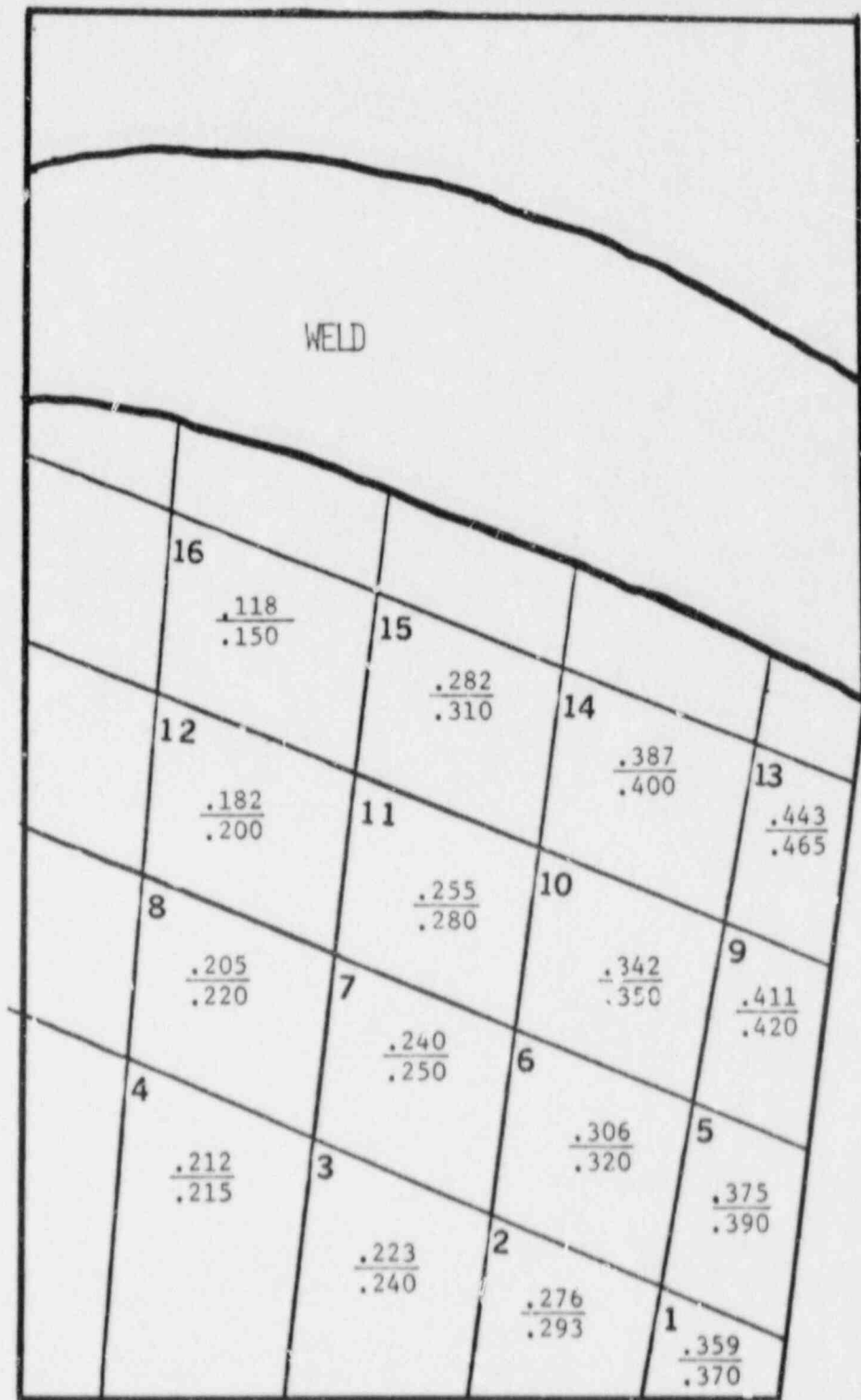


Figure 32. Sketch of the grid pattern used for the ultrasonic examination of specimen 4A- 2.

9. CONCLUSIONS

From the available literature, which has been almost completely covered in this review, it can be concluded that a qualitative assessment of the major influential factors in erosion-corrosion of carbon steel in high temperature flowing water is now complete. However, there are many discrepancies in the experimental results when studies conducted by different authors are compared. Furthermore, as the recent observations of Tomlinson and Ashmore^(37,38) show, erosion-corrosion could be extremely severe even at temperatures above 250°C. Several years ago Berge and Kahn⁽⁵⁵⁾ noted that the commonly accepted statement that erosion-corrosion does not occur beyond 200°C should be considered cautiously. In this regard it seems that differences between results of different authors could be assigned to the presence of residual elements that are not properly identified. In most of the studies on erosion-corrosion it is uncommon to have a full description of the chemical composition of the steel. As discussed, before, residual amounts of elements such as chromium may have a strong beneficial effect.

For these reasons, the most effective counter measure against erosion-corrosion is the choice of sufficiently resistant materials. In most of the applications under single phase conditions, low alloy steels containing 2% Cr seem to be a cost effective solution if modifications in design to reduce flow rates and local turbulences are difficult to implement. Under two-phase flow (wet steam) more highly alloyed materials are needed.

Under particular conditions, modifications in the water chemistry by rising the pH or by adding oxygen to the feedwater may be extremely effective to inhibit erosion-corrosion damage, as suggested by the experience in the U.K. and West Germany. In this case again, these types of countermeasures are more successful under single phase conditions.

Regarding the modelling efforts, it can be concluded that the prediction of accurate erosion-corrosion rates on the basis of laboratory data is still very limited. These models are capable of metal loss predictions within the range of data on which they are based. It should be noted, however, that small variations in the environmental conditions (dissolved oxygen concentrations varying in the range of few ppb, or presence of acidic impurities) may lead to unsuspectedly high rates of erosion-corrosion under certain circumstances. These variables, plus significant variations in the rate of mass transfer at specific locations may be the source of very large differences in erosion-corrosion rates from plant to plant, from component to component and in particular for different locations in the same component, even though no substantial changes in the overall hydrodynamic conditions could be suspected.

10. REFERENCES

1. "Water Chemistry and Corrosion in the Steam-Water Loops of Nuclear Power Stations," Conference ADERP, Electricite de France, Seillac, France, March 1980.
2. "Corrosion-Erosion of Steels in High Temperature Water and Wet Steam," Electricite de France, Ph. Berge and F. Kahn (ed), Les Renardieres, France, May 1982.
3. Water Chemistry of Nuclear Reactor Systems 2, British Nuclear Energy Society, London, 1981.
4. Water Chemistry of Nuclear Reactor Systems 3, Vol. 1 and 2, British Nuclear Energy Society, London, 1983.
5. Water Chemistry of Nuclear Reactor Systems 4, British Nuclear Energy Society, London, to be published. (Reprints from the Conference held in 1986 are available.)
6. G. Cragnolino, "Erosion-Corrosion in Nuclear Power Systems-An Overview," CORROSION/'87, NACE, Houston, Texas, 1987, Paper No. 86.
7. J. A. Beavers, A. K. Agrawal and W. E. Berry, "Corrosion-Related Failures in Feedwater Heaters," EPRI CS-3184, Electric Power Research Institute, Palo Alto, CA, July 1983.
8. L. Chanudeit, "Generateurs de Vapeur Chauffes au Gaz Carbonique dans les Centrales Nucleaires Francaises," Ref. 1.
9. G. J. Bignold, K. Garbett, R. Garnsey and I. S. Woolsey, Nuclear Engineering International, June 1931, p. 37.
10. J. M. Delplanque and L. Mougey, "Difficultes Reencontrees en Centrales E.D.F. Recherches Experimentales," Ref. 1.
11. C. J. Czajkowski, "Metallurgical Evaluation of an 18-Inch Feedwater Line Failure at the Surry Unit 2 Power Station," NUREG/CR-4868, Brookhaven National Laboratory, March 1987.
12. H. Keller, VGB, Kraftwerkstechnik, 54, No. 5, 292, (1974).
13. G. A. Delp, J. D. Robison and M. T. Sedlack, "Erosion-Corrosion in Nuclear Plant Steam Piping: Causes and Inspection Program Guidelines," EPRI NP-3944, Electric Power Research Institute, Palo Alto, CA, April 1985.
14. E. Kunze and J. Nowak, Werkstoffe und Korrosion, 33, 262, (1982).
15. R. Svoboda and G. Faber, "Erosion-Corrosion of Steam Turbine Components," Corrosion in Power Generating Equipment, M. O. Speidel and A. Atrens, eds., Plenum Press, New York, p. 269, 1984.

16. J. P. Cerdan, J. Gregoire and L. Lacaille, "Erosion-Corrosion in Wet Steam-Impacts of Variables and Possible Remedies," Ref. 1.
17. G. J. Bignold, K. Garbett, R. Garnsey and I. S. Woolsey, "Erosion Corrosion in Nuclear Steam Generators," Ref. 3, p. 5.
18. Ph. Berge, J. Ducreaux and P. Saint-Paul, "Effects of Chemistry on Erosion-Corrosion of Steels in Water and Wet Steam," Ref. 3, p. 19.
19. G. J. Bignold, C. H. de Whalley, K. Garbett, R. Garnsey, I. S. Woolsey, D. F. Libaert and R. Sale, Proc. 8th Int. Congress Metallic Corrosion, DECHEMA, West Germany, 1981, Vol. II, p. 1548.
20. G. J. Bignold, K. Garbett and I. S. Woolsey, Ref. 2, Paper No. 12.
21. G. J. Bignold, C. H. de Whalley, K. Garbett and I. S. Woolsey, Ref. 4, p. 219.
22. I. S. Woolsey, G. J. Bignold, C. H. de Whalley and K. Garbett, Ref. 5, p. 337.
23. J. Ducreaux, Ref. 2, Paper No. 14.
24. J. Ducreaux, Ref. 4, p. 227.
25. L. E. Sandrez Caldera, "The Mechanism of Corrosion-Erosion in Steam Extraction Lines of Power Stations," Ph.D. Thesis, Massachusetts Institute of Technology, 1984.
26. H. W. Townsed, Jr., Corrosion Sci., 10, 343 (1970).
27. P. R. Tremaine and J. C. LeBlanc, J. Soln. Chem., 9, 415 (1980).
28. E. G. Brush and W. L. Pearl, Corrosion, 28, 129 (1972).
29. L. Tomlinson, Corrosion, 37, 591 (1981).
30. F. H. Sweeton and C. F. Baes, Jr., J. Chem. Thermodynamics, 2, 479 (1970).
31. J. F. Gulich, D. Florjancic and E. Muller, "L'Erosion-Corrosion dans les Pompes d'alimentation et d'extraction. Recherches et Choix des Materiaux," Ref. 1.
32. B. Poulson, Corrosion Sci., 23, 391 (1983).
33. M. W. E. Coney, "Erosion-Corrosion: The Calculation of Mass Transfer Coefficients," CERL RD/L/N 197/80 Central Electricity Research Laboratories, Leatherhead, UK, November 1980.

34. F. P. Herber and K. F. F. L. Hue, *Int. J. Heat Mass Transfer*, 20, 1185 (1977).
35. V. H. Heitmann and W. Kastner, *VGB Kraftwerkstechnik*, 62, No. 3, 211 (1982).
36. M. Izumiya, A. Minato, F. Hataya, K. Ohsumi, Y. Ohshima and S. Ueda, "Corrosion and/or Erosion in BWR Plants and Their Countermeasures," Water Chemistry and Corrosion Products in Nuclear Power Plants, International Atomic Energy Agency, Vienna, Austria, 1983, p. 61.
37. L. Tomlinson and C. B. Ashmore, Ref. 5, p. 195.
38. L. Tomlinson and C. B. Ashmore, *Br. Corros. J.*, 22, 45 (1987).
39. W. R. Apblett, *Proc. Am. Power Conf.*, 29, 751 (1967).
40. R. K. Freier, *VGB Speisewassertagung*, 1969, p. 11.
41. P. H. Effertz, *Der Maschinenschaden*, 53, No. 6, 217 (1980).
42. W. Kaestner, K. Riedle and H. Tratz, *VGB Kraftwerkstechnik*, 64, No. 4, 411 (1984).
43. K. Tittle, P. W. Tasker and D. S. Eyre, Ref. 4, p. 253.
44. D. Penfold, G. S. Harrison, G. M. Gill, J. C. Greene and M. A. Walker, *Nucl. Energy*, 25, 257 (1986).
45. A. J. Bates, G. J. Bignold, K. Garbett, W. R. Middleton, D. Penfold, K. Tittle and I. S. Woolsey, *Nucl. Energy*, 25, 361 (1986).
46. G. Cragolino and T. Christman, *CORROSION/86*, NACE, Houston, Texas, Paper No. 86.
47. J. Garaud, Ref. 2, Paper No. 9.
48. R. Svoboda, G. Ziffermayer, S. Romanelli, H. G. Seipp and W. Kaufman, Ref. 4, p. 261.
49. H. Heitmann and P. Schub, Ref. 4, p. 243.
50. W. M. M. Huijbregts, *Materials Performance*, 23, No. 10, 39 (1984).
51. J. Ducreux, Ref. 2, Paper No. 19.
52. R. G. Keck, "Prediction and Mitigation of Erosive-Corrosive Wear in Steam Extraction Piping System," Ph.D. Thesis, Massachusetts Institute of Technology, 1987.

53. J. Marceau, "Erosion Corrosion by Wet Steam-Design Choices, Sizing, Materials, Manufacturing," Ref. 1.
54. W. Kastner, "An Empirical Model for Calculating Metal Loss Due to Erosion Corrosion," KWU Report R5/V6/R7/R73/, Kraftwerk Union AG, Erlangen, November 1986.
55. Ph. Berge and F. Khan, "Summary and Conclusions of the Meeting," Ref. 2.
56. "Power Reactor Events," USNRC, NUREG/BR-0051.
57. Telecon, C. Czajkowski, Region V, USNRC, May 1987.
58. Telecon, C. Czajkowski, R. C. Rupe (PGE), May 1987.
59. Telecon, C. Czajkowski, J. W. Carter (PGE), May 1987.
60. Telecon, C. Czajkowski, T. Trainor (Yankee Atomic), May 1987.
61. Jones, R., et al., EPRI Final Report, "Single-Phase Erosion-Corrosion of Carbon Steel Piping," February 19, 1987.

II. EROSION-CORROSION IN SINGLE-PHASE FLOWS (W. J. Shack)

1. Introduction

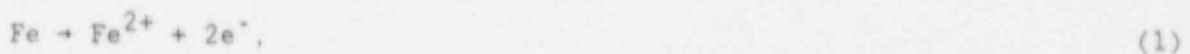
A substantial body of data and experience is available on erosion-corrosion in environments characteristic of secondary water systems in nuclear reactors.¹⁻¹³ In the U.S. attention was focussed on the problem by the catastrophic failure involving loss of life that occurred at the Surry Unit 2 in December 1986. The inspections triggered by this event have revealed numerous instances of significant erosion-corrosion at other U.S. reactors, primarily in wet-steam lines, but also in some single-phase lines. Although erosion-corrosion occurs most frequently in wet-steam systems,⁸ German data files for the period 1961 to 1976 show that one-third of the 96 cases reported were for single-phase conditions.¹⁴ Most of the available experimental data are based on tests under single-phase conditions.

There is fairly general agreement^{1,3,4,9} that the basic process of erosion-corrosion is an accelerated dissolution of the corrosion film caused by the enhanced mass transfer associated with turbulent flows. Mechanisms of erosion-corrosion caused by removal of the protective oxide by mechanical impact of particulate matter or droplets (somewhat analogous to raindrop erosion of aircraft windshields) have also been proposed.^{9,10} However, in most cases levels of suspended solids in nuclear reactor systems are very low, and examination of surfaces where erosion-corrosion has occurred shows no evidence of mechanical damage in the underlying material.^{9,11} Even in two-phase flows, erosion-corrosion is associated with wet steam rather than dry steam, which suggests that the presence of a liquid film is critical to the process. The strong dependence on pH and dissolved oxygen content of the two-phase, wet-steam case is also consistent with a dissolution process.

Temperature, pH, dissolved oxygen level, alloy content, and flow velocity have been shown to have significant effects on the erosion-corrosion rate.¹⁻⁹ However, although the qualitative changes in the erosion-corrosion rates expected with changes in these variables are reasonably well understood and materials that are highly resistant to erosion-corrosion are available for replacement or new construction, quantitative predictions of erosion-corrosion rates in existing carbon steel piping systems are subject to large uncertainties.

2. Phenomenology of the Erosion-Corrosion Process

In the deoxygenated solutions characteristic of typical secondary systems, the dissolution of iron,



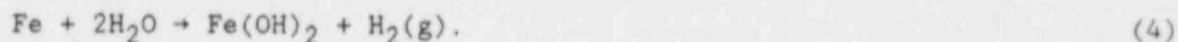
is accompanied by hydrogen evolution,



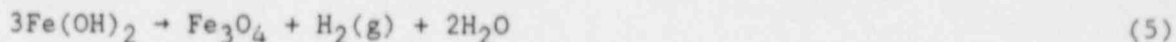
The ferrous ions then react with OH^{-} ions to form insoluble ferrous hydroxide,



The net corrosion reaction is then

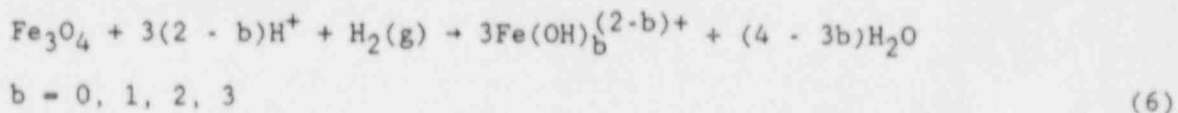


At the temperatures associated with the secondary systems of power plants, the insoluble ferrous hydroxide decomposes to form magnetite according to the Schikorr reaction:



The stability of this magnetite film controls the erosion-corrosion process.

Sweeton and Baes¹⁵ have shown that the dissolution rate of magnetite is a strong function of temperature, pH, and partial pressure of H_2 . Four soluble ferrous species are formed: Fe^{2+} , FeO^+ , $\text{Fe}(\text{OH})_2$, and $\text{Fe}(\text{OH})_3^-$. The general dissolution reaction is



The equilibrium concentration of soluble ferrous species can be expressed in terms of the equilibrium constant for this reaction, K_b , which is a function of temperature, the pH of the solution (or H^+ concentration), and the dissolved H_2 concentration.¹⁵ The solubility may be significantly increased locally by the hydrogen generated by the local corrosion processes [i.e., Eqs. (2) and (5)]. Turbulent flow of the bulk fluid accelerates the corrosion process by removing the soluble corrosion products.

A number of models of the basic physical processes involved in the accelerated dissolution have been proposed.^{1,4,12,13} Berge et al.¹² considered both the mass transport process and the dissolution process. Both processes are assumed to be governed by first-order equations. The mass transport equation is

$$\dot{m} = k(C - C_b) \quad (7)$$

where \dot{m} is the rate of loss of material, k is the mass transfer coefficient, C is the concentration of iron in solution at the oxide-solution interface, and C_b is the concentration of iron in the bulk solution. The equation for the rate of dissolution of the magnetite is

$$\dot{m} = k_c(C_{eq} - C) \quad (8)$$

where k_c is the dissolution rate constant and C_{eq} is the equilibrium concentration of iron in solution under the given environmental conditions. Eliminating C from Eqs. (8) and (9) then gives

$$\dot{m} = \frac{k \cdot k_c}{k + k_c} (C_{eq} - C_b) \quad (9)$$

The relative magnitudes of k and k_c indicate whether mass transfer or dissolution of the film is the rate-limiting process.

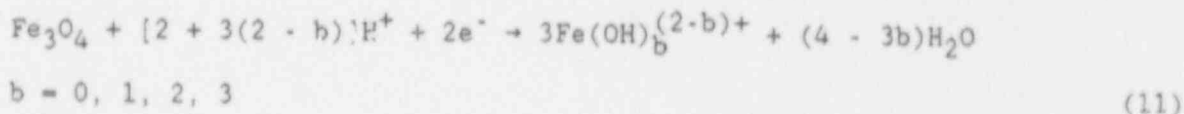
Sanchez-Caldera¹³ considers the formation of ferrous hydroxide [Eqs. (1)-(4)] at the metal-oxide interface to be the rate-limiting corrosion process, rather than the dissolution reaction [Eq. (6)] at the oxide-water interface. Since the formation of ferrous hydroxide can only occur where water can reach the inner surface, this model also includes the effects of oxide porosity and diffusion of the ferrous ions from the metal-oxide interface to the oxide-fluid interface. The resulting equation is similar in form to that of Berge et al.,¹²

$$\dot{m} = \left[\frac{2Dk k_f}{2Dk + k_f k L + k_f D} \right] \theta (C_{eq} - C_b) \quad (10)$$

but it now includes a diffusivity D for transport from the metal-oxide interface to the oxide-fluid interface, the oxide thickness L , and an oxide porosity factor θ . In addition, the reaction rate constant k_f now refers to a reaction occurring at the metal-oxide interface rather than at the oxide-solution interface.

Quantitative estimates of the dissolution rate constants k_c or k_f are difficult to obtain, although Sanchez-Caldera¹³ provides some data. In addition, the equilibrium concentration C_{eq} is a strong function of the hydrogen concentration. Because the hydrogen arises primarily from local corrosion processes, quantitative estimates of the concentration are difficult to make.

Bignold et al.¹ assume that the dissolution process is limited by the rate of mass transfer from the eroding surface and not by the dissolution process itself; in this case the erosion-corrosion rate \dot{m} is controlled solely by the transport process, Eq. (7). They note that the dissolution reaction Eq. (6) is the result of a reductive dissolution process



In Reference 1 the only soluble species considered is Fe^{2+} ; this corresponds to $b = 2$ in Eq. (6), and the appropriate Nernst equation is

$$E = E^0 - \frac{RT}{2F} \ln \left(\frac{[\text{Fe}(\text{OH})_2]^3}{[\text{H}^+]^2} \right) \quad (12)$$

where $[]$ denotes the activity (concentration) of the species involved, F is the Faraday constant, T is the absolute temperature, and R is the gas constant. Equation (12), together with Eq. (2) and the ionization reaction for water, gives

$$[\text{Fe}^{2+}] = \frac{[\text{H}^+]^{8/3}}{K_2} \exp \left(\frac{-2F(E - E^0)}{3RT} \right) \quad (13)$$

where

$$K_2 = \frac{[\text{Fe}(\text{OH})_2][\text{H}^+]^2}{[\text{Fe}^{2+}]}$$

Thus K_2 can be determined in terms of the equilibrium constants for the ionization of water and Eq. (3). The cathodic current i_c corresponding to hydrogen discharge at the surface of the magnetite film is assumed to vary exponentially with the potential,

$$i_c = -FB \exp\left(\frac{-\beta FE}{RT}\right) \quad (14)$$

where B and β are constants, and the corresponding anodic current i_a is assumed to be limited by the rate of removal of Fe^{2+} ions; i. e., i_a is proportional to the mass transfer rate [Eq. (6)]. Charge balance then requires

$$2Fk [\text{Fe}^{2+}] \cdot C_b = FB \exp\left(\frac{-\beta FE^0}{RT}\right) \quad (15)$$

If the bulk concentration C_b is much less than the local concentration and $\beta = 1$, then

$$[\text{Fe}^{2+}] = \frac{4k^2 [\text{H}^+]^8}{K_2^3 \cdot B^2} \exp\left(\frac{2FE^0}{RT}\right) \quad (16)$$

The solubility of the magnetite (in terms of Fe^{2+}) is thus dependent on the square of the mass transfer coefficient k ; Eq. (8) then implies that the overall dependence of the erosion-corrosion rate depends on k^3 . In Reference 4 this analysis is extended to consider all soluble species; the overall erosion-corrosion rate varies as k^3 plus additional terms k^2 and k . Although the phenomenological models of Berge et al.¹² and Sanchez-Caldera¹³ provide qualitative understanding of the relative roles of dissolution and mass transfer, only the model of Bignold et al.¹⁴ gives a result, the predicted dependence on k^3 can be readily tested by experiments. Because of the inherent complexity of the fundamental processes, most applications are based on phenomenological models; these will be discussed after the available data are reviewed.

3. Effect of Flow Velocity on Erosion-Corrosion Rates

Since the enhanced mass transfer associated with turbulent flows is the fundamental process in the accelerated dissolution of the magnetite corrosion film, the effect of the flow is best described in terms of the mass transfer coefficient k , which is a function of the flow velocity and geometry. For the flow conditions generally found in PWR secondary-system feedwater piping, typical values of k are $1-3 \text{ mm}\cdot\text{s}^{-1}$.

Correlations between the mass transfer coefficient and flow velocity and geometry are available for a variety of configurations.¹⁶ However, these

correlations give an average value of k and generally are based on the assumption of a fully developed flow. In real flows k may vary significantly over the component and may depend strongly on disturbances introduced upstream. The correlations are commonly expressed in terms of the nondimensional Sherwood number

$$Sh = kd/D \quad (17)$$

where d is the diameter of the pipe and D is the diffusion coefficient of iron in water. The Sherwood number is a measure of the relative contributions of turbulent mixing and molecular diffusion to the transport process. In reactor piping systems, Sh is very large, i.e., turbulent mixing dominates the transport processes.

For a straight pipe,¹ Sh is given by

$$Sh = 0.0165 Re^{0.86} Sc^{0.33} \quad (18)$$

where Re is the Reynolds number and Sc is the Schmidt number. The Reynolds number is

$$Re = \frac{Vd}{\nu} \quad (19)$$

where V is the velocity and ν the kinematic viscosity, and the Schmidt number is

$$Sc = \frac{\mu}{D} \quad (20)$$

In the analogous heat transfer situation, the groups denoted here as the Sherwood and Schmidt numbers are referred to as the Nusselt and Prandtl numbers.

The increased turbulence associated with changes in flow geometry increases the effective Sherwood number over that for the straight pipe. Figure 1 shows the relative increase in Nusselt number associated with a variety of tube inlet geometries;¹⁷ these results suggest that k can be 2-3 times higher than the value calculated for a straight pipe with the same nominal flow conditions. In some situations, even higher effective k values can probably be achieved. Inlet geometries are probably more severe than elbow geometries, where k values are 1.5-2 times higher than those for the straight pipe.¹⁸

The correlation for the mass transfer coefficient, Eq. (18), is valid only for single-phase flows. Transfer coefficients for two-phase flows are generally higher than those for single-phase flows with the same mass flow rate, because the reduction in the average density corresponds to higher velocities. Very little information is available for two-phase flows, and estimates must be obtained by analogy with corresponding heat transfer correlations¹⁹ or by estimates of the liquid film velocity.^{19,20}

As noted in Section 2, the model developed by Bignold et al.¹ suggests that the corrosion-corrosion rate is proportional to k^3 . The data shown in Figure 2 are in good agreement with this model at k values above a threshold of $1 \text{ mm}\cdot\text{s}^{-1}$. However, the data shown in Figs. 3 and 4 indicate that the

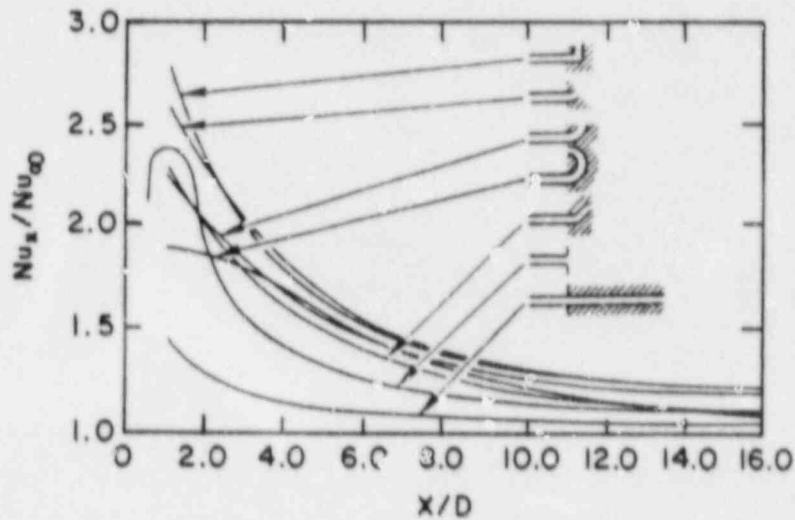


Fig. 1. Measured Nusselt numbers in the inlet region of a circular tube for various inlet configurations (from Reference 17).

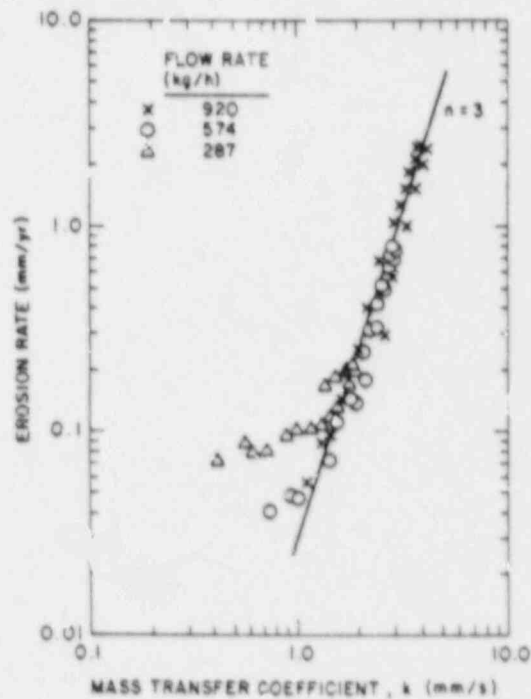


Fig. 2. Correlation of erosion-corrosion rate with the mass transfer coefficient (from Reference 1).

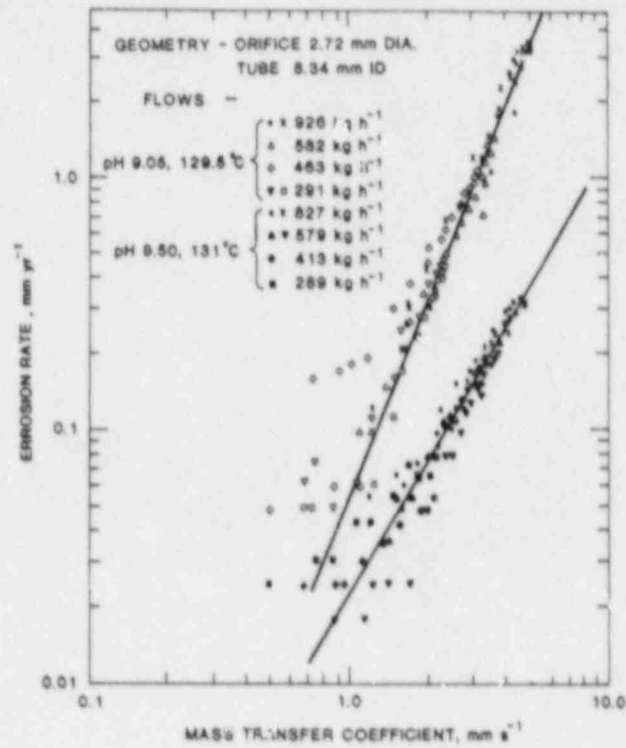


Fig. 3. Dependence of the exponent of the mass transfer coefficient on temperature for pH=9.05 (from Reference 5).

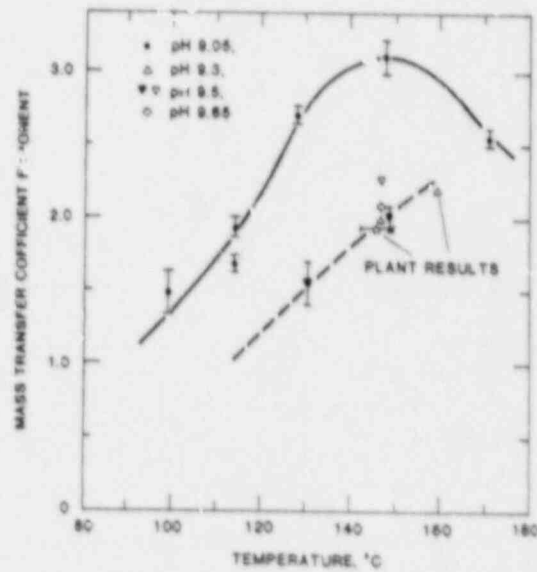


Fig. 4. Effect of pH on the variation of erosion-corrosion rates with the mass transfer coefficient (from Reference 5).

exponent n describing the k dependence is a function of temperature and pH.⁵ At higher temperatures the measured n varies between 2.5 and 3.3; i.e., n is close to 3. At lower temperatures n decreases, and at 99°C, n is 1.4. Bignold et al.⁴ argue that at lower temperatures or higher pH, the dissolution rates of the magnetite may become comparable to the mass transfer rates, which were assumed to be rate limiting in the development of the model; hence the apparent dependence on k diminishes.

The results of Ducreux,³ which are shown in Figs. 5-7, indicate that for k values above a threshold ($>5 \text{ mm}\cdot\text{s}^{-1}$) the erosion-corrosion rate depends linearly on k (Fig. 5). At lower values ($1-5 \text{ mm}\cdot\text{s}^{-1}$), which are more typical of feedwater piping systems (Figs. 6 and 7), the corrosion rate shows a nonlinear dependence on k . Analysis of these data suggests that in the nonlinear regime $n \approx 2.5$, which is close to the values reported by Bignold et al.^{1,4} for these environments, although the flow geometry used by Ducreux³ is very different from that used by Bignold. Additional data,²¹ which were obtained by using the same test loop but a different test geometry, are shown in Fig. 8. In this case the measured exponents range from 1.4 to 1.7 even for relatively low k values; in contrast the data of Bignold et al.⁵ would suggest that $k \approx 2.2$ for these environments.

Data for the dependence of the erosion-corrosion rate on velocity are also presented in Reference 2 and shown in Figs. 9 and 10. The velocities in these studies are high ($5-40 \text{ m}\cdot\text{s}^{-1}$); the values of the corresponding mass transfer coefficients are not given, but they seem likely to be high. Analysis of these data shows that for carbon steel with pH 7 the erosion-corrosion rate varies as $V^{1.3}$; with pH 9 the rate varies as $V^{1.6}$. Since only two velocities are reported, comparisons with the data of Bignold et al.,^{1,4} Ducreux,³ and Bouchacort²¹ are uncertain.

The exponent n describing the dependence of the erosion-corrosion rate on the mass transfer coefficient is clearly a function of temperature, pH, and flow rate (k). Even for a restricted set of conditions characteristic of secondary-system feedwater piping in PWRs (pH ≈ 9 , $T \approx 150-200^\circ\text{C}$, low oxygen, velocities of $10-15 \text{ ft}\cdot\text{s}^{-1}$ corresponding to $k \approx 0.75-3 \text{ mm}\cdot\text{s}^{-1}$), a fairly wide range of values of n (1-3) has been reported. The values obtained by using orifice test geometries^{1,4,5} tend to be higher than those obtained by using other test geometries. A strong dependence on k is intuitively appealing and seems consistent with field experience. Entire piping systems do not dissolve away; damage is concentrated at locations with high local turbulence corresponding to relatively high values of k .

4. Effect of Temperature on Erosion-Corrosion Rates

Data on the effect of temperature are reported in References 1, 2, 3, and 4 and shown in Figs. 11-13. [The data from Reference 1 are actually for two-phase wet-steam flow. The data from Reference 2 are for pH of 7 and high velocity ($35 \text{ m}\cdot\text{s}^{-1}$).] Qualitatively there is good agreement between the reported data. The erosion-corrosion rates drop off markedly at high and low temperatures with a strong peak at intermediate temperatures. However, there are considerable differences in the values obtained for the temperature at which the maximum rate occurs and in the temperature range for which erosion-corrosion rates are significant.

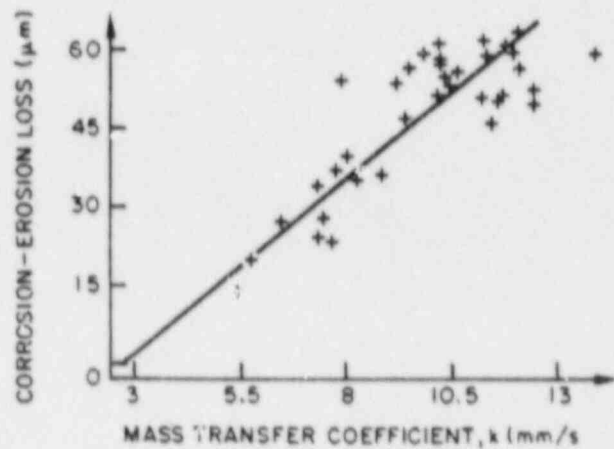


Fig. 5. Correlation of erosion-corrosion rate with mass transfer coefficient at pH=9, 180°C for a high mass transfer coefficient (from Reference 3).

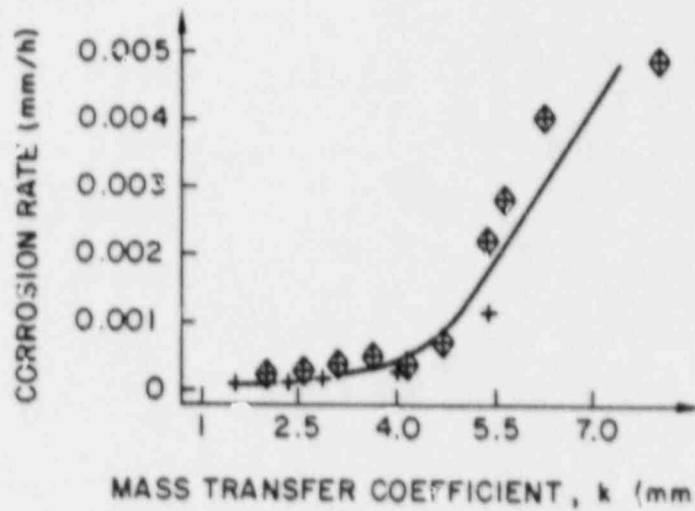


Fig. 6. Correlation of erosion-corrosion rate with mass transfer coefficient at pH=9, 180°C for a low mass transfer coefficient (from Reference 3).

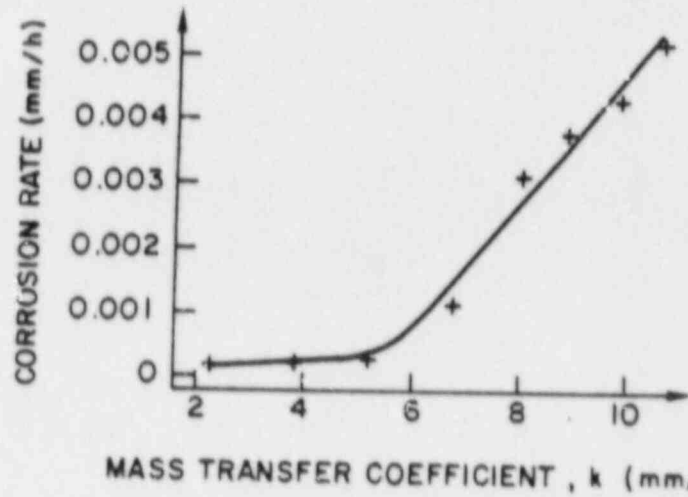


Fig. 7. Correlation of erosion-corrosion rate with mass transfer coefficient at pH=9, 210°C for a low mass transfer coefficient (from Reference 3).

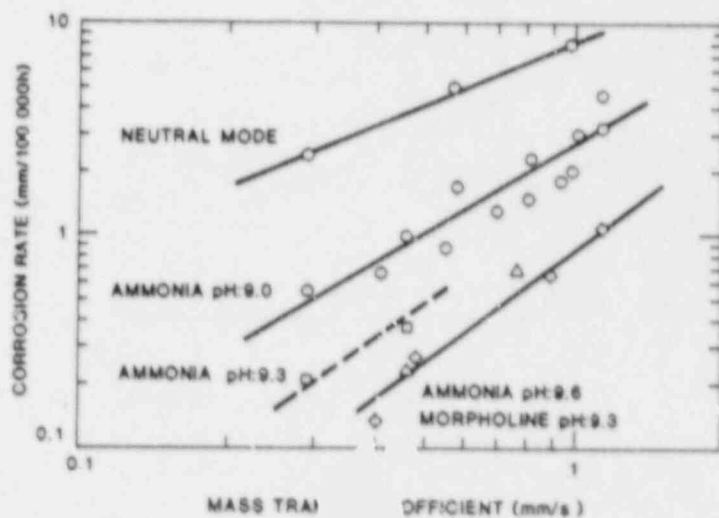


Fig. 8. Effect of mass transfer coefficient on erosion-corrosion rates in neutral and alkaline environments at 180°C (from Reference 21).

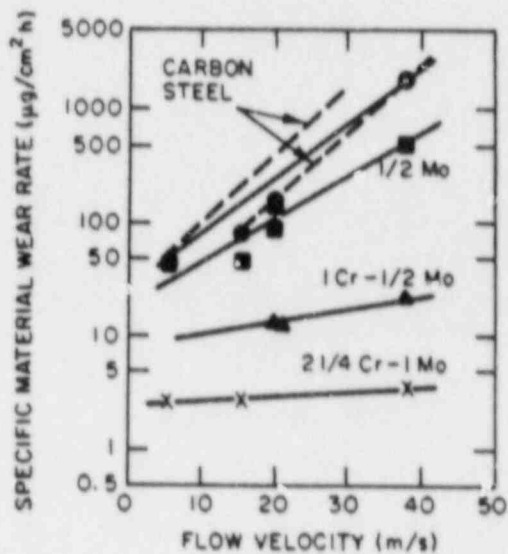


Fig. 9. Effect of flow velocity on erosion-corrosion rate in near neutral environments (pH=7) (from Reference 2).

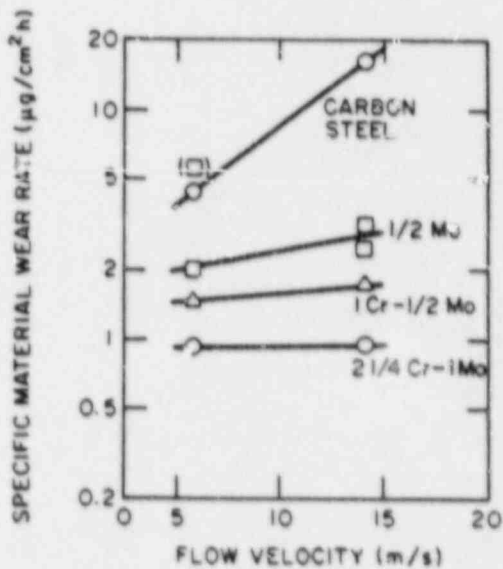


Fig. 10. Effect of flow velocity on erosion-corrosion rate in an environment with pH=9 (from Reference 2).

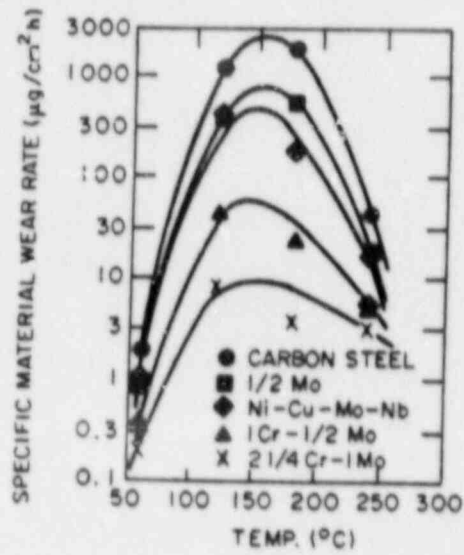


Fig. 11. Effect of temperature and alloy content on erosion-corrosion in pH=7 environment (from Reference 2).

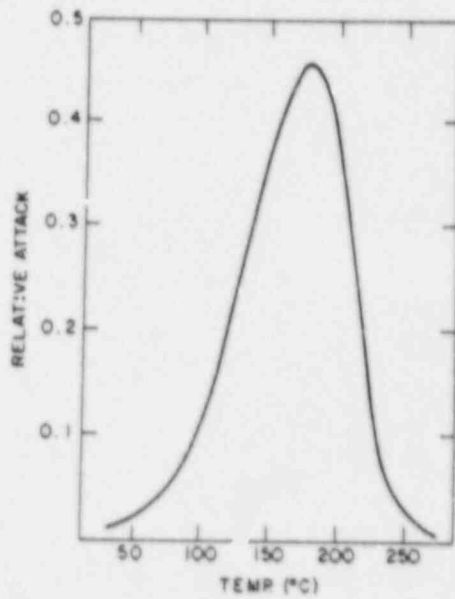


Fig. 12. Temperature effect on erosion-corrosion in pH=9 environment for two-phase wet-steam flow (from Reference 1).

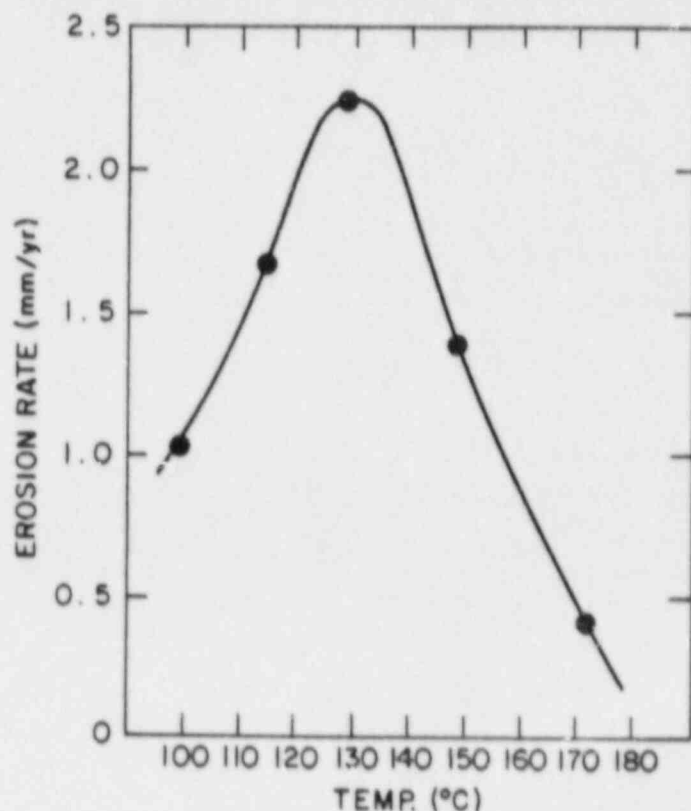


Fig. 13. Temperature effect on erosion-corrosion in pH=9 environment (from Reference 4).

In Fig. 14 the data from References 1, 2, and 4 are replotted in terms of a normalized erosion-corrosion rate (erosion-corrosion rate/maximum rate) to facilitate comparison. The temperatures at which the maximum rates occur range from ≈ 130 to 175°C . The data reported in Reference 4 show a much lower temperature for the maximum rate, and the rate decreases much more rapidly with increasing temperature than the rate from References 1 and 2. This may be due to the difference in environments. However, the data of Ducreux,³ which are shown in Figs. 6 and 7 and were obtained for environmental conditions and mass transfer rates similar to those in Reference 4, indicate relatively high erosion-corrosion rates and a decrease in rates between 180 and 210°C a factor of ≈ 2 . The temperature dependence inferred from these data is closer to that given in References 1 and 2 than that in Reference 4. The reasons for the differences in the data are unclear; Bignold et al.²² have suggested that they may be due to the higher chromium content ($\approx 0.1\%$) of the materials used in these studies. A "best guess" empirical fit for the temperature dependence based on all the available data is shown in Fig. 15.

Several mechanistic explanations for the observed temperature dependence have been proposed.^{4,9,13} Bignold et al.⁴ suggest that the decrease at high temperatures is due to the decrease in the solubility of magnetite with increasing temperature,¹⁵ while at lower temperatures dissolution is kinetically limited, although the equilibrium solubility is high. Keck⁹ and Sanchez-Caldera¹³ also attribute the decrease at low temperatures to a decrease in the kinetics of the dissolution reaction, but they attribute the rapid decrease at higher temperatures to changes in the porosity of the oxide

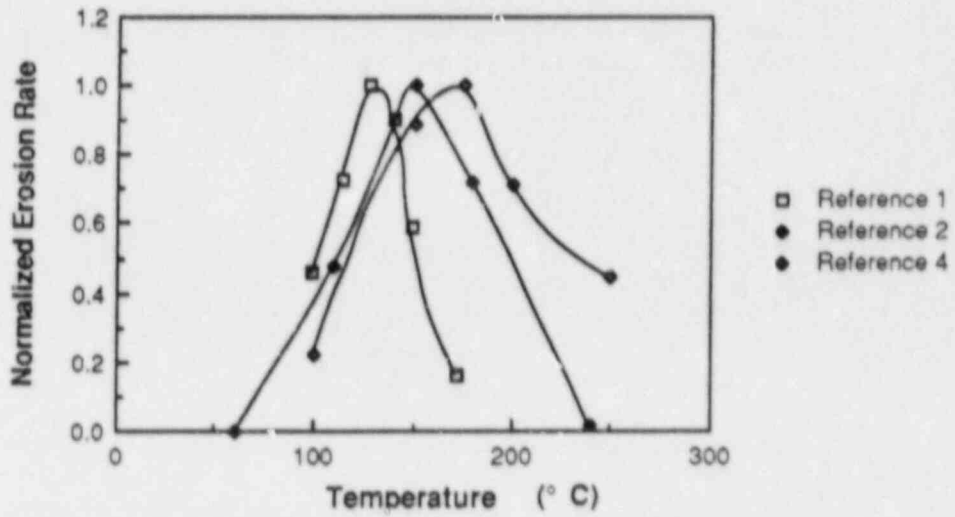


Fig. 14. Effect of temperature on normalized erosion-corrosion rates based on data from References 1, 2, and 4.

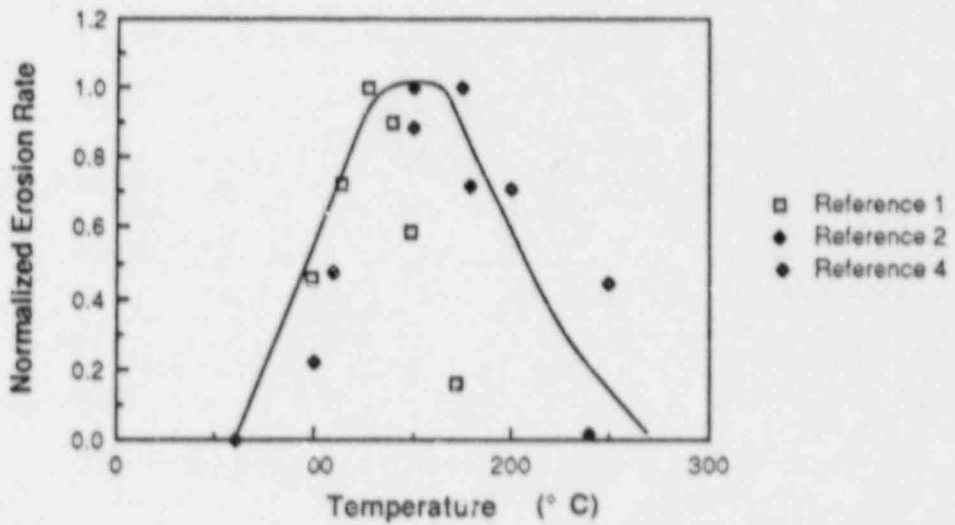


Fig. 15. Estimated temperature dependence of erosion-corrosion based on data from References 1, 2, and 4.

that inhibit access to the metal surface. With suitable choices of model parameters, both explanations give results fairly consistent with available data.

5. Effect of pH on Erosion-Corrosion

Erosion-corrosion rates are strongly dependent on pH over the range of interest in reactor water systems (\approx pH 7-10 at 25°C). Data from References 1 and 2 are summarized in Figs. 16-18. (Note that the data for carbon steel in Fig. 18 were obtained at 75°C.) The data are replotted in Fig. 19 in normalized form (erosion-corrosion rate/rate at pH 9). Although there is some scatter, the data consistently show a decrease of more than an order of magnitude in erosion-corrosion rates over the pH range 8.5-9.5 specified for secondary-system feedwater. In terms of the normalized rate, even low-alloy steels show a strong pH dependence, as is shown in Fig. 20. The data for carbon steel in the pH range 8.5-9.5 and a simple regression fit are shown in Fig. 21.

Figure 22, from Reference 21, shows a correlation between the erosion-corrosion rate and the solubility of magnetite at different pH values. The effect of pH appears consistent with its effects on the solubility of magnetite. However, the changes in erosion-corrosion rates are much more dramatic than the corresponding changes (\approx a factor of 2) in corrosion rates under low flow rates, as is shown in Fig. 23.

Although the effect of pH is conventionally described in terms of pH values at 25°C, the critical parameter is actually the corresponding high-temperature pH value. This value can be affected by the choice of control agents (e.g., morpholine or ammonia) and by impurities in the water. In two-phase flows the critical parameter is the pH of the liquid phase; this can be significantly affected by the partitioning of the control agent between the steam and liquid phases. Because morpholine has a lesser tendency to enter the gas phase, French PWRs use morpholine to control pH in the secondary system.

6. Effect of Oxygen on Erosion-Corrosion

Data on oxygen effects are reported in References 2, 6 and 7. The data in Reference 6 are summarized in Table 1.

Table 1. Effect of Dissolved Oxygen on Erosion-Corrosion Rates

Oxygen Level (ppb)	pH	Test Duration (h)	Wall Loss (mm)
<1	9.3	8000	450
5-20	9.5	10331	5
1	9.5	10331	40
5-10	9.4	6438	20
1-2	9.4	6438	20

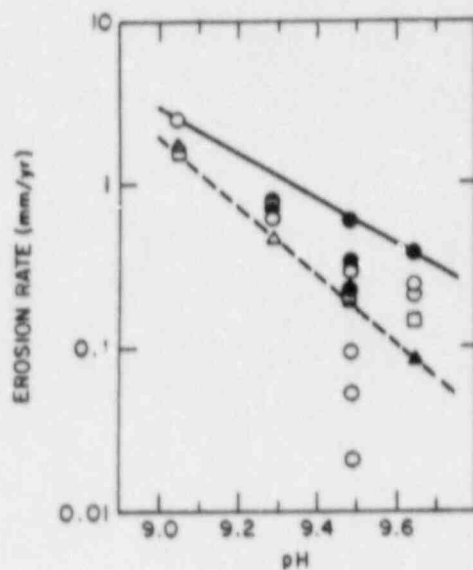


Fig. 16. pH dependence of erosion-corrosion rates at 157°C (from Reference 1).

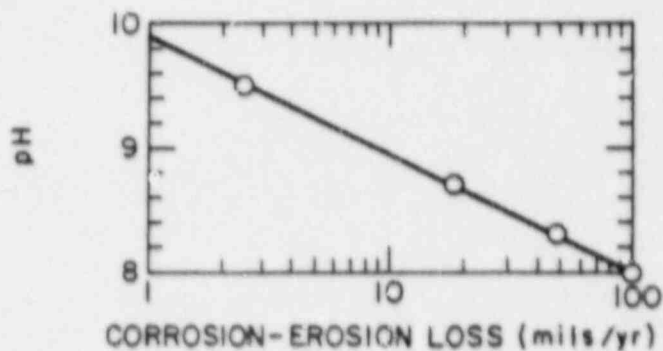


Fig. 17. pH dependence of erosion-corrosion at 99°C from rotating disc tests (from Reference 1).

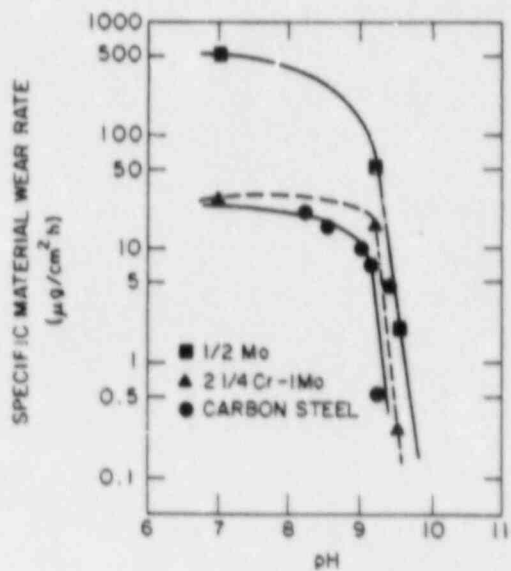


Fig. 18. pH dependence of erosion-corrosion for carbon and low-alloy steels (from Reference 2).

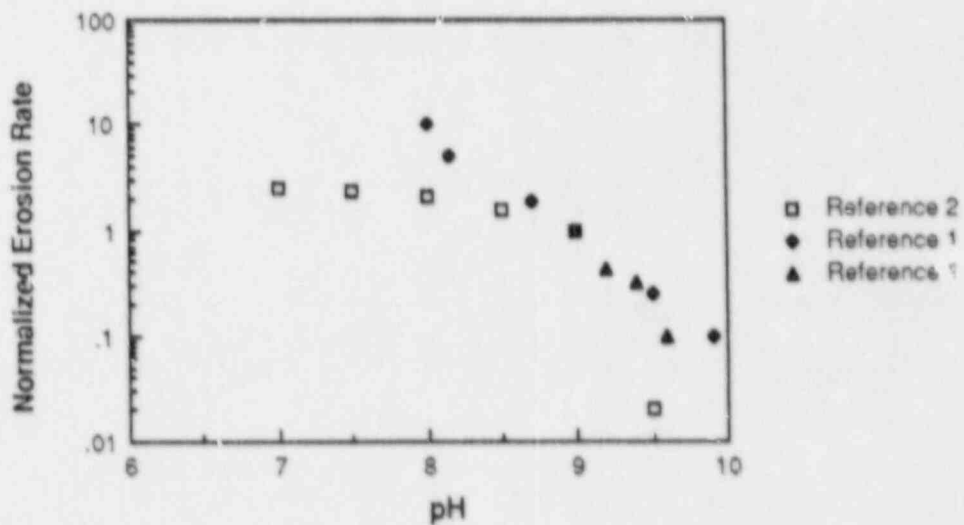


Fig. 19. pH effect on the normalized erosion-corrosion rate for carbon steel. The normalized wear rate is 1 at pH=9. (Based on data from References 1 and 2.)

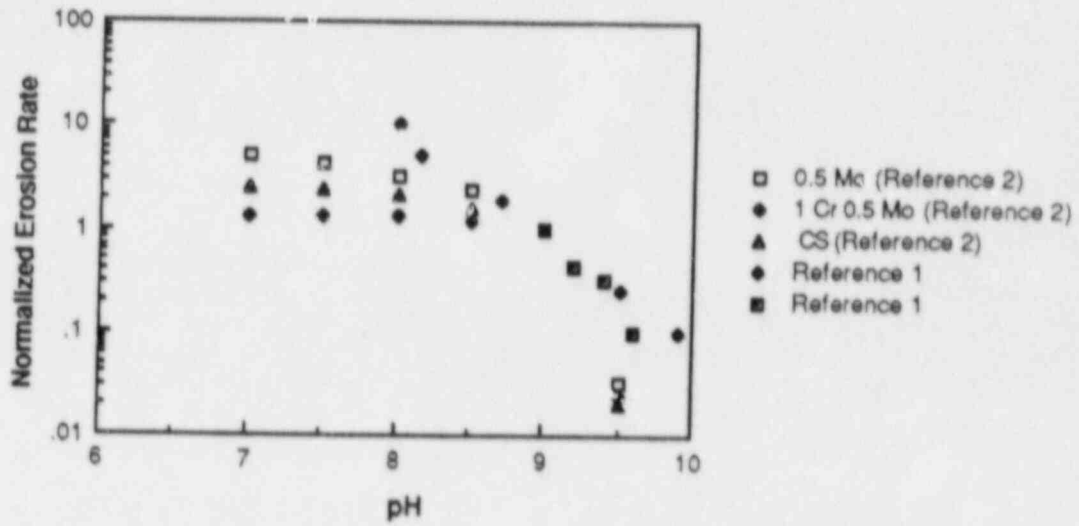


Fig. 20. pH effect on the normalized erosion-corrosion rate for carbon and low alloy steels. The normalized wear rate is 1 at pH=9. (Based on data from References 1 and 2.)

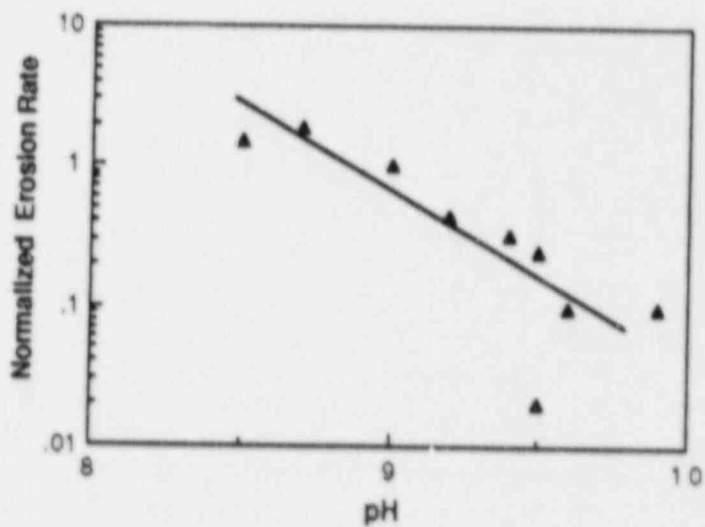


Fig. 21. Curve fit for the pH effect on the normalized erosion-corrosion rate for carbon steel.

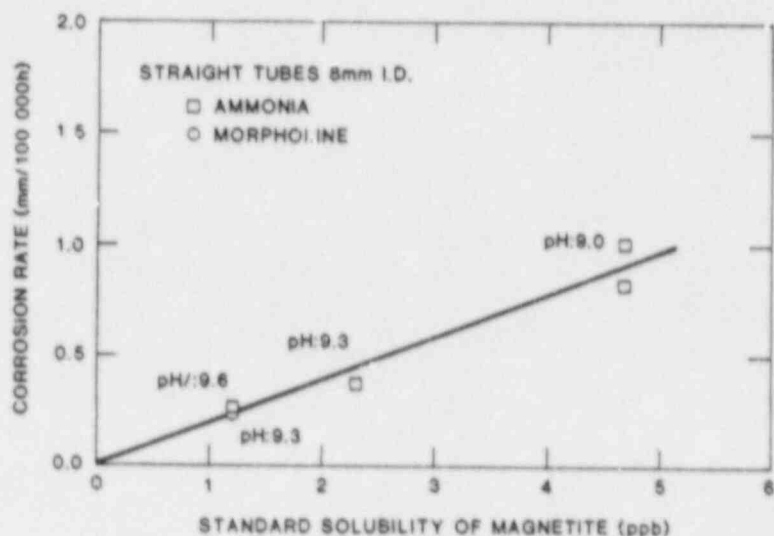


Fig. 22. Correlation between erosion-corrosion rates and the standard solubility of magnetite (from Reference 21).

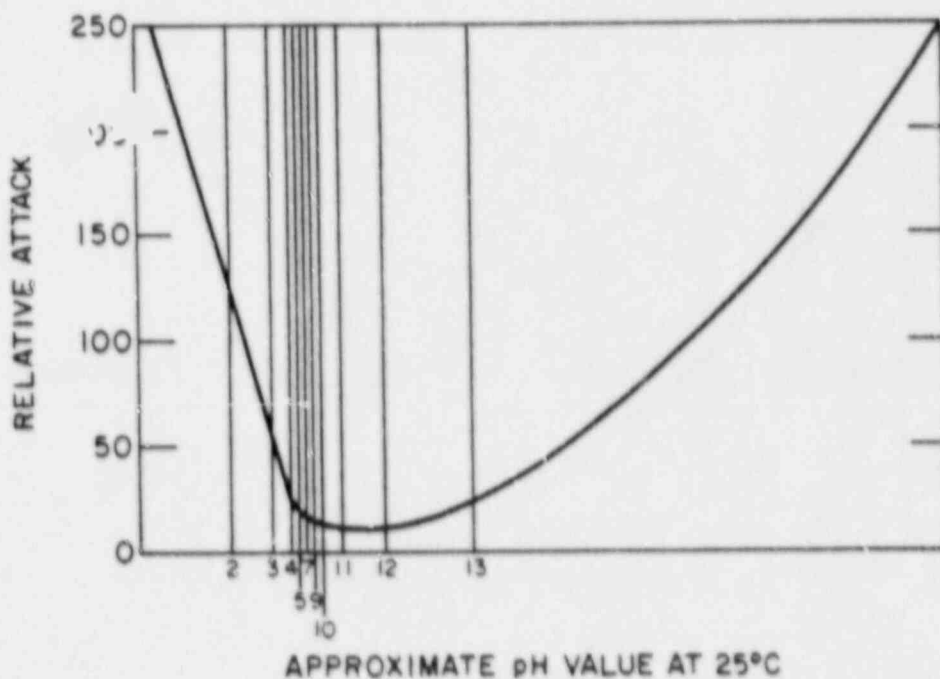
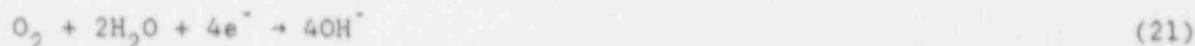


Fig. 23. pH dependence of corrosion rate of carbon steel under very low flow rate conditions at 310°C (from Reference 23).

Typical results from Reference 7 are shown in Fig. 24. Over the pH range considered, very small amounts of dissolved oxygen (on the order of 2-5 ppb) appear to have dramatic effects on the erosion-corrosion rates.

The data in Reference 2, which are summarized in Figs. 25 and 26, include results for both pH 7 and pH 9. They are qualitatively consistent with the results in References 6 and 7, but since only two oxygen levels are considered (<5 ppb and ≈500 ppb), they do not define the threshold level of dissolved oxygen needed to inhibit erosion-corrosion.

The effect of oxygen can be explained in terms of its effects on the nature of the oxide film. In the presence of oxygen, the film probably contains hematite (Fe_2O_3) as well as magnetite (Fe_3O_4). Since the solubility of hematite is much less than that of magnetite,²⁴ the oxide film is much more resistant to erosion-corrosion. This change in the film can also be interpreted in electrochemical terms. Recent tests²⁵ have shown that the inhibition of erosion-corrosion by oxygen addition is accompanied by a change in the electrochemical potential to a much more positive value. This is consistent with a change in the cathodic reaction of the corrosion process from hydrogen ion reduction [Eq. (3)] to oxygen reduction:



An upper bound for the oxygen level required to inhibit a particular rate of erosion-corrosion can then be estimated by assuming that the associated anodic dissolution will be completely balanced by oxygen reduction.²⁵

The strong effect of dissolved oxygen on erosion-corrosion raises the question of whether the use of hydrogen water chemistry in boiling water reactors (BWRs), which lowers the dissolved oxygen level in the reactor coolant, could increase the possibility of erosion-corrosion in the carbon steel portions of BWRs. Hydrogen water chemistry specifications²⁶ require that oxygen be added if necessary to maintain the dissolved oxygen content in the feedwater at 20 ppb. The oxygen content in the wet steam entering the moisture separators is harder to estimate, but it is almost certainly fairly high. Based on the data obtained at pH = 9, even 5 ppb of dissolved oxygen is enough to reduce erosion-corrosion to negligible levels. If this is also true in nearly neutral water, there appears to be little chance of erosion-corrosion problems developing in BWR carbon steel systems. However, additional data are needed to verify this conclusion.

7. Effect of Alloy Additions on Erosion-Corrosion

Field experience shows that alloying can greatly reduce susceptibility to erosion-corrosion.⁸ Chromium is probably the most important alloying element for improving resistance, although other elements may also have a beneficial effect. Austenitic stainless steels can be considered virtually immune, and even 2%Cr-1Mo steels give good performance in the field.⁸

The beneficial effect of chromium is readily understandable because of the high thermodynamic stability of chromium oxides. However, the degree of improvement associated with even low levels of chrome is somewhat surprising. This improvement is presumably due to a progressive enrichment of the corrosion film by chromium as the less-stable oxides are dissolved. The

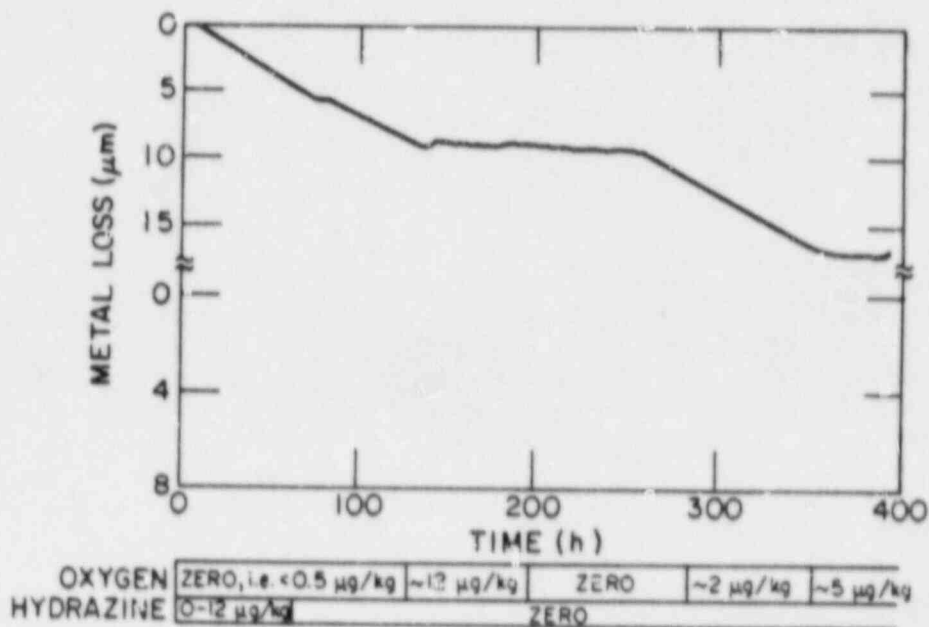


Fig. 24. Effect of dissolved oxygen content on erosion-corrosion (from Reference 7).

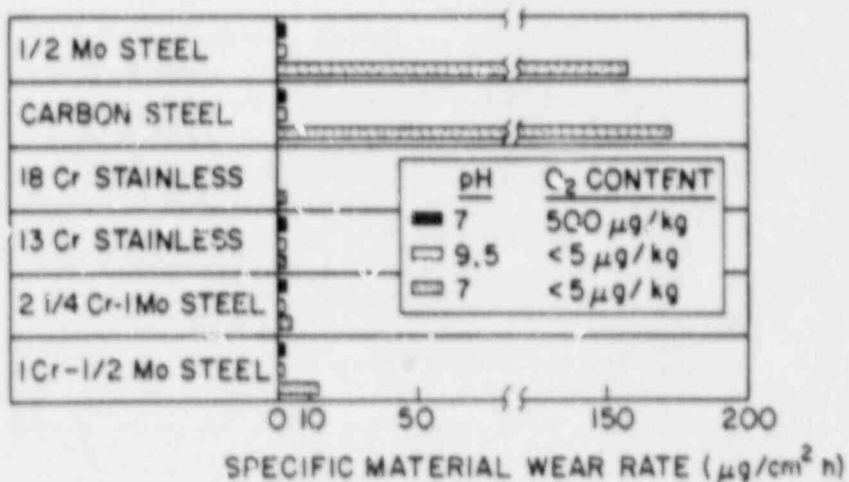


Fig. 25. Erosion-corrosion of various materials for different pH values and oxygen levels (from Reference 2).

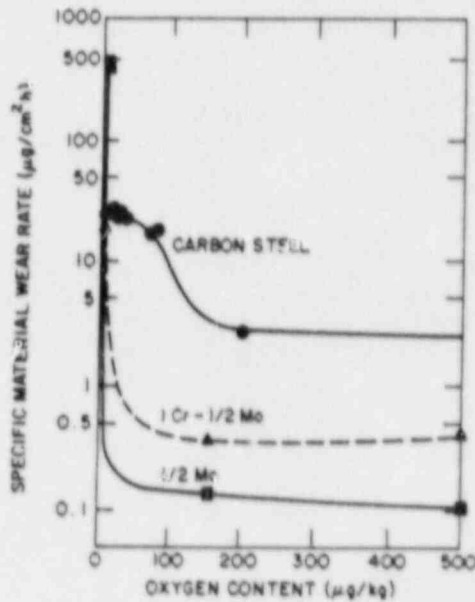


Fig. 26. Effect of dissolved oxygen content on erosion-corrosion of carbon and low alloy steels. The data for carbon steel are at 75°C and relatively low velocities (from Reference 2).

basis for the beneficial effects of molybdenum and copper are less clear,⁹ and experimental data and plant experience⁸ are less consistent in demonstrating a beneficial effect of these alloys.

Quantitative data on alloy effects were obtained by Ducreux²⁷ for alkaline water and by Huijbregts²⁸ for high pH, wet-steam conditions. The data of Ducreux²⁷ cover a wide range of alloy contents, while Huijbregts²⁸ considered only relatively low-alloy materials.

Empirical correlations between weight loss and alloy content were also developed by both authors. The one developed by Huijbregts is of the form

$$G = 94 - 100Cr - 120Cu - 35Mo \quad (C2)$$

where G, the weight loss, is given in milligrams and the alloy levels are given in wt.%. This can be rewritten in terms of a nondimensional weight loss R.

$$R = 1 - 1.06Cr^* \quad (r^2 = 0.58)$$

$$Cr^* = Cr + 0.35Mo + 1.20Cu \quad (23)$$

where R has been normalized with respect to the predicted weight loss of a material with no alloying, Cr* is an "effective" chromium content, and r² is the coefficient of correlation for the regression equation. Examination of

the data of Huijbregts shows that Cr, Mo, and Cu are all significant variables in a statistical sense.

Ducreux²⁷ presents correlations for materials with low alloy contents in several roughly equivalent forms:

$$g = 0.7 + 32.4Cr \quad (r^2 = 0.96) \quad (24a)$$

$$g = -5.2 + 28.9Cr + 51.9Cu + 11.5Mo \quad (r^2 = 0.99) \quad (24b)$$

$$g = 83.0Cr^{0.89}Mo^{0.20}Cu^{0.25} \quad (r^2 = 0.96) \quad (24c)$$

where g represents the increase in erosion-corrosion resistance relative to a reference material with 0.04%Cr, <0.01%Mo, and 0.13%Cu. Most of the observed variation in erosion-corrosion resistance in Ducreux's tests can be correlated solely in terms of Cr content, but the inclusion of Mo and Cu slightly improves the fit. Equations (24b) and (24c) give physically unrealistic results, i.e., vanishingly small erosion-corrosion resistance, for very low alloy contents. To avoid this difficulty, the data can be reanalyzed in terms of relative erosion-corrosion rates (=1/g). This gives

$$R = e^{-5.16Cr^{**}} \quad (r^2 = 0.94)$$

$$Cr^{**} = Cr + 0.19Mo + 0.40Cu \quad (25)$$

where again R has been normalized with respect to the predicted weight loss of a material with no alloying elements, and Cr** is an alternative definition of an "effective" chromium content. The coefficient of correlation for this regression equation is slightly smaller than those proposed by Ducreux, but the behavior at low alloying levels is more realistic. The data of Huijbregts can also be analyzed in terms of an equation of this form:

$$R = e^{-1.44Cr^*} \quad (r^2 = 0.61) \quad (26)$$

In this case the coefficient of correlation is slightly higher than that for Eq. (23), and unlike Eq. (23), R does not become negative for Cr levels > 0.94%.

The data obtained by Ducreux²⁷ for low-alloy materials and the regression equation (25) are shown in Fig. 27; the data of Huijbregts²⁸ and the corresponding regression equation (26) are shown in Fig. 28. A comparison of Eqs. (25) and (26) is shown in Fig. 29. For the low levels of alloy content that would characterize different heats of nominally carbon steel, Eq. (26) predicts relatively little effect for the alloying elements, while Eq. (25) predicts a much stronger effect. For higher levels of alloying more characteristic of low-alloy steels, both equations predict significant reductions in erosion-corrosion rates.

Ducreux²⁷ also obtained data, shown in Fig. 30, for more highly alloyed materials with Cr contents up to 13%. As expected, the higher chrome contents greatly reduce the erosion-corrosion rates. Similar results were obtained by Heitmann and Schub² for neutral pH conditions (Fig. 11).

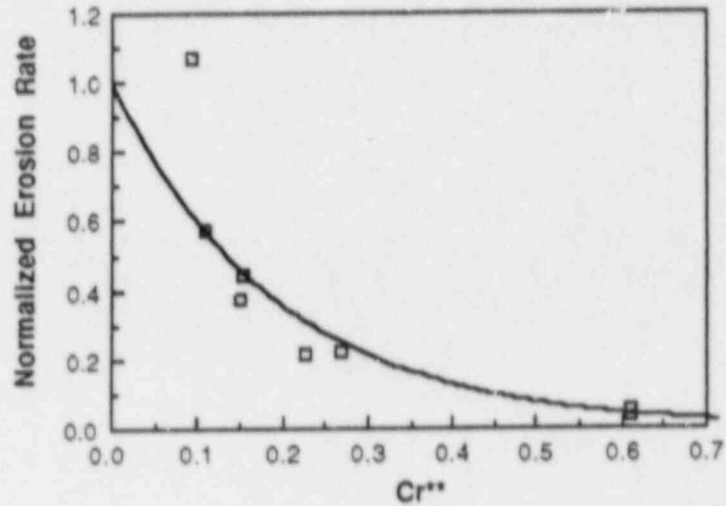


Fig. 27. Effect of low levels of chromium, molybdenum, and copper on erosion-corrosion rates in deoxygenated water with pH of 9 at a temperature of 180°C and a flow velocity of $56\text{ m}\cdot\text{s}^{-1}$ (from Reference 27). The data have been normalized so that the predicted erosion-corrosion rate for a plain carbon steel is 1.

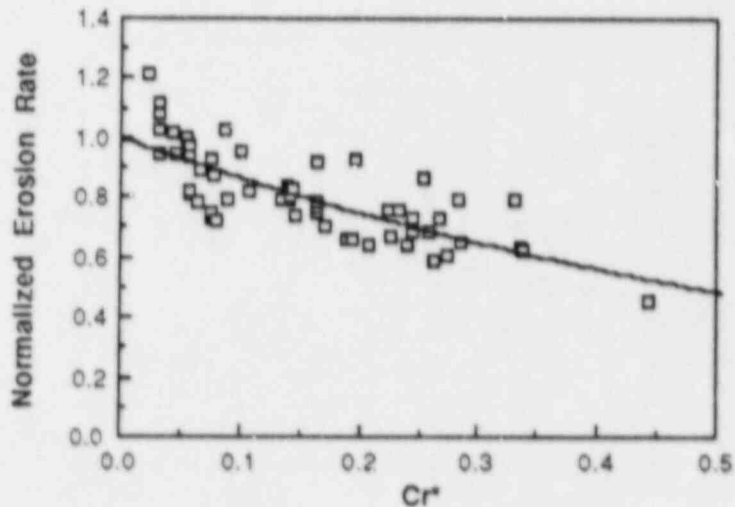


Fig. 28. Effect of low levels of chromium, molybdenum, and copper on erosion-corrosion rates in two-phase flow with 10% water and a steam velocity of $960\text{ m}\cdot\text{s}^{-1}$ at a metal temperature of 127°C (from Reference 28). The data have been normalized so that the predicted erosion-corrosion rate for a plain carbon steel is 1.

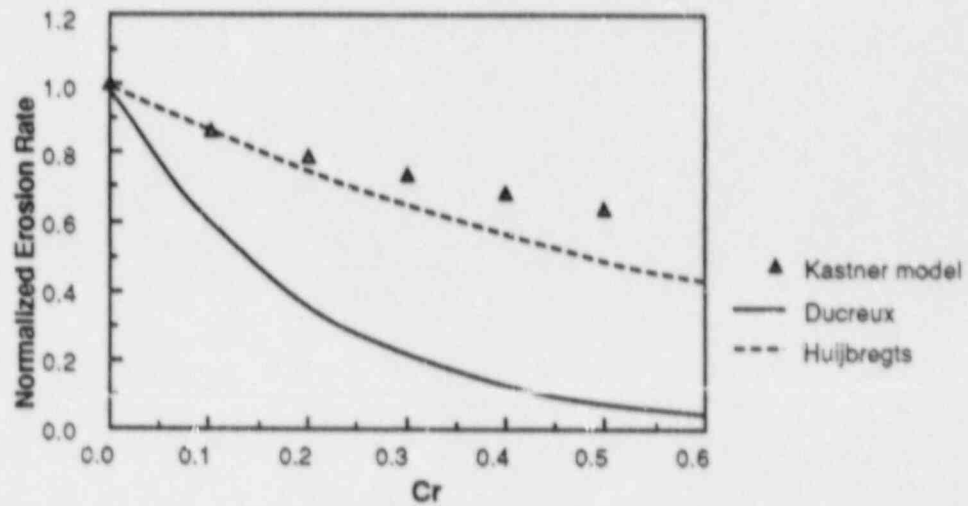


Fig. 29. Normalized erosion-corrosion rates as a function of Cr content predicted by regression equations based on the results of Ducreux²⁷ and Huijbregts.²⁸

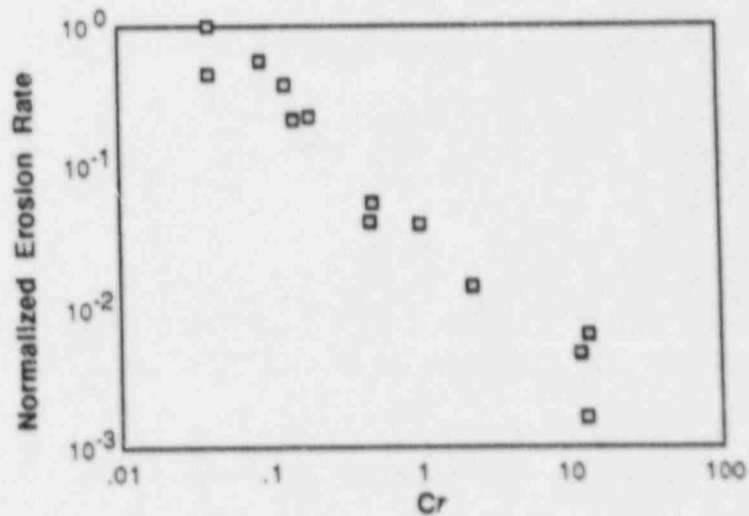


Fig. 30. Effect of chromium additions on relative erosion-corrosion resistance (from Reference 27).

8. Empirical Estimates of Erosion-Corrosion Rates

A number of empirical models that account for the major critical variables have been developed.^{9,19,20,22} The model in Reference 9 is based on the phenomenological model Eq. (9) for dissolution wear with modifications to account for the effect of alloying, a more accurate representation of temperature effects and a separate model for droplet impact. This model is discussed in detail in Reference 9, and a simplified procedure for the application of the model to piping systems is presented in Reference 29.

The model presented in References 21 and 19 was developed by researchers at Electricite de France (EDF), and is being adapted for use in the U.S. by NUMARC. This model is of the form

$$\dot{m} = F(k)FG \cdot FT \cdot FC \cdot FR \quad (27)$$

where $F(k)$ describes the mass transfer dependence, FG is the geometry factor introduced by Keller³⁰ except that it is normalized to make $FR=1$ for a straight pipe, FT is a temperature factor, FC is a water chemistry (pH) factor, and FR is a steel composition factor. The explicit expression for FR is simply the reciprocal of g as given by Eq. (24c). The corrections for pH are based on correlations for the solubility of magnetite,¹⁵ because, as is shown in Reference 21, this correlates well with erosion-corrosion rates. The factor is then normalized to be equal to 1 for conditioning with ammonia at $pH = 9$. Because the solubility calculations are based on the pH at temperature, the use of different control agents gives different predictions of the erosion-corrosion rates; e.g., an environment of $pH 9.3$ ($25^\circ C$) with morpholine control is equivalent to an environment of $pH 9.6$ ($25^\circ C$) with ammonia control.

For applications to two-phase flows, an appropriate value of k must be used. A simplified procedure to compute k for this case is given in Reference 19. In two-phase flows with ammonia control, an additional factor is used to account for the preferential partitioning of ammonia to the gaseous phase. Calculations with the model give good agreement with the observed behavior at the Surry 2 reactor.¹⁹

The model of Kastner²⁰ is strictly empirical. It is described by the following equations for the erosion-corrosion loss (in $mm \cdot h^{-1}$):

$$\dot{m} = 8.0 \cdot 10^{-6} k_c Be^{NV} [1 - 0.175(pH - 7)^2] 1.8e^{-0.118 \cdot g} + 1 [f(t)] \quad (28)$$

with

$$B = -10.5\sqrt{h} - 9.375 \cdot 10^{-4} T^2 + 0.79 \cdot T - 132.5$$

$$N = -0.0875 h - 1.275 \cdot 10^{-5} T^2 + 0.01078 \cdot T - 2.15 \quad 0 \leq h \leq 0.5$$

$$N = (-1.29 \cdot 10^{-4} T^2 + 0.109T - 22.07) \cdot 0.154e^{-1.2h} \quad 0.5 < h \leq 5$$

$$f(t) = C_1 + C_2 t + C_3 t^2 + C_4 t^3$$

where

$$C_1 = 0.9999934$$

$$C_2 = -0.335690 \cdot 10^{-6}$$

$$C_3 = -0.5624812 \cdot 10^{-10}$$

$$C_4 = 0.3849972 \cdot 10^{-15}$$

and k_c are the geometry factors of Keller,³⁰ g is the dissolved oxygen level in ppb, h is the sum of the chromium and molybdenum content (wt.%), the pH values are measured at 25°C, and t is time in hours.

Unlike the model described by Eq. (27), in which each important factor appears as an independent term, the variables in the Kastner model appear to be coupled. In addition, the velocity appears directly in this model instead of implicitly through the mass transfer coefficient. However, the actual numerical predictions of the two models appear to be similar in many cases.

The variation of erosion-corrosion rate with temperature predicted by the model of Kastner²⁰ for different pH values and velocities is shown in Fig. 31; experimental data from Reference 2 are also included for comparison. The coupling between the different variables is relatively weak, and a "separate factors" analysis like Eq. (27) would give comparable results. The variation of the normalized erosion-corrosion rate with pH predicted by the model is shown in Fig. 32 with corresponding experimental data. The variation with dissolved oxygen level is shown in Fig. 33. Detailed experimental data are not available for comparison, but the predictions seem conservative compared to the available information reviewed in Section 6. Typical predictions by the model for the effects of alloying are shown in Fig. 29; the dependence in the model seems to be similar to the results of Huijbregts.²⁸ Parametric calculations again show that alloying can be treated as a "separate factor" to a reasonable approximation.

The variation in erosion-corrosion rate with flow velocity is shown in Fig. 34. The variation predicted by the model cannot be described by a simple power-law, but for a restricted range of velocities ($1-10 \text{ m}\cdot\text{s}^{-1}$) a power law gives a reasonable approximation. For temperature and pH values for which the work of Bignold et al.⁵ suggested a dependence on the mass transfer coefficient k^{2-3} , corresponding to a velocity dependence of $V^{1.7-2.6}$ from Eq. (18), the model of Kastner gives an approximate value of $V^{0.4}$. However, the model is in reasonable agreement with the work of Bouchacourt²¹ shown in Fig. 8. In this case, the dependence is roughly k^{1-4} , corresponding to a dependence on velocity of V^{1-2} .

For applications to two-phase flows, the appropriate velocity to be used in Eq. (28) is the velocity of the fluid film at the wall. Kastner suggests a simplified method to calculate this quantity.²⁰ To account for the preferential partitioning of ammonia to the steam phase, under two-phase conditions the pH is assumed to be 7.

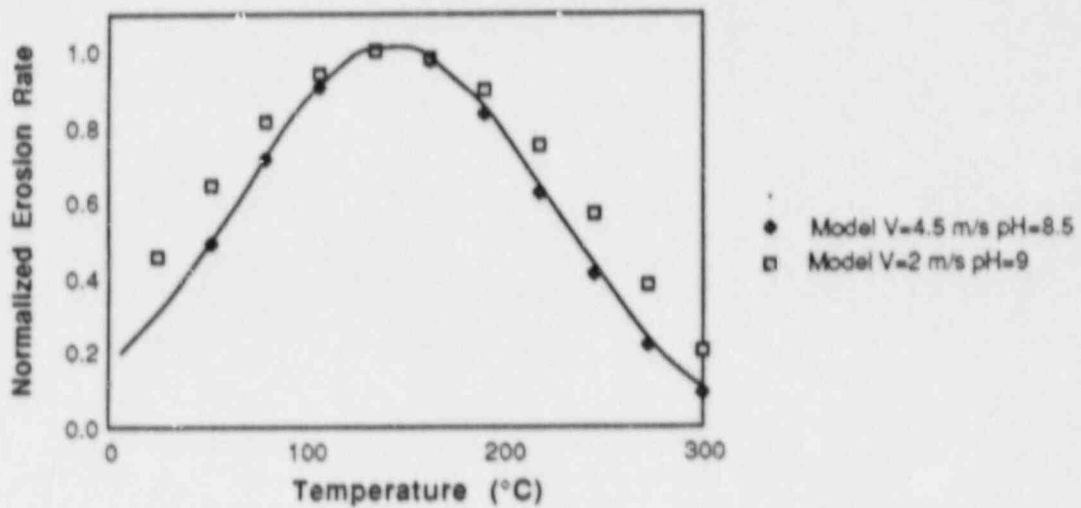


Fig. 31. Variation of erosion-corrosion rate with temperature predicted by the model of Kastner²⁰; the experimental data are from Reference 2.

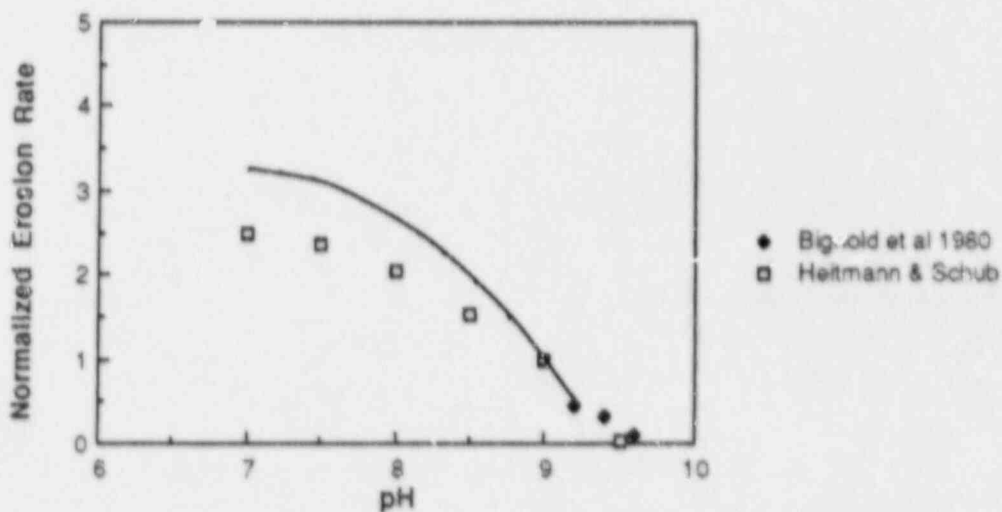


Fig. 32. Variation of erosion-corrosion rate with pH predicted by the model of Kastner²⁰; the data have been normalized to equal 1 for pH=9. The experimental data are from References 1 and 2.

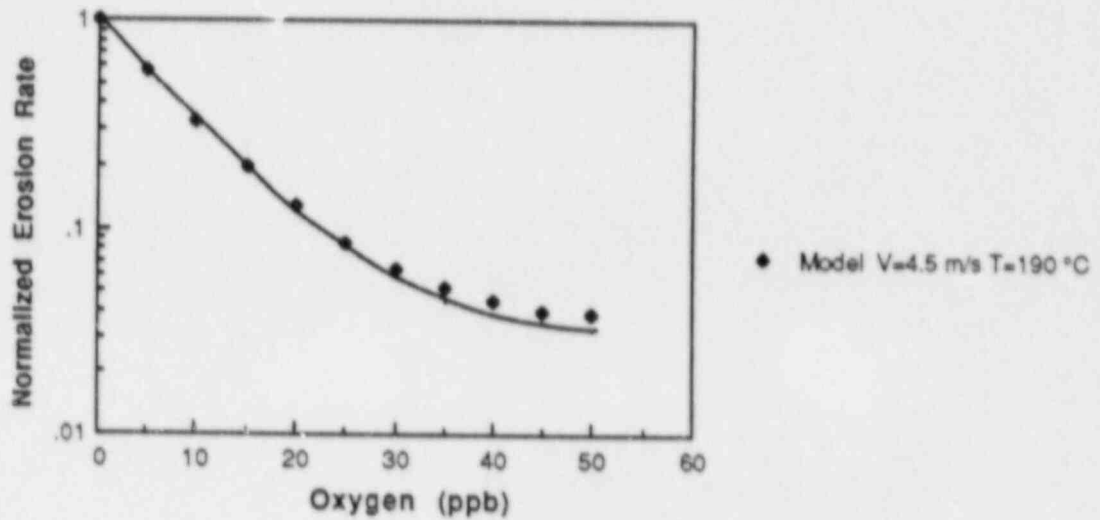


Fig. 33. Variation of erosion-corrosion rate with dissolved oxygen level predicted by the model of Kastner²⁰; the data have been normalized to equal 1 for vanishing dissolved oxygen levels.

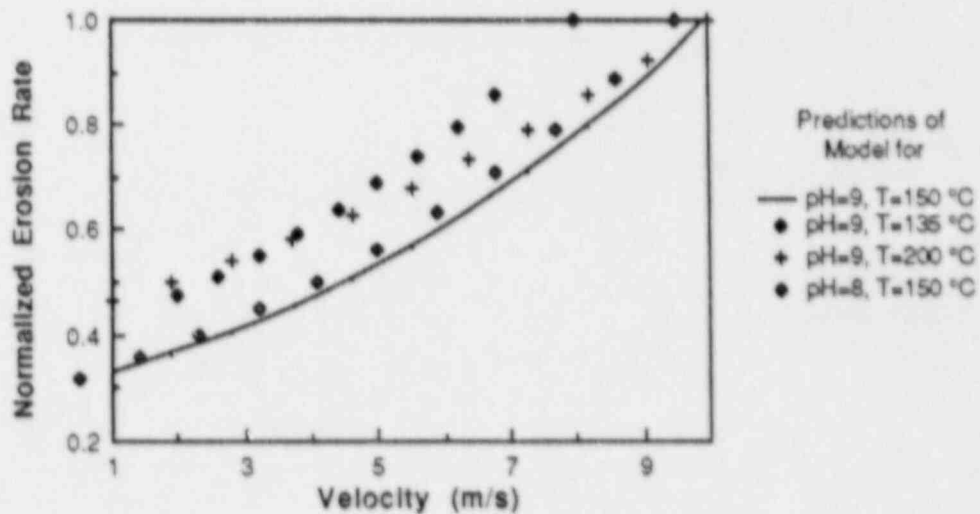


Fig. 34. Dependence of the erosion-corrosion rate on flow velocity predicted by the model of Kastner²⁰ for several pH and temperature conditions.

The model has been checked against 1049 cases of erosion-corrosion measurements in the laboratory and in power plants.²⁰ The data are widely scattered but in 85% of the cases the model gives conservative predictions of the losses. However, conservative predictions appear to be obtained more consistently for two-phase flow than for single-phase flows.

The models corresponding to Eqs. (27) and (28) account for local flow geometry by using the empirical geometric factors developed by Keller.³⁰ The model developed by Bignold et al.¹ suggests that the effect of geometry can be taken into account more fundamentally through the variation of the mass transfer coefficient k . In order to be able to test the use of a model of the form presented in References 1 and 4 for piping systems, the available data have been analyzed to develop simple empirical corrections to account for the effects of pH, temperature, oxygen, and alloy content. The resulting equation is similar in form to Eq. (27):

$$\dot{m} = CK_{\text{pH}}K_{\text{T}}K_{\text{O}_2}K_{\text{alloy}}k^n \quad (29)$$

where \dot{m} is the erosion-corrosion rate ($\text{mm}\cdot\text{yr}^{-1}$); K_{ij} are nondimensional factors accounting for the effect of pH, temperature, dissolved oxygen, and alloy content; k ($\text{mm}\cdot\text{s}^{-1}$) is the mass transport coefficient; n is taken from Reference 5, as is shown in Figs. 3 and 4; and C is a constant. Although the assumption that each factor can be considered independently of the others is not strictly correct, the generally consistent results obtained in the normalized data plots (Figs. 14, 20, 28) suggest that it is not an unreasonable approximation. The explicit expressions for the K factors are derived from regression analyses of the normalized plots (Figs. 14, 20) and the correlation with alloy content developed in Reference 28. They are scaled so that K_{pH} is exactly 1 at pH 9, K_{T} is exactly 1 at a temperature of 156°C, and K_{alloy} , taken from Huijbregts²⁸ [Eq. (26)], is exactly 1 for a plain carbon steel. The resulting expressions are:

$$K_{\text{pH}} = 9.6 \times 10^{10} e^{-2.81 \cdot \text{pH}} \quad (30)$$

$$K_{\text{T}} = 1.86 \cdot 175/T \quad (T < 156^\circ\text{C})$$

$$= 1.21 + 349/T \quad (T > 156^\circ\text{C})$$

$$K_{\text{O}_2} = 1 \quad \text{for the systems of interest}$$

$$K_{\text{alloy}} = e^{-1.44 \cdot \text{Cr}^*} \quad \text{Cr}^* = \text{Cr} + 0.35\text{Mo} + 1.20\text{Cu}$$

The value of C is 0.037 for k in $\text{mm}\cdot\text{s}^{-1}$ and \dot{m} in $\text{mm}\cdot\text{yr}^{-1}$; it has been chosen to match the data in Reference 1 (Fig. 2).

9. Application of the Empirical Models to the Surry 2 Feedwater Line

The basic physical parameters describing the flow in the Surry 2 feedwater line are given in Table 2.

Table 2. Flow Parameter and Geometry in Surry 2 Feedwater Line

Pipe Diameter (d)	18 in. (0.46 m)
Flow Velocity (V)	17 ft·s ⁻¹ (5.2 m·s ⁻¹)
Kinematic Viscosity (ν)	1.5 × 10 ⁻⁷ m ² ·s ⁻¹
Diffusivity of Fe ⁺⁺	7.7 × 10 ⁻⁹ m ² ·s ⁻¹
Temperature	375°F (190°C)
pH	9.0

The models described by Eqs. (27-29) have been used to evaluate the erosion-corrosion observed at Surry Unit 2. For these conditions and a "tee" geometry, the model of Kastner²⁰ gives an estimated erosion-corrosion rate of 1.3 mm·yr⁻¹, which is reasonably consistent with the observed behavior. Predictions made using the model developed by EDF [Eq. (27)] are given in Reference 19. No details of the analysis are given, but the calculated rates are ≈1.4 mm·yr⁻¹, similar to that predicted by the model of Kastner.

Equation (29) gives a predicted erosion-corrosion rate in a straight pipe under these conditions of 0.04 mm·yr⁻¹. Hence even after 10 years of operation very little metal loss is expected in straight pipe under these conditions. The applicable mass transfer coefficient correlations¹⁶ indicate that the inlet flows are more critical geometries than the elbows. The data shown in Fig. 1 suggest that the effective k is approximately three times the value computed for the straight pipe. With this value for k , Eq. (29) predicts an erosion-corrosion rate of 1.1 mm·yr⁻¹, which is again consistent with the observed behavior.

Although all three models give results in fairly good agreement with the observed behavior at Surry, such calculations are subject to large uncertainties. All of the models are very limited in their capability to consider the effect of complex piping geometries. Disturbances in turbulent flows can propagate a distance of many diameters in piping systems. Thus the behavior at a particular location depends not only on the geometry at that location, but also on the upstream flow geometry. Even in the case of an isolated component, geometry effects are taken into account in the EDF and Kastner models through the geometric factors of Keller. These were developed empirically based on two-phase flow experience; their application to single-phase flows is somewhat suspect. There are also significant differences between the models with respect to the predicted effect of variables like flow velocity and alloy content. These differences largely represent the range of results obtained in laboratory tests. These discrepancies may be due to the attempt to isolate "separate factors" in what is truly a complexly coupled problem.

References

1. G. J. Bignold, K. Garbett, K. Garnsey, and I. S. Woolsey, "Erosion-corrosion in nuclear steam generators," in Proceedings of the Second Meeting on Water Chemistry of Nuclear Reactors, British Nuclear Engineering Society, London, pp.5-18 (1980).
2. H. G. Heitmann and P. Schub, "Initial experience gained with a high pH value in the secondary system of PWRs," in Proceedings of the Third Meeting on Water Chemistry of Nuclear Reactors, British Nuclear Engineering Society, London, pp.243-252 (1983).
3. J. Ducreux, "The influence of flow velocity on the corrosion-erosion of carbon steel in pressurized water," in Proceedings of the Third Meeting on Water Chemistry of Nuclear Reactors, British Nuclear Engineering Society, London, pp.227-233 (1983).
4. G. J. Bignold, C. H. De Whalley, K. Garbett, and I. S. Woolsey, "Mechanistic aspects of erosion-corrosion under boiler feedwater conditions," in Proceedings of the Third Meeting on Water Chemistry of Nuclear Reactors, British Nuclear Engineering Society, London, pp.219-226 (1983).
5. G. J. Bignold, K. Garbett, and I. S. Woolsey, "Mechanistic aspects of the temperature dependence of erosion-corrosion," in Corrosion Erosion of Steels in High Temperature Water and Wet Steam, Electricite de France, Les Renardieres (May 1982).
6. K. Tittle, P. W. Tasker, and D. S. Eyre, "The use of oxygen in feedwater to counter erosion-corrosion of mild steel boiler feed pipework," in Proceedings of the Third Meeting on Water Chemistry of Nuclear Reactors, British Nuclear Engineering Society, London, pp.253-259 (1983).
7. D. Penfold, G. S. Harrison, G. M. Gill, J. C. Greene, and M. A. Walker, "The Control of Erosion-Corrosion of Mild Steel Using an Oxygen-Ammonia-Hydrazine-Dosed Feedwater," Nuclear Energy, 25, pp.257-266 (October, 1986).
8. G. A. Delp, J. D. Robinson, and M. T. Sedlack, Erosion/Corrosion in Nuclear Plant Steam Piping: Causes and Inspection Program Guidelines, EPRI NP-3944, Electric Power Research Institute, Palo Alto (April, 1985).
9. R. G. Keck, Prediction and Mitigation of Erosive-Corrosive Wear in Steam Extraction Systems, Ph. D. Thesis, Department of Mechanical Engineering, Massachusetts Institute of Technology, Cambridge, Massachusetts (1987).
10. S. Giampapa, Erosion-Corrosion Seminar, Toledo Edison Co., Toledo, Ohio (March, 1987).
11. C. J. Czajkowski, Metallurgical Evaluation of an 18-Inch Feedwater Line Failure at the Surry Unit 2 Power Station, NUREG/CR-4868 (March 1987).

12. P. Berge, J. Ducreux, and P. Saint-Paul, "Effects of chemistry on corrosion-erosion of steels in water and wet steam," in Proceedings of the Second Meeting on Water Chemistry of Nuclear Reactors, British Nuclear Engineering Society, London, pp.19-23 (1980).
13. L. E. Sanchez-Caldera, The Mechanism of Corrosion-Erosion in Steam Extraction Lines of Power Stations, Ph. D. Thesis, Department of Mechanical Engineering, Massachusetts Institute of Technology, Cambridge, Massachusetts (1987).
14. Kunze and J. Nowak, "Erosion Corrosion Damage in Steam Boilers," Werkstoffe und Korrosion, 33, pp.262-273 (1982).
15. F. H. Sweeton and C. F. Baes, Jr., "The Solubility of Magnetite and Hydrolysis of Ferrous Ion in Aqueous Solutions at Elevated Temperatures," J. Chem. Thermodynamics, 2, pp.479-500 (1970).
16. M. W. E. Coney, Erosion-Corrosion: The Calculation of Mass-Transfer Coefficients, RD/1/N 197/80, Central Electricity Research Laboratories (November 1980).
17. L. M. K. Boelter, G. Young, and H. W. Iversen, An Investigation of Aircraft Heaters- Distribution of Heat-Transfer Rate in the Entrance Section of a Circular Tube, NACA TN 1451, Washington, D.C. (July 1948).
18. R. A. W. Shock, "Convective Heat Transfer in Annular Flow," in Two-Phase Flows and Heat Transfer, D. Butterworth and G. F. Hewitt, Eds., Oxford University Press, London, pp. 170-199 (1979).
19. F. N. Remy, "Flow Assisted Corrosion: Consequences for the French Units," EPRI Workshop on the Erosion Corrosion of Carbon Steel Piping, Washington, D.C., April 14-15, 1987.
20. W. Kastner, "Erosion-Corrosion - Experiments and Calculation Model," EPRI Workshop on the Erosion Corrosion of Carbon Steel Piping, Washington, D.C., April 14-15, 1987.
21. M. Bouchacourt, "Identification of Key Variables: EDF Studies," EPRI Workshop on the Erosion Corrosion of Carbon Steel Piping, Washington, D.C. (April, 1987).
22. G. J. Bignold, C. H. Whalley, K. Garbett, and I. S. Woolsey, "CERL Single Phase Erosion-Corrosion Studies Under Boiler Feedwater Conditions," EPRI Workshop on the Erosion Corrosion of Carbon Steel Piping, Washington, D.C. (April, 1987).
23. H. Uhlig, Corrosion Handbook, McGraw Hill, New York (1949).
24. A. Seidell, Solubilities of Inorganic and Metal Organic Compounds, D. Van Nostrand Co., New York (1942).

25. I. S. Woolsey, G. J. Bignold, C. H. Whalley, and K. Garbett, "The influence of oxygen and hydrazine on the erosion-corrosion behaviour and electrochemical potentials of carbon steel under boiler feedwater conditions," Proceedings of the Fourth Meeting on Water Chemistry of Nuclear Reactors, British Nuclear Engineering Society, London, pp 337-344 (1986).
26. W. Bilanin, J. Blomgren, R. Cowan, W. Kirkley, B. Mueller, J. Pleva, S. Sawochka, J. Svenson, and F. Walschot, BWR Water Chemistry Guidelines, EPRI NP-3589-SR-LD, Electric Power Research Institute, Palo Alto (April, 1985).
27. J. Ducreux, "Theoretical and experimental investigation of the effect of chemical composition of steels on their erosion-corrosion resistance," in Corrosion Erosion of Steels in High Temperature Water and Wet Steam, Electricite de France, Les Renardières (May, 1982).
28. W. M. J. Huijbregts, "Erosion-Corrosion of Carbon-Steel in Wet Steam," Materials Performance, 23, pp.39-45 (1984).
29. R. G. Keck and P. Griffith, Prediction and Mitigation of Erosive-Corrosive Wear in Secondary Piping Systems of Nuclear Power Plants, NRC-04-87-106 (June, 1987).
30. V. H. Keller, "Erosion-corrosion in damp steam turbines," Kraftwerkstechnik, 54, p.292 (1974).

Distribution for NUREG/CR-5156 (ANL-88-25)

Internal:

O. K. Chopra	P. S. Maiya	C. E. Till
H. M. Chung	J. Y. Park	R. A. Valentin
D. R. Diercks	W. E. Ruther	R. W. Weeks
B. R. T. Frost	W. J. Shack (5)	ANL Patent Dept.
T. F. Kassner (10)	W. K. Soppet	ANL Libraries
D. S. Kupperman	E. M. Stefanski	TIS File (3)
		ANL Contract File

External:

NRC, for distribution per R5 (315)
DOE-OSTI (2)
Manager, Chicago Operations Office, DOE
R. Dalton, DOE-CH
P. Alexander, Combustion Engineering, 400 West Avenue, Rochester, NY 14611
G. A. Arlotto, Office of Nuclear Regulatory Research, USNRC, Washington
C. Y. Cheng, Office of Nuclear Reactor Regulation, USNRC, Washington
G. Cragnolino, Comision Nacional de Energia Atomica, Gerencia de Procesos Quimicos,
Avda Del Libertador 8250, 1429 Buenos Aires, Argentina
D. Cubicciotti, Electric Power Research Inst., P. O. Box 10412, Palo Alto, CA 94303
W. H. Cullen, Materials Engineering Assoc., Inc., 9700 B. George Palmer Highway,
Lanham, MD 20706
C. J. Czajkowski, Dept. of Nuclear Engineering, Brookhaven National Laboratory,
Upton, NY 11973 (5)
J. C. Danko, U. Tennessee, Knoxville, TN 37966-2000
B. J. Elliot, Office of Nuclear Reactor Regulation, USNRC, Washington
M. Fox, APTECH, 1257 Elko Drive, Sunnyvale, CA 94089
S. J. Green, Electric Power Research Institute, 3412 Hillview Avenue, Palo Alto,
CA 94303
R. A. Greenkorn, Purdue University, Hovde Hall, Room 222, West Lafayette, IN 47907
S. D. Harkness, Bettis Atomic Power Laboratory, P. O. Box 79, West Mifflin,
PA 15122
W. S. Hazelton, Office of Nuclear Reactor Regulation, USNRC, Washington
L. J. Jardine, Bechtel National, Inc., 45 Fremont Street, 11/B33, San Francisco,
CA 94105
O. Jonas, Jonas Inc., 1113 Faun Road, Wilmington, DE 19803
R. E. Johnson, Office of Nuclear Reactor Regulation, USNRC, Washington
R. L. Jones, Electric Power Research Inst., P. O. Box 10412, Palo Alto, CA 94303
C. Y. Li, Cornell University, Dept. of Materials Science & Engineering, Bard Hall,
Ithaca, NY 14853
J. Muscara, Office of Nuclear Regulatory Research, USNRC, Washington
D. M. Norris, Electric Power Research Inst., P. O. Box 10412, Palo Alto, CA 94303
E. J. Rowley, Commonwealth Edison Co., P. O. Box 767, Chicago, IL 60690
E. F. Rybicki, Dept. of Mechanical Engineering, U. Tulsa, Tulsa, OK 74110
R. E. Scholl, URS/John A. Blume & Associates, 150 Fourth Street, Sixth Floor,
San Francisco, CA 94103
P. M. Scott, UKAEA AERE-Materials Development Division, Harwell, Didcot,
OX11 0RA, UK
C. Z. Serpan, Office of Nuclear Regulatory Research, USNRC, Washington
P. G. Shewmon, Dept. of Metallurgical Engineering, Ohio State U., Columbus,
OH 43210

External (Contd.):

- R. Smith, EPRI NDE Center, 1300 Harris Blvd., Box 217097, Charlotte, NC 28213
- A. Taboada, Office of Nuclear Regulatory Research, USNRC, Washington
- B. Tomkins, Risley Nuclear Power Development Labs., U K. Atomic Energy Authority, Risley, Warrington, WA3 6 AT, England
- E. Venerus, Knolls Atomic Power Laboratory, P. O. Box 1072, Schenectady, NY 12301
- J. R. Weeks, Brookhaven National Laboratory, Upton, NY 11973
- K. R. Wichman, Office of Nuclear Reactor Regulation, USNRC, Washington
- F. Witt, Office of Nuclear Reactor Regulation, USNRC, Washington

NRC FORM 338 12 841 NRDM 1102 3201 3202 SEE INSTRUCTIONS ON THE REVERSE		U.S. NUCLEAR REGULATORY COMMISSION	1. REPORT NUMBER (Assigned by TRD/C add Vol. No. if any) NUREG/CR-5156
2. TITLE AND SUBTITLE Review of Erosion-Corrosion in Single-Phase Flows		3. LEAVE BLANK	
5. AUTHOR(S) G. Cragnolino, C. Czajkowski, and W. J. Shack		4. DATE REPORT COMPLETED MONTH: April YEAR: 1988	
7. PERFORMING ORGANIZATION NAME AND MAILING ADDRESS (Include Zip Code) Brookhaven National Laboratory Upton, NY 11973 Argonne National Laboratory Argonne, IL 60439		6. DATE REPORT ISSUED MONTH: June YEAR: 1988	
10. SPONSORING ORGANIZATION NAME AND MAILING ADDRESS (Include Zip Code) U. S. Nuclear Regulatory Commission Office of Nuclear Regulatory Research Washington, D. C. 20555		8. PROJECT/TASK/WORK UNIT NUMBER ANL-88-25	
		9. FILL OR GRANT NUMBER A2212	
		11. TYPE OF REPORT Technical; Topical	
12. SUPPLEMENTARY NOTES		13. PERIOD COVERED (Include Month)	
13. ABSTRACT (200 words or less) This report contains two literature reviews (prepared by Brookhaven National Laboratory and Argonne National Laboratory, respectively) on the available data and current mechanistic understanding of erosion-corrosion, and a failure analysis (prepared by Brookhaven National Laboratory) of a tee-elbow joint from the Surry Unit 2 reactor that failed by erosion-corrosion in December 1986. It also includes suggestions for additional research that should be performed by the USNRC to increase the capability to rank plants and/or location within plants in terms of susceptibility to erosion-corrosion and to ensure that proposed inspection and mitigation programs are soundly based.			
14. DOCUMENT ANALYSIS - KEYWORDS/DESCRIPTORS Erosion-Corrosion Corrosion water Chemistry Erosion		15. AVAILABILITY STATEMENT Unlimited	
16. IDENTIFIERS/OPEN ENDED TERMS		16. SECURITY CLASSIFICATION (This page) Unclassified (This report) Unclassified	
		17. NUMBER OF PAGES 91	
		18. PRICE	

120555139217 1 1AN1RS
US NRC-OARM-ADM
DIV FOIA & PUBLICATIONS SVCS
RES-POR NUREG
P-210
WASHINGTON DC 20555